Linking Cellular and *In Vitro* Microtubule Behavior: Reconstitution Assays to the Rescue

Luca Signorile

ISBN: 978-94-6299-701-1

Cover design: Lena Kourkouta
Layout: Luca Signorile
Printed by Ridderprint BV, The Netherlands

The studies presented in this thesis were conducted at the Department of Cell Biology, Erasmus Medical Center (Rotterdam, the Netherlands) and financially supported by the NWO Graduate Programme Erasmus MC - Medical Genetics Grant: 022.004.002.

Linking Cellular and *In Vitro* Microtubule Behavior: Reconstitution Assays to the Rescue

---

Vergelijking Tussen het Cellulaire en *In Vitro* Gedrag van Microtubuli:
Beter Inzicht met Behulp van Reconstitutie Experimenten

Thesis

to obtain the degree of Doctor from the
Erasmus University Rotterdam
by command of the
rector magnificus

Prof.dr. H.A.P. Pols

and in accordance with the decision of the Doctorate Board.

The public defence shall be held on
Wednesday 27th of September 2017 at 11:30 hours

by

Luca Signorile

born in Bari, Italy

Erasmus University Rotterdam

Doctoral Committee:

Promotors:	Prof.dr. D.F.E. Huylebroeck Prof.dr. F.G.Grosveld
Other members:	Prof.dr. A.M. Dogterom Dr. G. Jansen Dr.ir. J.H.G. Lebbink
Co-promotor:	Dr.ir. N.J. Galjart

To my family and friends

Table of Contents

Abbreviations

AAA	ATPase Associated with diverse cellular Activities
AchR	Acetylcholine receptor
ATP	adenosine 5'-triphosphate
ATPase	adenosine 5'-triphosphate hydrolase
BPTI	bovine pancreatic trypsin inhibitor
CAMSAPs	calmodulin-regulated spectrin-associated proteins
CCP	cytoplasmic carboxypeptidase
CHD	calponin-homology domain
CLASP	cytoplasmic linker associated protein
CLIP	cytoplasmic linker protein
COS	CV-1 (simian) in Origin, and carrying the SV40 genetic material
DNA	deoxyribonucleic acid
EB	end-binding protein
EBH	end-binding homology
EGFP	enhanced green fluorescent protein
EM	electron microscopy
fs	femtosecond
GMPCPP	guanosine-5'-[(α ,β)-methyleno]-triphosphate
GSK3β	glycogen synthase kinase 3β
GTP	guanosine 5'-triphosphate
GTPase	guanosine 5'-triphosphate hydrolase
HDAC	histone deacetylase
HIV	human immunodeficiency virus
i.e.	*id est*
IF	immunofluorescence
IFs	intermediate filaments
IL	interleukin
K_d	equilibrium dissociation constant
k_{off}	dissociation rate constant
k_{on}	association rate constant
KD	knock down
KO	knock out
kDa	kiloDalton
KIF	kinesin family
min	minute
mRNA	messenger RNA
ms	millisecond
MAP	microtubule-associated protein
MD	molecular dynamics
MM	molecular mechanics
MT	microtubule
MTOC	microtubule-organizing center
nM	nanomolar
NMR	nuclear magnetic resonance
ns	nanoseconds
pf	protofilament

pN	picoNewton
ps	picosecond
PTM	post-translational modification
QM	quantum mechanics
RC	ring complex
RNA	ribonucleic acid
s	seconds
STOPs	stable tubule only polypeptides
TAP	tubulin-associated protein
TAT	tubulin acetyltransferase
TIRF	total internal reflection fluorescence microscopy
TOG	tumor-overexressed gene
TuRC	tubulin ring complex
TTL	tubulin tyrosine ligase
TTLL	tubulin tyrosine ligase-like
UV	ultra-violet
wt	wild-type
ZED	ζ-,ε-,δ-tubulin module
µL	microliter
µM	micromolar
Å	angstrom
+end	plus end
-end	minus end
+TIP	plus end tracking protein

Scope of the thesis

The cytoskeleton is composed of intermediate filaments, the actin network and microtubules (MTs); it is a dynamic cellular web that serves multiple purposes which go beyond a mere structural function. The cytoskeleton allows complex morphological changes in cells, which are critical for cell specialization and functions. This thesis describes how MT behavior can be influenced by subtle changes in its building block, the tubulin protein, and by a subset of MT-associated proteins (the so-called "+end-tracking proteins", or +TIPs), which associate to the dynamic, fast-growing ends of MTs. The studies presented in this thesis widen our knowledge on MTs, tubulin and +TIPs. Three major issues are discussed: 1) the discovery of novel tubulin-associated proteins (TAPs) as well as the effects of some tubulin mutations involved in neurodevelopmental disorders on the MT network stability in cells and on TAP binding; 2) the effects of these same mutations on tubulin structure within a protofilament, investigated *in silico* with molecular modelling and molecular dynamics simulations; 3) the regulation of MTs by +TIPs, in particular the cytoplasmic linker proteins (CLIPs).

Chapter 1 provides an overview of MT function, structure and behavior, together with the structural features, isotypes and post-translational modifications of its building block, the tubulin dimer. Since regulation of MTs is carried out by +TIPs, a description of the structure and role of the main ones presented in this thesis is also provided. Finally, a brief introduction to molecular dynamics simulations is given to guide the reading of **Chapter 3**.

Chapter 2 describes our strategy and studies centered on the identification of novel TAPs via purification of isotypes of α- and β-tubulin. We also report on the binding of TAPs to two tubulin mutants found in patients with neurodevelopmental disorders, and the effects of these mutations on the MT network in cells.

Chapter 3 describes the effects of the tubulin mutations (discussed in **Chapter 2**) on tubulin and protofilament structure at the atomic level, by using molecular modelling and molecular dynamics simulations. The model proposed helps in understanding possible mechanisms leading to tubulin/MT dysfunction in cells (**Chapter 2**).

Chapter 4 focuses on the roles in MT dynamics of the +TIP CLIP-115 compared to those of its close relative CLIP-170. These two proteins have always been considered redundant in function, but our studies suggest that they also have distinct properties.

Finally, **Chapter 5** discusses the major findings presented in the other chapters, and some aspects of current methodologies commonly used in the field, such as *in vitro* reconstitution assays; the implications of the studies presented in this thesis and future prospects are addressed.

Chapter 1

General Introduction

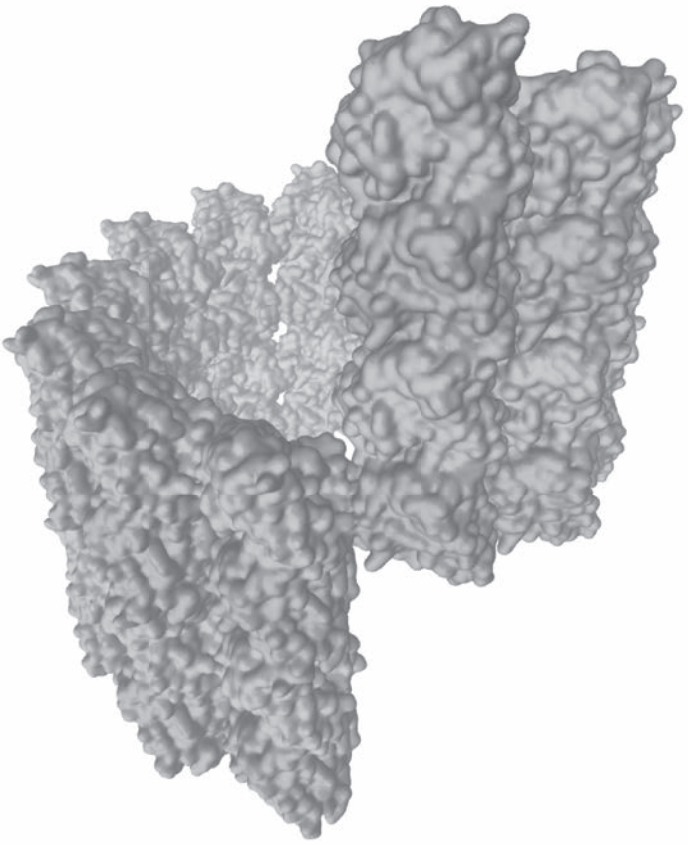

Microtubules

The cytoskeleton and its functions

The cytoskeleton plays a crucial role in structural stability, motility, intracellular transport and cellular division in all eukaryotic cells [1]. It is represented by three types of network, i.e. intermediate filaments (IFs), actin filaments and microtubules (MTs) (for review, see [2]). Briefly, IFs are non-polar structures mainly responsible for mechanical support; motor proteins cannot associate or move along IFs given the lack in polarity [3]. By contrast, the actin and MT networks are polar structures and support cell shape and intracellular transport. One of the major functions of the actin cytoskeleton is to induce changes at the plasma cell membrane by constituting, for example, filopodia [4] and lamellipodia [5,6]. Actin achieves this by exerting pushing and pulling forces but also by employing actin-based motors, called myosins [3,7–9]. MTs, the subject of this PhD thesis, are hollow tubes made up of tubulin subunits. MTs are important for cell shape and mitosis, and play a critical role in regulating cell polarity [10] and organizing the cytoplasm [11,12].

MTs are also involved in various other processes, including the directional movement of cells [13–15]. MTs direct long-range transport of organelles in cells [15], by serving as "cellular railways" over which organelles and vesicles can be transported by MT-based motor proteins, such as kinesins [16–18] and cytoplasmic dynein [19]. Transport mediated by the cytoskeleton achieves displacement of organelles, vesicles, proteins, and chromosomes during cell division, in a much more efficient and specific manner than diffusion. Since MTs are essential for long-range intracellular trafficking, they are of critical value for highly polarized and elongated cells such as neurons. The spatio-temporal organization of the three cytoskeletal networks (i.e., actin and intermediate filaments, and MTs) their regulation by proteins that interact with them (e.g. MT-associated proteins, or MAPs), and the prompt responses, in particular of the actin and MT cytoskeletons, to external cues and mechanic stimuli, together with their cross-signaling [20,21], are of paramount importance for the proper functioning of all cells in our body.

Tubulin

Tubulin structure

MTs are dynamic hollow tubes made of αβ tubulin heterodimers stacked longitudinally into protofilaments, thirteen of which form a MT through lateral interactions. This description of the MT network is started by describing its building block: the tubulin heterodimer. Tubulin was first discovered by Weisenberg, Borisy and Taylor in 1968 as a "colchicine-binding protein of mammalian brain" [22]. The 8 nm-long tubulin heterodimer consists of two polypeptides of 55 kDa each, α- and β-tubulin, each capable of binding the nucleotide guanosine 5'-triphosphate (GTP) (Figure 1). The nucleotide-binding pocket of α-tubulin, located at the interface between α- and β-tubulin, is called the N-site. Here, GTP cannot be exchanged or hydrolyzed, and this GTP plays a structural role [23]. By contrast, GTP at the β-tubulin E-site can be hydrolyzed; this site can also bind guanosine 5'-diphosphate (GDP), resulting from GTP hydrolysis after MT polymerization [24], and exchange it again for GTP once the dimer returns to the pool of soluble tubulin after MT depolymerization [25]. The 40% sequence identity in their primary structure [26,27] leads to a nearly identical tertiary structure for α- and β-tubulin, each monomer being composed by two β-sheets surrounded by twelve α-helices [25,28]. In both α- and β-tubulin, the N-terminal domain contains a Rossmann fold, important for the binding of GTP, with the signature Gly-Gly-Gly-Thr-Gly-Ser-Gly [29]. The nucleotide is further stabilized by hydrogen bonding with the residues Asn206 and Asn228 (Figure 1, top right). In particular,

this specificity is obtained by hydrogen bonding of the 2-exocyclic amino group in GTP to the hydroxyl groups of Asn206 and Asn228, and by hydrogen bonding of the 6-oxo group of GTP to the amino group of Asn-206 (see Figure 1A, top right) [25]. The intermediate domain comprises the strands S7–S10 and the helices H9–10 (Figure 1, bottom left) [30]. In β-tubulin, this domain contains a binding site for taxol, a MT-stabilizing drug (depicted as green stick model in Figure 1). This site is represented by a pocket facing the MT lumen in proximity to the so-called M-loop, which is involved in lateral interactions with the adjacent protofilament. In α-tubulin, the corresponding space is occupied by an eight-residue insertion in the loop between β strands S9 and S10 (Figure 1, bottom left) [31], hindering the binding of the drug. Finally, the C-terminal helices (H11 and H12) are a major site for the binding of MAPs (Figure 1, bottom left) [28,32].

The stability of the tubulin heterodimer relies also on its non-covalent bonds, mainly longitudinal hydrogen bonds at the inter-monomer interface [33]. In concert with these bonds, further stabilization is accomplished by a Mg^{2+} ion [23] coordinating the surrounding residues and the GTP accommodated at the N-site (Figure 1, bottom right).

Tubulin C-terminal tails

The disordered projections that arise from the heterodimer at the C-terminal domain are commonly known as the tubulin "tails". Although unstructured elements, they are highly important. For example, the tails are subjected to a number of post-translational modifications (PTMs, see section 1.3) that modify the properties of tubulin itself or of the affinity of MAPs for MTs [34]. The C-terminal residues of α- and β-tubulin (starting with Ser439 in α-tubulin and Ala430 in β-tubulin) are mainly represented by glutamate (hence the name E-hooks), and (together with aspartate residues) these greatly contribute to the acidic character of the tubulin tails and to their disordered structure [35].

The structures of each of the tubulin tails has not been solved experimentally, but can be modeled as part of the tubulin (Figure 1). This is due to their flexibility and intrinsic disordered status, resulting in a number of possible distinct conformations that are averaged out during the reconstruction process of X-ray crystallography or cryo-electron microscopy (cryo-EM). Alternatively, it has been proposed that the heterogeneity of tubulin forms present in brain tissue, which is the main source of tubulin used for most studies, could lead to the loss of structural information. This could be caused by the differences in conformation of isotype-specific tails, but also by PTMs (see *Post-translational modifications of tubulin* later in this section) [34]. It is interesting to note the functional role of the aforementioned structural disorder. As reviewed by Roll-Mecak [34], the flexibility of the tails and their high radius of gyration would result in an increased probability of fruitful interactions with binding partners, increasing in turn the association rate. At the same time, their intrinsically disordered structure would also increase the "off" rate, since part of the interface would dissociate. Since the structural ordering of a disordered region upon binding is an energetically-unfavorable process, the net result is that the flexible, disordered tails would engage in highly specific, but weak interactions with their binding partners [36]. This is in line with experimental observations, since many MT-MAP affinities have been shown to be in the μM range [34].

An interesting, recent study used NMR to investigate the tubulin tails. Although they were found to be disordered they did have a propensity for β-sheet conformation [37], in contrast with the α-helix conformations predicted by molecular dynamics (MD) simulations (see the dedicated section later in this chapter) [38,39]. However, in both experimental and *in silico* investigations, the tails were found to interact with the heterodimer body. Specifically,

in MD simulations α-tubulin tails mainly interacted with the helix H11 of β-tubulin, and β-tubulin tails with the respective helix in α-tubulin. Alternating interactions of α-tubulin's H10/B9 loop between the C-terminal tail of α-tubulin and the H11 helix of β-tubulin caused more fluctuations within the intermediate domain. This would mean that the C-terminal tails could alter the conformation of the heterodimer, thus possibly influencing assembly properties (in disagreement, however, with more recent studies, see next paragraph) and MAP binding [39].

Tubulin superfamily and tubulin isotypes

Different tubulin genes, belonging to the so-called "tubulin superfamily", code for α- and β-tubulins, but also for γ- (gamma), δ- (delta), ε- (epsilon), ζ- (zeta), η- (eta), ι- (iota) and κ- (kappa) tubulins [40]. Furthermore, several tubulin isoforms, commonly referred to as "isotypes", are expressed in most eukaryotes [41]. Humans have at least seven α- and eight β-tubulin isotypes [42], and two γ-tubulin forms. These three tubulins are synthesized in every eukaryotic organism investigated so far. By contrast, the genes encoding the various tubulin isotypes have different tissue and temporal expression patterns, suggesting that they could confer specific characteristics to the MTs they constitute [43–46], leading to the "multi-tubulin hypothesis" [42,47]. However, the different isotypes do not form distinct isotype-specific pools of MTs, but they can all co-polymerize into the same MT, forming a heterogeneous pool of MTs with different isotypes [46,48].

Studies with tubulin isolated from bovine brain showed that tubulin heterodimers with different β isotype composition have distinct dynamic instability parameters. Specifically, MTs with a higher βII/βIII isotype ratio were less dynamic than when βIII was more abundant [49,50]. Importantly, it was recently shown what confers different isotype-specific properties to dynamic instability parameters and polymerization in MTs reconstituted *in vitro*. The residues within the conserved β-tubulin core are the determinants conferring the different MT dynamics behavior, rather than those of the C-terminal tail [51], which is instead mainly involved in interactions with MAPs. Most of the isotype sequence differences are located in approximately 25 residues of the tails, which are susceptible of many PTMs that can modulate these interactions [52,53].

Gamma (γ)-tubulin is present mainly in MT-organizing centers (MTOCs) and, together with other proteins of the γ-Tubulin Ring Complex (γ-TuRC) (for MT nucleation structures described here, see *Microtubule nucleation and nucleation centers in cells* later in this section), is involved in MT nucleation [54–56] (Figure 2) . In 2008, an interesting functional adaptation was found for γ tubulin. Two isoforms of γ-tubulin (γ-T1 and γ-T2) were discovered in the Antarctic ciliate *Euplotes focardii.* Comparison of the three-dimensional structures of the γ-tubulin of the congeneric species of temperate climates revealed differences at specific residues in their primary structure. In particular, these were located in regions involved in inter-dimer longitudinal and lateral contacts (M-loop) and in the T3 loop (Figure 1, bottom left), responsible for GTP binding. These adaptations are most likely to promote the nucleation of MTs at low temperatures. Moreover, a different cellular localization of the two isoforms was observed, with the γ-T1 being present in basal bodies and γ-T2 in the centrosomes of the micronuclear spindles [57]. These observations suggest that not only subtle residue changes can greatly influence tubulin behavior and stability properties, but also that different isoforms can contribute to different functions.

There is still little known about δ- and ε-tubulin. They were both identified in the human genome by sequence similarity to other tubulins [58], the former specifically by similarity to its homologue in *Chlamydomonas* [59]. Both are conserved in vertebrates and are not incorporated into MTs. Rather, they localize to the centrosome, as found by

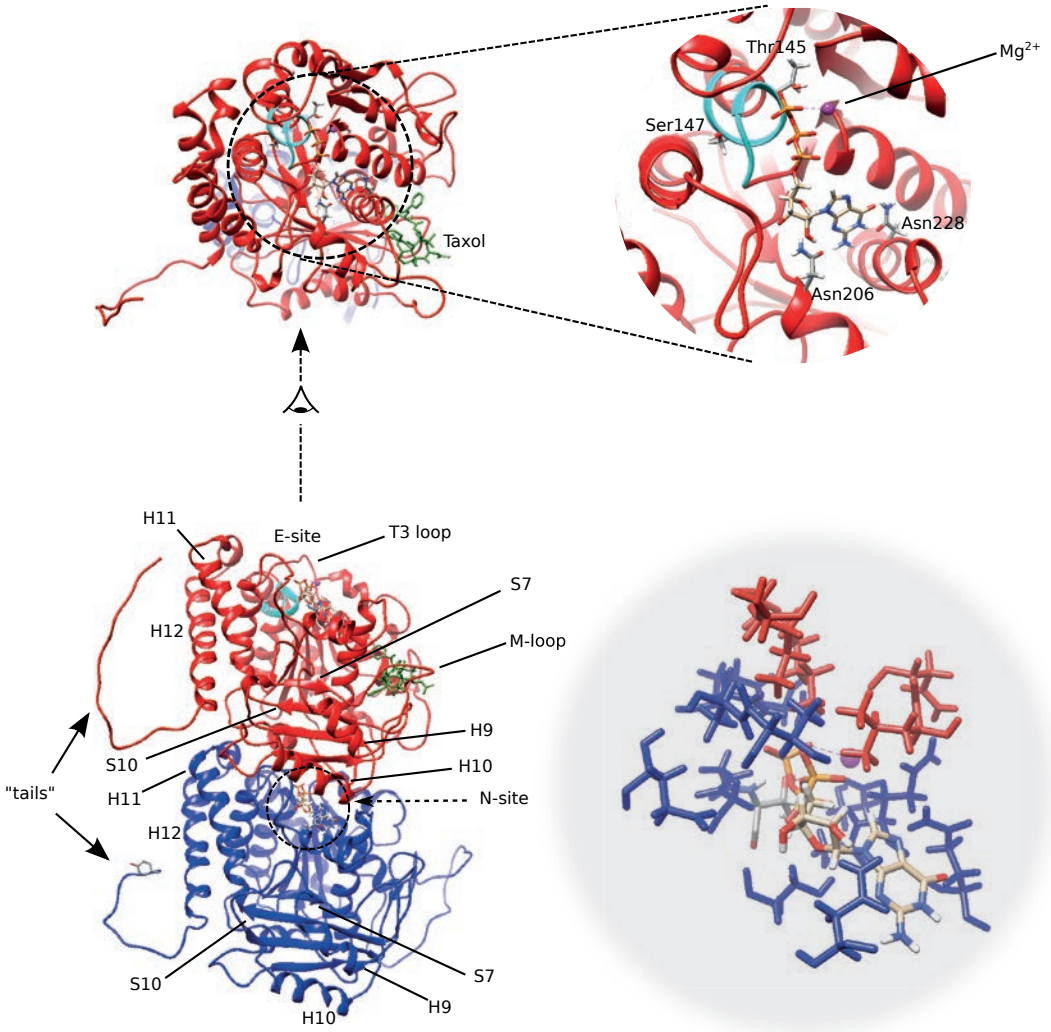

Figure 1. Full model of the tubulin heterodimer. **Bottom left,** tubulin structure modelled based on the structure deposited by Nogales et al. (Löwe *et al*. 2001) with PDB entry 1JFF. Red: β-tubulin, blue: α-tubulin. The deposited structure was modified as follows. The Zn^{2+} ion was removed; the GDP at the E-site was substituted by GTP and Mg^{2+} using the translated coordinates of the GTP and Mg^{2+} at the N-site. The α-tubulin N-terminal loop (residues 35 to 60) was reconstructed by homology with the corresponding β-tubulin loop. The secondary structure elements cited in the text are marked accordingly ("H": α-helix; "S": β-strand). The C-terminal tails were modelled *ab initio* using the software Modeller (Webb and Sali 2014); the C-terminal α-tubulin tyrosine residue is depicted as sticks. The taxol molecule is depicted in green behind the M-loop. The residue signature Gly-Gly-Gly-Thr-Ser-Gly is represented in cyan; the residues threonine and serine are depicted as sticks. **Top left,** top view of the heterodimer, looking towards the E-site. **Top right,** close-up view of the area enclosed by the dashed circle with the residues Thr145, Ser147, Asn206 and Asn228 depicted as sticks. **Bottom right,** close-up view of the N-site (dashed circle) highlighting the residues within 4 Å of the GTP or Mg^{2+} ion colored by chain (same color-code as in the model). Figure generated with Chimera (Pettersen et al. 2004).

immunofluorescence experiments in human osteogenic sarcoma cells (U2OS cells). However, δ-tubulin was found between centrioles, suggesting a role in centriole bridging, for Paintrand and co-workers observed fibers linking the two centrioles [60], or centriole separation. In fact, the pattern of localization resembles that of Skp1, a component of the SCF ubiquitin ligase, which is required for centriole separation [61].

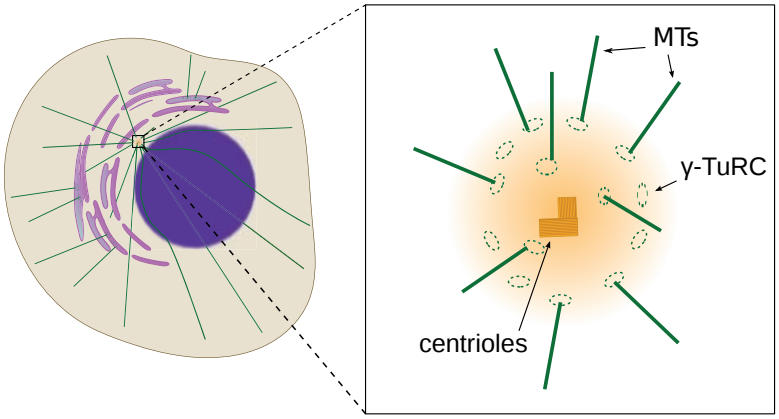

Figure 2. Centrosomal and non-centrosomal MT nucleation. Simplified and schematic representation of an animal cell highlighting the organization of MTs (green lines) nucleating from a centrosome (inset) or the trans-Golgi apparatus (pink stacks surrounding the nucleus, in purple). Inset: the yellow shaded area is the pericentriolar material, the perpendicular elements the pair of centrioles and the green dashed circles the γ-TuRC as indicated by the arrows.

Epsilon (ε)-tubulin localizes to the pericentriolar material of the centrosome during and after mitosis. This tubulin isotype might be involved in the regulation of a cell-cycle-specific function, such as centrosome duplication, or cell-cycle-specific recruitment of other molecules to the centrosome [62].

Zeta (ζ)-tubulin is the last tubulin characterized in vertebrates. A recent study by Turk and co-workers suggested a conserved pattern: first, organisms lacking ε-tubulin always also lack δ- and ζ- tubulins; second, the presence of ε-tubulin is always accompanied by that of δ- and/or ζ-tubulin. Therefore, ζ-tubulin, together with δ- and ε- tubulins, has been classified as a member of the so-called ZED tubulin module [63]. Zeta (ζ)- and δ- tubulin are evolutionarily interchangeable: in humans ζ-tubulin is not produced, in contrast to δ-tubulin. In *Xenopus* multiciliated cells, ζ-tubulin is a component of the basal foot, a centriolar appendage that connects centrioles to the apical cytoskeleton, and co-localizes there with ε-tubulin. It has been proposed that ZED tubulins are important for centriole functionalization and for orientation of centrioles with respect to cellular polarity axes [63].

Eta (η)-tubulin was first identified by genetic screening in *Paramecium* [64]. It has been suggested that the function of η-tubulin might be to tether γ-tubulin-containing complexes to the sites of basal body duplication (since γ-tubulin is required for this function [65]), where it might either stabilize nascent MTs in developing basal bodies or transduce a signal for basal body duplication [66].

Finally, genomic sequences for ι-, κ-, and θ-tubulin from *Paramecium* species have been reported in databases, but their cellular functions are still unknown.

Post-translational modifications of tubulin

Tubulin can be post-translationally modified, and this occurs mainly at its tails. The main PTMs include detyrosination (Arce et al. 1975; Barra, Arce, and Argaraña 1988), glutamylation [69,70], acetylation [71], methylation [72] and glycylation [73], and these will be described below. Other modifications (phosphorylation, polyamination, palmitoylation, ubiquitination, glycosylation, arginylation, sumoylation (reviewed by [74]) have also been identified but have not been investigated in detail.

The major PTMs occur after the dimers have been incorporated into MTs [75], which could explain the observation that taxol-induced stable MTs often accumulate more of these modifications than dynamic ones [76–79]. In fact, since incorporated tubulin dimers are retained for much longer times in stable MTs than those of dynamic MTs, they have an increased likelihood of acquiring PTMs. PTMs can influence MAP binding and, indirectly, MT dynamics and stability, and are therefore critical to MT function [80].

Detyrosination

This PTM occurs only on α-tubulin. Detyrosination was the first MT-associated PTM to be discovered, about 40 years ago [81]. The last C-terminal residue of the α-tubulin isotypes, except for TUBA4A and TUBA8, is tyrosine, which can be removed specifically by an unidentified tubulin carboxypeptidase once α-tubulin is incorporated into MTs [76,82]. Little is known about this process. An increased level of detyrosination is observed on stable MTs, as their prolonged lifetime allows them to acquire the PTM in ever increasing quantities. It is unclear whether detyrosination induces *per se* the formation of stable MTs; however, experiments in Vero cells showed that detyrosinated MTs were more resistant to depolymerization at higher concentrations of nocodazole (a MT-depolymerizing compound) than tyrosinated MTs [83]. Detyrosination has also been shown to protect MTs from kinesin-2 mediated depolymerization [84].

Importantly, de-tyrosinated tubulin can be tyrosinated again by the enzyme tubulin tyrosine ligase (TTL). This enzyme is able to recognize the three-dimensional structure of the curved tubulin dimer in the cytoplasm and to perform the ligation reaction [85]; this reaction does not occur when the tubulin dimer is within the MT; TTL even prevents its incorporation by capping the dimer longitudinally [75,85]. Loss of TTL results in morphological abnormalities and it is involved in cancer [75]. Interestingly, studies in Madin-Darby Canine Kidney (MDCK) epithelial cells showed that the level of MT detyrosination increased as the cells approached confluency, and then decreased when the cells became polarized at confluency [86,87].

An example of functional co-existence of these PTMs is given by neurons, where immunoelectron microscopy studies with an antibody against tyrosinated tubulin showed that axonal MTs are dynamic (and tyrosinated) at the +end of the more stable, non-tyrosinated MTs [88,89]. This was later confirmed at a higher resolution on individual MTs [90]. These observations suggest that axonal MTs are composed by a more recently-assembled domain (tyrosinated tubulin-rich) extending from a stable domain (tyrosinated tubulin-poor) (Figure 3). Also, tyrosinated tubulin was prevalently found in growth cones [90,91]. As for the functional role of tubulin tyrosination, a *Ttl*-null mouse model showed that the lack of TTL leads to abnormal neuronal morphology and respiratory problems and is lethal within 1 day after birth [92]. Therefore, tubulin tyrosination and detyrosination are essential events that need to occur in MTs in a specific and regulated manner.

Δ2- /Δ3-modifications

Detyrosinated α-tubulin can undergo removal of another residue, i.e. the ultimate glutamate [93]. This deglutamylation is carried out by one of six specific cytosolic carboxypeptidases (CCPs) (CCP1 [94], CCP2/3 [95], CCP5 [96], and CCP4/6 [97]). Remarkably, the newly-exposed glutamate residue cannot be tyrosinated; Δ2-α-tubulin is mostly found in stable MTs and is enriched in neurons, centrioles and cilia [98,99]. Although this modification is highly present in brain MTs [99], its exact function has not yet been elucidated.

Recently, another modification of the α-tubulin terminus has been identified in rat

brain tissue. It consists of the removal of the ultimate glutamate residue produced after the aforementioned Δ2-modification process, and is therefore named Δ3-modification [100]. All the CCPs cited above, except for CCP2 and CCP3, are able to remove the ultimate glutamate on Δ2-tubulin. Discrepancies have been observed for CCP5, which appears to act only on the isotype α4A and not on α1B tubulin –when fused to mCherry- (see [96] and [100]). Δ3-tubulin appears to have similarities with tyrosinated tubulin, in that they were both recovered to a larger extent in the soluble fraction (44% and 30%, respectively) rather than in the microtubular fraction after treatment with nocodazole and high-speed centrifugation, perhaps indicating that the Δ3-modification could be associated to only mildly stable MTs. This was in contrast to the behavior of detyrosinated tubulin, which is recovered predominantly in the microtubular fraction (96%). In the same study Δ4-β-tubulin (lacking the last four residues) was also identified, raising the question whether more PTMs with further trimming of the tubulin tail are still to be found.

The only example of β-truncation in mammals is reported by Miller and co-workers [101], who demonstrated the removal of the C-terminal alanine and the penultimate valine residues from the β2-tubulin isotype in rat liver tissue. As for Δ2, the functions of all of these PTMs need to be elucidated.

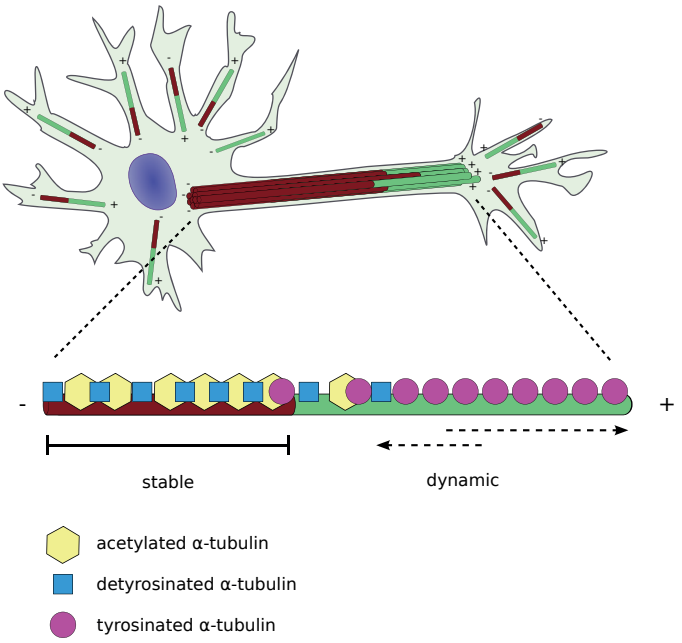

Figure 3. PTMs in neurons. Simplified and schematic representation of a neuron, highlighting the stable and dynamic segments of MTs, together with their polarity (+: +end, -: -end). Axonal MT bundles possess a homogeneous distal +end polarity, in contrast to MTs in dendrites. The inset shows the most abundant PTMs present on an axonal MT: the dynamic portion is enriched in tyrosinated α-tubulin, whereas the older, stable segment is abundant in detyrosinated and acetylated α-tubulin.

Acetylation

Discovered about 30 years ago [71,78], this PTM occurs at the residue lysine 40 (Lys40 or K40) of α-tubulin [102]. Since K40 is located on a loop facing the lumen of the MT, the enzyme has to reach the inside of the MT tube to perform its activity, in contrast to modifications occurring

at the C-terminal tails. The transfer of the acetyl moiety from acetyl-CoA to Lys40 is catalyzed specifically by the enzyme tubulin acetyltransferase 1 (TAT1, also known as MEC-17) [103]. Using a combination of *in vitro* experiments and computer simulations, it was recently shown that TAT1 enters the lumen of the MT either from the –preferentially tapered- ends, where the enzyme concentrates, or through transient bends and breaks in the MT lattice [104]. These results are in contrast to the model proposed by Shida and co-workers, according to which the entry of TAT1 would be allowed by regular MT lattice breathing [105]. Alterations in MT structure could modulate the affinity of TAT1 for its binding sites, determining the extent of acetylation. The slow diffusion of TAT1 within the MT lumen would explain the acetylation patches observed in stable MTs in cells [78,106,107]. In fact, the long lifetimes of stable MTs increase the probability of lattice defects, leading to an increased TAT1 accumulation and thus, a higher degree of acetylation. Acetylated MTs are enriched in cilia and flagella; loss of TAT1 is associated with defective axonal morphology and neurodegeneration in the nematode worm *Caenorhabditis Elegans* [108,109] and, although viable, *Tat1* knockout mice showed sperm defects [110]. Acetylation is associated with MT stability, although it does not appear to act directly on MT structure [111], and experiments showed that this modification did not influence MT dynamics [112]. However, *in vitro* experiments showed that a decreased level of MT acetylation causes reduced binding and motility of the molecular motor kinesin-1 on the MT [113]. Increased MT acetylation, conversely, promoted dynein and kinesin-1 recruitment [114]. Thus, the extent of MT acetylation has to be finely regulated by the cell to ensure proper levels of binding and motility of these motor proteins.

Acetylation of α-tubulin is reversible. While acetylation occurs in MTs, deacetylation of K40 of α-tubulin occurs on free tubulin dimers [115] and is performed by the histone deacetylase 6 (HDAC6) [116] (for a brief overview on histones, see section *"Methylation"*) or by the non-classical HDAC (sirtuin) SIRT2 [117]. Both enzymes have several other target proteins; strikingly, *Sirt2* knockout and *Sirt2*/*Hdac6* double knockout mice are viable and normal [118]. Interestingly, no change in α-tubulin acetylation was observed in *Sirt2* knock-out cells, whereas cells from *Hdac6* knock-out mice showed an increased MT acetylation compared to wild-type controls, but still without producing any remarkable phenotype [119]. The main effects regarded behavior, since *Hdac6* knock-out mice were hyperactive, less anxious and with a lower depression tendency than wild-type mice [120]. HDAC6 could also play a role in inflammation, as MT acetylation would result in an increased production of the anti-inflammatory interleukin (IL) IL-10 [121]. Taken together, these studies suggest a pivotal role played by HDAC6 rather than by SIRT2 in MT deacetylation. However, the exact function of acetylation on MTs remains elusive (for a comprehensive review, see [122]).

Glutamylation

Glutamylation consists of the addition of one or more glutamate residues (poly-glutamate chains) to the tail of α- or β-tubulin. It occurs through the formation of peptide bonds branching off the γ-carboxyl groups of the existing glutamates [69]. This PTM is catalyzed by enzymes called glutamylases, nine of which have been identified in mammals [123]. They have different preferences for the tubulin subunit they act upon, and also with different abilities in starting or extending the glutamylation process [124]. These enzymes belong to the TTL-like (TTLL) family, as they contain a TTL-homology domain that allows ligation of different amino acids to tubulin [123,125]. It has been shown that the number of added glutamate residues ranges from 1 to 6 and the position of the PTM depends on tubulin subunit and isotype: at Glu445 in the tubulin isotypes α1 and α2 [69], Glu443/445 in α4 [126], Glu438 in β6 [127], Glu435 in β2 and β3 [70,128,129], Glu434 in β4 and Glu441 in β5 [130]. Interestingly, the abundance

of glutamylated β-tubulin and the extent of this modification was found to increase during neuronal differentiation [131,132]. However, Wolff and colleagues, who developed the GT335 antibody to detect glutamylated tubulin, found that α-tubulin was more glutamylated than β-tubulin in mouse brain, whereas only β-tubulin was glutamylated in non-nervous tissues, although to a lower extent than in brain [133]. In other tissues, glutamylated MTs are enriched in axonemes of cilia and flagella, but also in centrioles [62,129].

It has been proposed that glutamylated MTs contribute to intracellular traffic and in the regulation of motility in cilia and flagella, by acting on the binding of the cytoplasmic and axonemal dynein molecular motors [134–136] (see section 2). Cellular and *in vitro* assays showed that glutamylation can also mediate MT severing. In fact, long polyglutamate chains (formed by TTLL6, and often abundant in brain tissue) induced a higher degree of MT severing by spastin than shorter chains (added by TTLL4) [137–139].

The extent of polyglutamylation has been shown to be crucial in the regulation of MAP binding to MTs: Tau, kinesins, MAP1B and MAP2 all show preferential binding with increasing affinity for mono-, di-, or triglutamylated MTs, the last modification being responsible for the highest relative affinity. As the glutamate chain grows further, the affinity progressively decreases [140–142]. An exception to this mechanism is represented by MAP1A, which maintains high affinity for longer polyglutamyl chains in α- and β-tubulin [142].

The reversal of polyglutamylation (deglutamylation) is catalyzed by the CCPs (discussed above, section 1.3.2). However, only one of them (CCP5) preferentially removes the branching glutamates added by the TTLLs [97,143]. Nevertheless, similarly to the other CCPs, CCP5 is able to remove not only TTLL-added glutamates, but also those that are present in tubulin itself [96]. The neurodegeneration phenotype of the *pcd (Purkinje cell degeneration)* mouse model [144,145] was shown to be due to a mutation of the *Ccp1* gene. Hyperglutamylation was observed in brain areas that undergo degeneration (such as the cerebellum and the olfactory bulb [97]). A possible explanation for the neurodegeneration could be the effect of polyglutamylation on MAP binding and MT severing by spastin (as described earlier). Nevertheless, despite the efforts made so far, it is still difficult to ascribe specific functional roles to MT polyglutamylation. Interestingly, survival of Purkinje cells was observed when *Ttll1* was also knocked-out, suggesting that balancing the glutamylation level on MTs is crucial for neuronal survival [94,97].

Glycylation

This PTM consists of the addition of glycine residues to the terminal glutamate of α- or β-tubulin [146,147] and is abundant in cilia and flagella, the only structures where this modification has been found so far [148]. Similar to glutamylation, glycylating enzymes are members of the TTLL family described above. In mammals, TTLL3 and TTLL8 are responsible for the formation of a γ-linked isopeptide bond between the glycine and the terminal glutamate of α- or β-tubulin [146,147]. The chain can then be further extended by TTLL10, which indeed is an elongating glycylase [149]. However, in humans, this protein has lost its enzymatic activity presumably due to two amino acid changes, and thus MTs in cilia and flagella MTs are monoglycylated [150]. An example is represented by MTs in human sperm flagella, which are in fact monoglycylated. Thus, it appears that MT monoglycylation is able to sufficiently fulfill the functions of protein glycylation [150] and that the lack of polyglycylation does not impede ciliary beating [151].

Interestingly, conventional knock-out mice for *Ttll3* show lack of MT glycylation in the colon, indicating that TTLL3 is the only functional glycylase present in this tissue. Here, the

lack of this PTM leads to decreased number of primary cilia and increased development of colon tumors [152]. The lower amount of cilia compared to wild-type mice could be explained by the fact that non-glycylated axonemes (see section "*Microtubule nucleation and nucleation centers in cells"*) disassemble after initial assembly, impairing normal ciliogenesis and leading to the phenotype [150,153]. Interestingly, development of cancer due to defective ciliogenesis was also observed in human breast cancers [154], indicating that misregulation of ciliogenesis (via lack of MT glycylation or via down-regulation of cilia-associated genes, as for the study on breast cancer just mentioned) is an important factor for cancer development.

Methylation

Tubulin methylation is in fact a tri-methylation (the addition of three methyl groups) event and occurs at Lys40 of α-tubulin. This modification was first identified in tubulin of *Toxoplasma gondii* [72], and recently new insight was gained through a study by Park *et al*., who discovered a common player in the well-known "histone code" and the more recently proposed "tubulin code" (see below). Briefly, histones are basic, dimeric proteins interacting with the 2'-deoxyribonucleic acid (DNA) [155]. Histones H2A/H2B, H3 and H4 constitute the octameric nucleosome core, around which 146 base pairs (bp) of DNA are wrapped [155]. Histone association compacts chromatin and any PTM that alters histone association can thus affect transcriptional activity. Indeed, certain PTMs at histone tails do regulate chromatin accessibility of the transcription machinery, as well as the recruitment of non-histone chromatin modifiers and transcription factors (TFs) according to the combination of modifications present (reviewed by [156]). The "histone code" represents the combinations of PTMs at the terminal protrusions ("tails") of histones [157].

Modifications of histone and tubulin tails have always been considered to belong to distinct machineries. The histone methyltransferase SET-domain containing 2 (SETD2, or KMT3A) is involved in transcriptional elongation by performing trimethylation of lysine 36 of the histone H3. Strikingly, SETD2 is another example of "histone-tubulin code bridge" (see HDAC6, discussed above). SETD2 is, in fact, a common "writer" of methylation of both histones and tubulin [158]. Specifically, SETD2 performs trimethylation of lysine 40 of α-tubulin, the same residue being also subject to acetylation, during mitosis and cytokinesis. Co-immunoprecipitation experiments confirmed the direct interaction between SETD2 and α-tubulin. Knock-out cells for this enzyme showed non-methylated MTs, anomalies in mitosis, cytokinesis, micronuclei and polyploidy. Interestingly, rescue experiments restored this normal phenotype, whereas synthesis of a SETD2 mutant protein, which was unable to perform methylation of α-tubulin, but not of the histone H3, failed to do so. This led to the conclusion that trimethylation of lysine 40 of α-tubulin, and not that of lysine 36 of histone H3, is needed for normal mitosis. This modification would play a role in preventing aberrant chromosome segregation and thus genomic instability, potentially leading to cancer [159]; in fact, mutations of *SETD2* have been found in various types of cancer (as reviewed by [160]).

Structure and dynamic behavior of microtubules

Structure of microtubules

As mentioned above, MTs are made of the protein tubulin, whose functional form is the α-/β-tubulin heterodimer (Figure 1). In MTs the heterodimers stack in a head-to-tail fashion to constitute a protofilament [161–165]; in cells, 13 protofilaments associate laterally to ultimately form a hollow MT tube of approximately 25 nm in outer diameter [166,167] (Figure 4 and Figure 5). Having a high persistence length –up to about 3 mm for tens of μm-long MTs - [168], MTs

are rigid filamentous structures. Early EM studies showed the existence of two possible MT lattice conformations: the “A-lattice”, which describes only heterotypic (α-β) inter-protofilament contacts, and the “B-lattice” [169]. In the latter, lateral contacts occur via adjacent α-tubulin - α-tubulin or β-tubulin - β-tubulin interactions (homotypic contacts). In the B-lattice, MTs show a helical symmetry, conferring a pitch to the tubulin subunits, represented by a rise of 3 tubulin monomers after one complete turn (3-start helix). This results in lateral α-β tubulin contacts at the “seam” [170,171], which are presumably weaker than the homotypic contacts (Figure 4 and Figure 5). The B-lattice has been shown to be the natural-occurring lattice conformation [170]. In *in vitro* reconstitution and polymerization assays with purified tubulin, MTs are usually constituted by 14 protofilaments, although it has been observed that this number ranges from 11 to 16 or even 17 [172]. Variation in the number of protofilaments has been observed even within the same MT [173,174], perhaps due to the flexibility of the lateral loops mediating the inter-protofilament interactions.

Dynamic behavior of microtubules

MTs are highly dynamic in order to quickly reorganize according to the needs of a cell. Due to the nature of the α-/β-heterodimer, MTs are polarized structures, and consequently their ends have different structural and functional characteristics. The end exposing the β-tubulin to the cytoplasm is termed the “ plus end” (from now on referred to as “+end”) and its polymerization rate is higher than the other end, called “ minus end” (from now on referred to as “ –end”), which exposes α-tubulin [175] (Figure 4 and Figure 5). The +end explores the cytoplasm and engages in interactions with other proteins, cellular structures and the cell cortex [176], whereas the -end is less dynamic and is usually embedded in nucleation centers [177].

MTs can grow and shrink repeatedly in a process termed dynamic instability [162,178] and they can therefore be considered to be in a continuous “search-and-capture” process where the ends are constantly “exploring” the cytoplasm of cells in “search” of other structures (e.g. kinetochores) that can be “captured” [179,180]. Dynamic instability is regulated by GTP hydrolysis in β-tubulin; the transition from MT growth to shrinkage, which eventually leads to protofilaments curling outwards, is called catastrophe, while the transition from shrinkage to a growth phase is called rescue. Growth and shrinkage rates, together with catastrophe and rescue frequencies, represent the four basic parameters describing MT dynamic behavior. MT dynamics would be a stochastic process without a regulatory system. Such system is represented by a large variety of MAPs, among which are also the so-called MT “+end tracking proteins”, or +TIPs, which specifically associate with the +ends of growing MTs (see section 2). +TIPs greatly influence MT behavior and, indeed, the +end is where much of the MT dynamics regulation takes place [180].

GTP hydrolysis and GTP cap model

A key feature needed for MT dynamics is represented by GTP hydrolysis at the inter-dimer interface. This interface is formed when the α-tubulin subunit of an incoming tubulin heterodimer establishes longitudinal contacts with the solvent-exposed E-site on the β-tubulin (bound to GTP) of another heterodimer, in a protofilament of the growing MT. After dimer incorporation into the elongating protofilament, GTP hydrolysis takes place [181], thereby leading to a MT lattice prevalently constituted by tubulin dimers with GDP at their E-sites, and a MT +end constituted by tubulin dimers still binding GTP, not yet hydrolyzed. However, studies with non-hydrolyzable analogues (such as guanosine-5’-[(α ,β)-methyleno]-triphosphate, or GMPCPP) suggested that GTP hydrolysis is not required for MT polymerization, but rather for its depolymerization

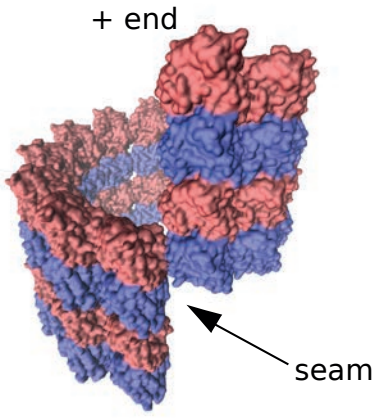

Figure 4. Computational reconstruction of an MT segment. 13 protofilaments interact laterally with a rise of 3 monomers after one complete turn (13-3 microtubule). Red: β-tubulin, blue: α-tubulin. The "seam", where heterotypic contacts take place, is clearly visible. The reconstruction was carried out by fitting in the cryo-EM density map (EMD-5193 (Sui and Downing 2010)) of a microtubule the minimized modelled dimer (exclusive of tails) and by performing the necessary symmetry operations. Figure generated with Chimera (Pettersen et al. 2004).

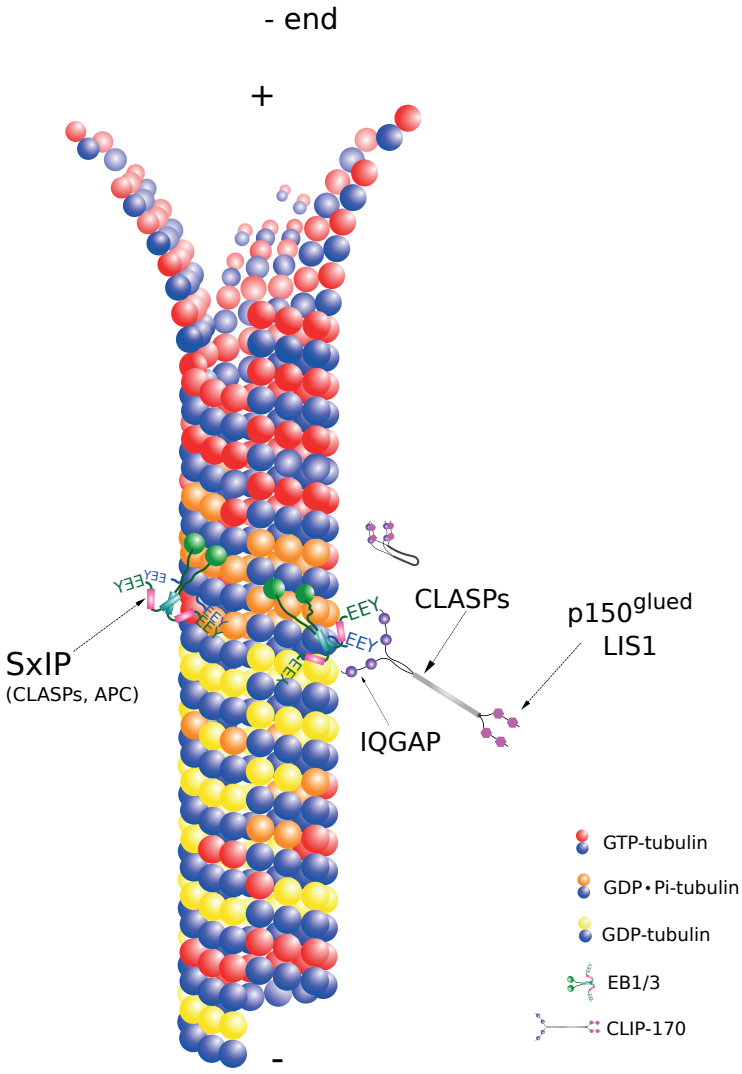

Figure 5. Schematic representation of a polymerizing MT. The "GTP cap" is represented by the GTP-tubulin dimers (red β-tubulin). The transition state GDP-Pi at β-tubulin is depicted in orange; EBs preferentially recognize and bind this state (Maurer et al. 2011, 2012, 2014), but can also dock onto GTP-tubulin (not shown in figure). Note that the calponin-homology domain (CHD, green sphere) contacts four tubulin monomers (2β-2α), except at the seam. The EEY terminal sequence is labeled at the C-terminus of EBs and of α-tubulin (blue tails and labels). SxIP motif-containing proteins bind EBs via the EB homology domain (EBH).The supposed interaction between CLIP-170 and EBs is also shown; note that the first CAP-Gly domain of CLIP-170 contacts the tyrosine of EBs (to which it has higher affinity), whereas the second CAP-Gly domain contacts the tyrosine of the α-tubulin tail. Some of the interacting proteins and binding regions are marked. The closed conformation of CLIP-170 while not engaged in any interaction is depicted in the background. "+" and "-" represent the plus- and minus-ends, respectively. More details and references for the interactions can be found in the section on +TIPs.

and for maintaining proper MT dynamics [182,183]. Also, Hyman *et al*. proposed that GTP hydrolysis could inhibit spontaneous MT nucleation, which instead occurred in the presence of GMPCPP [182]. Regarding the mechanical reason of depolymerization driven by GTP hydrolysis, Caplow *et al.* [184] showed that the free energy change derived from GMPCPP hydrolysis was almost zero in MTs, indicating that the MT lattice becomes thermodynamically unstable as the hydrolysis events take place within the MT. This energy, accumulated as strain in the lattice, is released during MT depolymerization. To counteract this energy release, since GTP hydrolysis occurs rapidly during polymerization, a model was proposed in which a stabilizing feature was present at the end of the growing MT. This "GTP cap" model [178] was suggested also in light of the long kinetic lag between tubulin polymerization and GTP hydrolysis [185]. Experimental evidence was provided by ultra-violet (UV) micro-beam cutting and micro-needle severing of single MTs: the new +end rapidly depolymerized, while the original remained intact [186,187]. Furthermore, it was proposed that a monolayer of GTP-tubulin would be sufficient to exert this protective effect against depolymerization [188], although it has also been suggested that up to 200 dimers could constitute the GTP cap [189].

Microtubule nucleation and nucleation centers in cells

MT nucleation, the formation of the first part of the MT through tubulin assembly, is a thermodynamically unfavorable process, which is believed to occur with at least a two-step mechanism [190,191]. The initial energetic barrier for tubulin polymerization and protofilament assembly is overcome via so-called MT nucleation-promoting complexes. In cells, this is the γ-tubulin ring complex (γ-TuRC), comprising γ-tubulin and γ-tubulin complex proteins (GCPs) [192,193]. The structure of the γ-TuRC complex is such that it can both provide the basis for the 13 PFs observed in cellular MTs, as well as for the B-type lattice. *In vitro*, MT nucleation occurs at pre-formed MT seeds (Note: seeds are short MTs, usually stabilized with taxol or GMPCPP, often used in *in vitro* assays as a template for MT growth). A recent study revealed a second energetic barrier for MT nucleation [191].

Using *in vitro* single-molecule assays it was shown that certain MAPs can stimulate or inhibit the rate of MT nucleation in the presence of nucleation-promoting complexes. Experiments showed that there was a kinetic barrier preventing MT nucleation; in fact, no MT nucleation was observed in a range of tubulin concentrations (4 μM to 6 μM) above the critical concentration (Cc, ca. 1.3 μM) for MT elongation, which was extrapolated from the fitting of the curve of growth rate in function of tubulin concentration (Note : in its simplest form the Cc is defined as $Cc=k_{off}/k_{on}$, where k_{off} is the dissociation rate constant of tubulin subunits from the MT and k_{on} the apparent association rate constant [191]). An increase in tubulin concentration to 15 μM resulted in nucleation of MTs from GMPCPP seeds in the absence of any MAP; decrease of the tubulin concentration to lower values (4 μM) was sufficient to maintain MT elongation after nucleation, but was insufficient to generate MTs in the absence of a growth-promoting MAP. Furthermore, catastrophe-promoting factors like MCAK (a MT depolymerase [194]) and EB1 [195], delayed the onset of nucleation, whereas anti-catastrophe proteins (such as Tpx2) and a processive MT polymerase, XMAP215 [196,197] (chTOG in human), shortened the time lag before observing MT nucleation. Therefore, MT nucleation does not occur with tubulin alone at low protein concentrations (1.3 μM - 6 μM), despite being above the Cc. Instead, anti-catastrophe factors are needed to overcome this second energetic barrier, thus playing a pivotal role in this process.

In cells MT nucleation occurs at MTOCs, where the MT nucleation-promoting complexes (i.e., γ-TuRCs) accumulate. In many cells the centrosome is the major MTOC [198,199], but

in differentiated animal cells (e.g. muscle cells, epithelial cells and neurons), the centrosome becomes inactive by losing proteins of the pericentriolar material (see below) - that re-localize e.g. to the cytoplasmic membrane or to the nuclear envelope - and non-centrosomal MT nucleation occurs [200,201]. Besides the centrosome, also the Golgi apparatus [202–206] or severed MTs [207,208] can act as nucleation sites.

The centrosome is composed of a pair of centrioles, which attract (and are therefore embedded in) pericentriolar material, composed of many different proteins [209]. The pair of centrioles is oriented perpendicularly (Figure 2), and each centriole consists of a set of 9 triplets of MTs organized in a cylindrical array. Centrioles have a relatively confined dimension, measuring about 0.5 μm in length and 0.2 μm in diameter [210]. It is unknown how this is regulated, but several proteins associate to centrioles to stabilize them. The protein CP110 is a strong candidate for this function: it localizes to centriole tips and its depletion leads to the formation of abnormally long centrioles; the excessive length makes them prone to fragmentation, thus allowing MT nucleation at multiple sites, ultimately originating abnormal mitotic spindles [211,212].

The centrioles not only organize the centrosome, being therefore required for chromosome segregation [200,213]; they are also necessary for ciliogenesis [200], a process leading to the formation of cilia and flagella, whose core, the axoneme, is made of MTs. Axonemes of primary (non-motile) cilia are composed of 9 MT doublets arranged radially [214,215]. This type of cilia is mainly involved in sensing extracellular cues and in activating the downstream intracellular signaling pathways [216]. Primary cilia are found, for instance, in the nasal cavity as olfactory sensors, and on luminal surfaces of renal tubules, biliary ducts, and vascular endothelial cells, as mechanosensors of fluid flow [217,218]. Axonemes of motile cilia and flagella are composed of 9 MT doublets surrounding two central MTs (“9+2 axonemes”) [215]. This type of structures are capable of performing regular beating through the action of the axonemal dyneins (see section *“Molecular motors”*), which are responsible for the sliding of adjacent MT doublets relative to each other [3,219]. Motile cilia and flagella allow the movement of fluid relative to the cell. For instance, motile cilia can be found on the ependymal cells lining the ventricles of the brain, to ensure cerebrospinal fluid flow by coordinated beating, and flagella allow sperm cell motility in a similar fashion [220]. Ciliogenesis is initiated by one centriole being tethered to the plasma membrane, known as basal body. This process involves an intricate network of several proteins playing a role in the initial docking of the basal body, but also in the elongation of the axoneme itself. Furthermore, cilia are dynamic structures that require a continuous supply of molecules for their maintenance; this is based mainly on transport, in which molecular motors play a pivotal role [220].

As stated above, centrosomes are not essential in all cells; many animal cells do not have them [200] as in the flatworm *Planaria,* which possesses centrioles to form the cilia, but not centrosomes [221]. Centrosomes do not exist in higher plants either. Mammalian oocytes lack centrosomes, and bipolar spindles can form in the vicinity of chromosomes [222]. This is achieved through a pathway that involves the small GTPase Ran and the action of MT motors and MT-bundling proteins [223]. As an example, one of the proteins involved in MT nucleation at this location is the protein Tpx2 [224,225], which serves as a stabilizing factor of early MT nucleation intermediates to promote MT nucleation in concert with the protein chTOG [226].

Microtubule-associated proteins

Regulation of MT behavior is essential for the proper orchestration of cellular activities. In fact, while a population of MTs can be probing the cytoplasm, another can be considerably less

dynamic. MTs can engage in interactions with target structures in order to re-localize them within the cell. MTs can perform such functions by virtue of their dynamic instability, which provides mechanical pushing/pulling forces during assembly or disassembly, respectively [227]. MTs also represent the “cellular tracks” onto which motor proteins with their cargos can dock and move. Several MAPs play a role in mediating and regulating these tasks. They can be broadly classified as structural MAPs, molecular motors, -end (“-end”) tracking proteins (-TIPs) and +end tracking proteins (“+ TIPs”), which specifically associate with -ends and +ends, respectively. +TIPs are particularly important for MT dynamic instability properties.

Structural MAPs

Structural MAPs, mainly found in neurons, were originally discovered by Murphy and Borisy in 1975 [228] as interacting factors during tubulin purification performed with repeated cycles of polymerization-depolymerization from brain lysates [229,230]. These MAPs tend to be elongated proteins with repeated domains that allow simultaneous interactions with multiple tubulin dimers [231], a characteristic that could be responsible for their MT-stabilizing role. They associate along the MT lattice during interphase and, upon entry in mitosis, they become phosphorylated. A kinase responsible for mitotic entry, Cdk1, is responsible for phosphorylation of β-tubulin, as well as of MAPs (such as MAP4), and molecular motors [232].

Phosphorylation decreases the affinity between the MAPs and the MTs [233,234] or reduces their MT-stabilizing activity [235]. As another example, the family of protein kinases MARK phosphorylates the proteins Tau, MAP2 and MAP4; overexpression of MARKs in cells leads to hyper-phosphorylation of these MAPs on KXGS (lysine-any amino acid-glycine-serine) motifs and to disruption of the MT array, resulting in morphological changes and cell death. [234]. Removal of phosphate groups from these proteins is achieved through phosphoprotein phosphatases (PPPs) such as PPP1, PPP2 and PPP3; removal of the phosphate groups reverses the effects induced by phosphorylation. The finely-tuned interplay between kinases and phosphatases is crucial in cells, and especially in neurons, as described very recently [236].

Although structural MAPs are normally associated with MT stabilization, a recent study [237] uncovered a new, important role for MAP1 proteins (MAP1A and MAP1S), which goes beyond their “classical” MT-stabilizing action. They observed that MAP1A and MAP1S interact with the HIV-1 capsid protein p24, mediating its trafficking towards the nucleus with a saltatory motion. Such behavior could involve detachment and reattachment to MTs using MAP1 proteins as anchor points [237]. MAP1-knockown cells showed an overall nuclear import defect, and an accumulation of viral capsids away from the nucleus [237]. Therefore, MAPs confer stabilizing properties to MTs, but they can also facilitate (at least in the case of MAP1A and MAP1S) HIV-1 early infection.

Another group of MAPs is represented by the “stable tubule only polypeptides” (STOPs), which confer MT resistance to cold. This effect is achieved through MT-binding motifs that can also simultaneously bind calmodulin, to which STOPs owe their regulation. Their function seems to be particularly important in neurons, since STOPs promote neuronal differentiation and are almost permanently associated to neuronal MTs; knock-out mice for these proteins displayed synaptic defects associated with neuroleptic-sensitive behavioral disorders, caused by a two-fold reduction in pre-synaptic vesicle density in CA1 hippocampal neurons compared to wild-type mice [238]. Behavioral abnormalities included disorganized activity, nurturing defects, anxiety-related behavior, inability to perform object recognition tests, and social withdrawal [238]. The wide range of effects suggested that the synaptic

defects were present throughout the brain, and not specific to some of its structures. However, STOP proteins are also present in other tissues [239]. In cycling cells, STOPs are localized on the mitotic spindle, whereas during interphase little localization on MTs is observed. This suggests that in dividing cells the role of STOP proteins is restricted to mitosis to ensure the fidelity of the process [239].

Given the interest in uncovering novel MAPs, or in quickly retrieving all the related information for those known, a new bioinformatic tool has been developed by Zhou *et al*., which is called MAPanalyzer [240]. It consists of a manually-curated database of all known MAPs and of a MAP prediction tool. The prediction of new MAPs is achieved through a combination of two separate components. The first one is the Basic Local Alignment Search Tool (BLAST)(https://blast.ncbi.nlm.nih.gov/Blast.cgi) [241], which identifies regions of local similarity between sequences of amino acid residues. The second component consists of machine-learning algorithms, trained on a subset of the database. It resulted that MAPanalyzer performed better than BLAST and another homology-searching tool, PSI-BLAST (Position Specific Iterated BLAST), when they were tested separately [240]. In fact, performance comparisons on the curated testing datasets indicated that the sensitivity of MAPanalyzer was higher at the different stringency thresholds used for benchmarking. This suggested that MAPanalyzer is a reliable tool for predicting novel MAPs.

Molecular motors

MTs represent the railways for long range cellular trafficking, but the actual movement of vesicles, organelles and other cellular structures is performed by proteins that are able to bind and move along MTs while binding their cargo at the same time. Motor proteins of the kinesins family (KIF) are mostly +end directed, although some exceptions exist (see *Kinesins* later). The major -end directed motor protein in cells is not a KIF member, but is cytoplasmic dynein-1 (see section *"Dyneins"*). At present it is thought that there are at least 45 mammalian *KIF* genes; however, alternative mRNA splicing can give rise to multiple KIF isoforms, possibly leading to twice as many KIF proteins [242]. Kinesins and dyneins convert the energy associated to ATP hydrolysis into movement along MTs through complex conformational changes in their motor domains.

Kinesins

Kinesins are elongated dimeric proteins with a MT-binding, globular domain with ATPase activity, which is mostly positioned at the N-terminus and is linked to a long intermediate domain (the "stalk"). Between the head and the stalk there is a linker region ("neck"), which has been shown to be important for the concerted, hand-over-hand movement of all kinesin motors; conformational changes occur in a nucleotide- and MT-dependent manner [243–247]. Finally, the C-terminal region is capable of binding adaptor proteins or directly their cargo. According to the location of the head domain, kinesins can be classified as N-terminal kinesins, C-terminal kinesins, or I-kinesins. In I-kinesins, such as the kinesin-13 family, constituted by KIF2A, KIF2B and KIF2C (MCAK) [248]), the head domain is located internally and the energy from ATP hydrolysis is used to depolymerize the MTs, rather than to transport cargos [249]. The N-terminal kinesins constitute the most abundant group of kinesins (at least 15, see [250]) and are mainly +end-directed motors, in contrast with C-terminal kinesins (at least three, see [250]), which are -end-directed [251]. One head domain of the dimer binds the MT when bound to ATP; subsequent hydrolysis results in a decreased affinity of the domain for the MT, leading to its detachment from the MT, movement "over" the other head domain (now bound

to the MT), and translocation to a next tubulin dimer (8 nm) on the MT lattice [252–255]. At this point, exchange of ADP for ATP increases the affinity of this head domain for the MT, and the cycle starts again for the other head domain. These concerted motions allow the motor protein to processively "walk" with a hand-over-hand mechanism on MTs [256]. It has been observed that kinesins can perform hundreds of steps before dissociating from the MT, even in the presence of a load from an optical trap [252,257–259].

It should be noted that not all kinesins follow the paradigm "N-terminal head – +end directionality". For instance, the kinesin-5 *S. cerevisiae* homolog, Cin8, despite having an N-terminal head domain, moves towards the -end at high ionic strengths and towards the +end at low ionic strengths [260,261]. Directionality and processivity seem to be dictated by the neck linker and its interactions with one of the ATP-bound head domains, orienting the other (ADP-bound) towards the +end, and so on (reviewed in [263]). It was recently found that phosphorylation in the catalytic site increased velocity and promoted -end directionality, and decreased the binding affinity between MTs and the motor domain [262].

Dyneins

Dyneins are large motor proteins: the –end-directed human cytoplasmic dynein-1 complex (referred to as "cytoplasmic dynein-1"), for instance, is approximately 1.4 MDa in molecular weight [19,264]. The first dynein was identified in *Tetrahymena pyriformis* in 1963: it was the first MT-associated ATPase capable of force generation to be described [265]. Dyneins can be classified in cytoplasmic and axonemal dyneins; the former is involved in cargo transport, including mRNA, mitochondria and vesicles [266,267], whereas the latter is responsible for generating the beating forces in cilia and flagella [264]. Dyneins are complexes formed by heavy, intermediate and light chains. Due to their large size, it has been difficult so far to determine their complete structure. However, it is known that the core of cytoplasmic and axonemal dyneins is formed by a homodimer of heavy chains (approximately 500 kDa each in molecular weight), whose conserved C-terminal regions contain the AAA (ATPase Associated with diverse cellular Activities) domains necessary for the ATPase function [268]. More specifically, 6 AAA domains are organized into a ring structure, stabilized by an N-terminal stalk structure folding on it; the stalk is also necessary for interactions with the cargo [269,270]. The interaction with the MT is mediated by a stem emerging from the "ATPase" ring; the propelling force is expressed through the movement of the stem via conformational changes in the AAA-ring following ATP hydrolysis [271].

Dynein cargo specificity is determined by the intermediate and light chains. Specifically, the intermediate chains contain WD repeats that are responsible for the interactions with $p150^{glued}$ [272,273], the largest of the 11 subunits of the dynactin complex [274]. This large complex (approximately 1 MDa in molecular weight) is one of the cofactors of cytoplasmic dynein, and is capable of binding different cargos, thus serving as an "adaptor" complex between cargo and dynein [274,275]. This function is crucial in cells, since only one dynein is responsible for cytoplasmic MT -end-directed transport and mitotic processes [276]. The affinity of dynein for $p150^{glued}$ is modulated by the dynein intermediate chain phosphorylation status [272,273]. The importance of dyneins can be exemplified in neurons. In these cells defects of cytoplasmic dynein motility, or disrupted interactions between cytoplasmic dynein and its adaptor proteins, are linked to neurodegeneration as a consequence of the impaired retrograde axonal transport (reviewed in [277]).

Cytoplasmic dyneins can be further divided in two subclasses: dynein-1 and dynein-2. The former is involved in -end –directed cargo transport along cytoplasmic MTs and is involved

in a number of processes, such as karyokinesis, cytokinesis [278] and maintenance of the Golgi apparatus [279]. The latter, instead, takes part specifically in retrograde intraflagellar trafficking [280,281], with roles in the assembly and maintenance of cilia and flagella [282]. Cytoplasmic dyneins are characterized by a processive motion along MTs just like the kinesins (see section 2.2.1); however, contrary to kinesins, the precise mechanism of dynein processivity is yet to be elucidated. Recent studies indicated that the motions of the two heads are almost independent of each other [268,283], except when they are further apart, when a tension-driven mechanism seems to induce coordinated stepping along the MT [284].

Axonemal dyneins, on the other hand, are responsible for the bending of cilia and flagella (described in section 1.4.4). Axonemal dyneins bridge adjacent MT doublets of the axoneme, using one of these as a track onto which their motor domains can slide, and the other one as a stably-bound cargo [219,264]. The sliding of MT doublets is counteracted by other axonemal components, resulting in bending. There are two types of axonemal dyneins in the axoneme, classified according to their location: inner-arm dyneins, facing the axoneme lumen and located every 96 nm, and outer-arm dyneins, on the opposite side and spaced by 24 nm. The outer-arm dyneins are particularly important for generating the proper beat frequency [264], The processes leading to this specific arrangement of dyneins and to the coordination of the beating motions are still largely unknown. Given the roles presented, dyneins can be seen as ubiquitous proteins ensuring proper cell functionality.

Minus-end tracking proteins (-TIPs)

-TIPs are a class of MAPs which has not been extensively studied yet. MT - ends are often clustered and embedded in nucleation structures (such as the centrosome); therefore, it is difficult to study the properties of individual MT -ends by light microscopy. Until recently, the only structure known to associate to -ends was the γ-TURC [285]. Recently, it was shown that proteins belonging to the CAMSAP/Patronin/Nezha family also specifically bind MT -ends and regulate their dynamics, mainly by preventing tubulin incorporation and by protecting them against kinesin-13-induced depolymerization [286–288].

CAMSAPs (calmodulin-regulated spectrin-associated proteins), include three homologues, CAMSAP1, CAMSAP2 (KIAA1078/CAMSAP1L1) and CAMSAP3 (KIAA1543/Nezha), These proteins are characterized by the presence of a common domain, called CKK (“C-terminal domain common to CAMSAP1, KIAA1078 and KIAA1543”, also known as domain of unknown function DUF1781) [287]. At their N-terminus, these proteins have a calponin homology domain (CHD), found also in other actin and MT-binding proteins [289]. However, the CHD of CAMSAPs does not interact with any cytoskeletal structure. Instead, for CAMPSAP1, the CKK domain interacts only weakly with the -end of MTs, and more strongly when together with its third coiled-coil and its preceding unstructured linker region. CAMSAP2 and CAMSAP3 bind and stabilize the MT lattice via an additional MT binding domain located in the unstructured region between the second and the third coiled-coil. In particular, CAMSAP3 is the most potent -end growth inhibitor and MT-stabilizing protein among the members of this family; this effect is due to an additional MT binding domain located between the third coiled coil and the CKK domain.

CAMSAPs bind to dynamic or static MT -ends, and fluorescently-tagged CAMSAPs (especially CAMSAP2 and CAMSAP3) have been seen to accumulate stably (with a low turnover rate) as dots at the tip of MT -ends *in vitro* [290]. CAMSAP1 associates to -ends only transiently, in contrast to CAMSAP2 and CAMSAP3, which instead remain associated to the MT lattice once deposited on the newly-polymerized MT at the -end. Previous studies

indicated that the main function of CAMSAPs is to stabilize the -ends of free or non-centrosomal MTs: in fact, depletion of CAMSAP2/3 led to a decrease of non-centrosomal MTs. Moreover, CAMPSAPs could play a central role in the stabilization of MTs soon after the γ-TURC-initiated nucleation phase (reviewed by [290]). Further investigations are needed to elucidate whether other –TIPs exist and, if so, what roles they may play.

Plus end tracking proteins (+TIPs)

+TIPs are a subset of MAPs that are crucial for the regulation of MT dynamics. The first protein of this class, CLIP-170 (encoded by the *CLIP1* gene), was discovered by Perez *et al.* in 1999 [291]. It was proposed that this endosome-MT linker could specifically recognize the "structure of a segment of newly polymerized tubulin", as GFP-CLIP-170 fluorescence was visible as "comet-like" dashes at the ends of growing MTs [291]. Since then, more than 20 +TIPs have been identified [292]. Although structurally and functionally heterogeneous, they all recognize and bind growing +ends. One feature that characterizes +ends is the so-called "GTP-cap" (see section *"GTP hydrolysis and GTP cap model"*); it has been suggested that +TIPs can recognize and bind this region with higher affinity than the rest of the MT lattice due to specific conformations present in the cap (see Figure 5 for a schematic and simplified representation). *In vitro* reconstitution assays revealed that the protein EB1 can recognize and bind specifically GTP-loaded +ends because it is able to "sense" the nucleotide state of the tubulin heterodimer within the MT wall [293]. In agreement with these observations, EBs show affinity for MTs assembled from GTP-γ-S, a nucleotide analogue with a conformation that mimics GTP in the transition state GDP-Pi [294,295].

+TIPs can be classified in 4 groups according to structural characteristics and mode of binding to MT ends: EB proteins (EB1, EB2 and EB3), CAP-Gly proteins (including CLIPs, $p150^{glued}$, CEP350, and others), SxIP motif-containing proteins (e.g. CLASPs, APC, MCAK, STIM1, Navigators, KIF18B, SLAIN2, and others), and the TOG domain-containing protein chTOG [296,297].

End-binding (EB) proteins

Mammalian EB proteins (EBs) belong to a family comprised of three members: EB1, EB2 and EB3 [298]. EBs are crucial in interphase as well as mitosis [299]. Interestingly, they not only mediate interactions between MT ends and other structures, but can apparently also associate with the actin cytoskeleton [300–302]. Furthermore, overexpression of EB1 in mouse MAP-1B-deficient hippocampal neurons was shown to compensate for the detrimental lack of MAP-1B during axonogenesis, suggesting that EB1, when overexpressed, can stabilize MTs [303].

EBs are generally homodimers of 64 kDa, but EB1 and EB3 can also heterodimerize [304]. While EB2 expression varies across different cell lines, EB1 is ubiquitously expressed, and EB3 is preferentially expressed in the central nervous system [305]. The N-terminus of EBs is a calponin-homology domain (CHD) which interacts directly with the surface of the MT. The CHD is followed by a disordered linker region, which connects the CHD to the C-terminal coiled coil domain; the latter mediates dimerization. At the end of the coiled-coil is the so-called EB-homology domain (EBH), which engages in interactions with SxIP motifs present in other +TIPs (such as CLASPs, described later). Following the EBH there is a flexible C-terminal tail of about 25 residues; the last residues (DEY in EB3 or EEY in EB1; note: the EEY sequence is present also at the C-termini of α-tubulin) interact with CAP-Gly domain-containing +TIPs (such as CLIPs, see later). EBs are capable of performing autonomous +end tracking, meaning that they do not require additional proteins to track +ends [195]. EBs are, together

with the TOG-domain proteins (see section 2.4.3) the only proteins capable of autonomous +end tracking to date. Since their discovery, a growing number of proteins interacting with EBs has been identified; virtually all +TIPs require EBs to perform MT +end tracking [297]. This has obvious important consequences on the organization and regulation of the cytoskeleton, and disruptions of interactions between EBs and other +TIPs would therefore be detrimental for the cell. Therefore, given the independent +end tracking ability of EBs and the multitude of interacting proteins, EBs are often classified as "core +TIPs" (for review, see [297]).

Cryo-EM studies with the EB1 *Saccharomyces pombe* homolog Mal3 led to a pseudo atomic model for the interactions between the CHD and the MT [293]. The CHD contacts 2 adjacent α- and 2 adjacent β- tubulin subunits in the MT lattice but not at the MT seam (where there are α/β lateral contacts) (Figure 3). Importantly, the CHD contacts the helix H3 of one β-tubulin, which is directly connected to the E-site, allowing it to "sense" the nucleotide state [293]. Recent very high-resolution (3.5 Å or better) cryo-EM studies of MTs together with EB3 [306], provided improved structural information. EB3 was found to promote inter-dimer longitudinal compaction; the closer distance of the residue E254 in helix H8 of α-tubulin (hypothesized to catalyze GTP hydrolysis, as discussed in **Chapter 3**) to the GTP in the E-site would promote GTP hydrolysis and therefore the MT maturation, as previously suggested [307]. Also, it could explain the catastrophe-promoting activity *in vitro* [191,308]. This mechanism could also be an explanation for the observed enhanced nucleation and sheet closure ability of EB1 [308].

However, a recent study reported that EB1 inhibited nucleation [191]. This apparent discrepancy can be explained by considering the differences in (i) the type of assays used, and (ii) the different concentrations of tubulin and EB1. In fact, the former study used turbidity as a measure of MT nucleation, whereas the latter used a TIRF microscopy-based assay. Second, the EB1 concentration used by Vitre *et al.* was 1.5 μM, whereas it was 200 nM in the study by Wieczorek; similarly, Vitre and colleagues used 45 μM or 90 μM of tubulin in their study, whereas Wieczorek and colleagues used concentrations of tubulin ranging from 0 to 20 μM. At high concentrations EB1 not only binds the +end, but also the MT lattice, inducing a stabilizing effect. This, in turn, would promote rescues and nucleation events [308]. However, Wieczorek and colleagues observed that even when decreasing EB1 lattice binding by increasing the ionic strength of the assay buffer, the outcome remained unchanged. Nevertheless, it can be concluded that EBs, by virtue of their sheet closure ability (observed by electron microscopy by Vitre and colleagues), are able to induce faster GTP hydrolysis and thus higher catastrophe frequencies. In turn, this would represent an obstacle for MT nucleation, as found by Wieczorek and colleagues, at lower tubulin concentrations. Other experimental set-ups would perhaps allow a more direct comparison and an easier interpretation of the results.

In a recent study [309], high-resolution *in vitro* experiments with TIRF microscopy showed that, upon tubulin dilution, longer EB-covered regions ("EB caps") correlated with an increased MT stability. This was in line with previous observations [293], in which the size of the EB binding region was found to decrease before catastrophe. In particular, Duellberg *et al.* [309] provided evidence, for the first time after the original proposal in 1984 [178,310], that faster-growing MTs possess longer protective "caps", which stabilize MTs and prevent them from undergoing catastrophe. Thus, EBs are not only indispensable "core" +TIPs ensuring proper localization of other +TIPs on MTs; *in vitro* studies show that EBs also influence MT dynamics *per se*, by increasing growth rates, and rescue and catastrophe frequencies; moreover, they can promote MT sheet closure and MT stability, the latter by "capping" the +ends. Finally, EBs alone would play an inhibitory role on MT nucleation at concentrations of about 200 nM with tubulin concentrations up to 20 μM (the latter presumably similar to that found in cells [311]). The diversity in functions and effects of EBs suggests complex regulatory

mechanisms.

CLIPs

Cytoplasmic Linker Proteins (CLIPs) comprise CLIP-170 (of 170 kDa) and CLIP-115 (of 115 kDa). CLIP-170 was first discovered in HeLa cells in 1990 [312] as a generic “170K protein”. The discovery was achieved using an antiserum raised against a microtubule-binding protein from HeLa cells. This protein (later named CLIP-170) was proposed to be involved in linking MTs to endocytic vesicles and was found to interact with MTs via a domain, the N-terminal CAP-Gly domain (cytoskeleton-associated protein glycine-rich), that was found to be present also in Blk1 in yeast and in the protein Glued in *Drosophila* [313]. Affinity-purified antibodies against this protein used in immunofluorescence showed a significant accumulation at the distal ends of MTs: it was the first +TIP to be identified, in 1999 [291].

CLIP-170 is an elongated dimer; two CAP-Gly domains (per monomer) are responsible for the interactions with tubulin via GKNDG residues that are the hallmark of the CAP-Gly domains. Structural studies revealed that the shallow, positively-charged grooves in the CAP-Gly domains harbor the GKNDG residues, which contact the EEY C-terminal residues of α-tubulin and EB1 [314,315]. In particular, it has been shown that the second CAP-Gly domain (more towards the C-terminal) has a higher affinity than the first for the EEY tail of α-tubulin and EB1, leaving the first CAP-Gly domain available for electrostatic interactions with the tail of β-tubulin. This would explain the even higher affinity for the tubulin dimer when both domains are in tandem [315]. The CAP-Gly domains in CLIP-170 are surrounded by three serine-rich regions which can modulate the binding to MTs [316]. Despite their high sequence similarity, it was shown that the two domains are not equivalent. The second CAP-Gly domain possesses a more basic groove than the first, and therefore the binding to the negatively charged terminal residues of EB and tubulin is enhanced [315]. This is in line with the observations by Gupta *et al.*, who identified the second CAP-Gly domain, together with the third serine-rich stretch, as the minimal +end tracking unit in cultured cells and as nucleation/elongation factor *in vitro* [317]. Nevertheless, for optimal +end tracking a combination of CAP-Gly domains and three serine-rich stretches is required [317].

The central region of CLIP-170 is predicted to be a long coiled-coil mediating dimerization and causing the elongated shape of the protein; two zinc-finger domains (“zinc knuckles”), located at the C-terminus, can interact with other CAP-Gly-containing proteins (such as the dynactin $p150^{glued}$ subunit) or with the N-terminal CAP-Gly domains of the same protein. This interaction leads to a folding-back of CLIP-170, resulting in a “closed” conformation [314,316] that cannot interact with MTs or other proteins. Interestingly, the binding determinants are the same basic grooves and the GKNDG motif involved in the interactions with tubulin, EB1 or $p150^{glued}$ [318].

The +end-tracking ability of CLIP-170 relies on composite sites formed by the EEY motifs in EBs and tubulin [319]. Importantly, this implies that CLIP-170 requires tyrosinated tubulin in order to bind MT ends; in a model proposed by Ligon and colleagues, CLIP-170 could interact simultaneously with one EB dimer and one tubulin dimer, thus forming a “co-polymerization complex” directed at the tip of the polymerizing MT [320].

CLIP-170 is present in many tissues, with highest mRNA expression in muscle, liver, testis and brain. CLIP-170 was found to be essential for spermatogenesis, as knock-out mice for *Clip1* were viable and apparently normal, but sub-fertile [321]. CLIP-170 interacts at its C-terminus with different proteins, for example LIS1, which has been suggested to mediate the recruitment of the cytoplasmic dynein on MTs [322]. In macrophages, CLIP-170

is necessary for phagocytosis via its direct interaction with mDia1, a protein promoting actin nucleation; in this way, CLIP-170 plays an important role in actin cytoskeleton remodeling during phagocytosis [323]. This cross-talk with the actin cytoskeleton through mDia1 has been recently confirmed using *in vitro* reconstitution assays and TIRF microscopy [324]. In fact, it was observed that from CLIP-170-mDia1 complexes at the growing MT +ends, actin nucleation was about 18 times as fast as free barbed-end-growth of actin filaments [324]. In addition, knock-down experiments of *Clip-170* in rat primary cortical neurons led to a reduction in neuronal processes. Expression of a full-length, wild-type CLIP-170 rescued this phenotype. Thus, CLIP-170 was found to be necessary for proper dendritic morphology and its association with mDia1 was suggested to be crucial. Our group has reported that MT dynamics is affected in CLIP-170-deficient hippocampal neurons [325], suggesting that a combined MT/actin defect may underlie neuronal dysfunction.

CLIP-170 is also involved in cellular polarization. Its direct interaction with IQGAP1 links it to Rac/Cdc42 at the cell cortex of the leading edge, driving the polarization process [326]. Finally, CLIP-170 also interacts with CLASPs, which will be discussed later in this section (Figure 3). The observation that *Clip1* knock-out mice showed only spermatogenesis defects raises questions as to why depletion of such an important protein does not cause a more severe phenotype, in particular in the brain. This could be justified by the existence of a close homologue of CLIP-170, CLIP-115, whose functions (at least as a rescue factor in cells and *in vitro* experiments) have been suggested of being redundant with those of CLIP-170 [327].

CLIP-115 is the closest homologue of CLIP-170. It is expressed preferentially in the brain and is capable of performing +end tracking in the presence of EBs [328]. CLIP-115 shares about 30% of overall identity in primary sequence with CLIP-170; however, its two CAP-Gly domains share a much higher degree of identity (79% for the first CAP-Gly domain, 95% for the second). The CAP-Gly domains, surrounded by serine stretches, are followed by a shorter coiled-coil domain; the C-terminus lacks the Zn knuckles present in CLIP-170 [329]. Knock-out mice for *Clip2* (i.e. the gene encoding CLIP-115) display characteristics similar to those of patients with Williams Syndrome (WS), which is caused by a hemizygous deletion of a chromosomal region of about 1.6 Mb on chromosome 7, encompassing at least 17 genes including *CLIP2* [330,331]. WS is a developmental disease leading to a multitude of defects, including cardiovascular abnormalities, unusual facial features, mental and statural deficiency, characteristic dental malformation, and infantile hypercalcemia [330,332]. The behavioral and neurological characteristics include poor spatial perception, lack of fear, and coordination problems. In line with these features, *Clip2* knock-out mice showed growth deficits and mild brain malformations, including a larger brain-ventricle volume and a smaller corpus callosum when compared to wild-type mice. Behavioral tests indicated also mild motor coordination defects, as well as affected hippocampal-dependent memory processes, together with a lower synaptic plasticity in the hippocampus [333].

In a study by Komarova *et al.* [327], an engineered CLIP-170 protein was expressed in CHO cells. This engineered protein ("Δhead-CLIP-170") lacked the MT-binding, N-terminal region comprising the two CAP-Gly domains and the surrounding basic sequences. However, the coiled-coil region required for dimerization and the C-terminal region (involved in interactions with $p150^{glued}$ and other proteins) were still present. Overexpression of this Δhead-CLIP-170 reduced the +end decoration of endogenous CLIP-170 and CLIP-115, while it increased their cytoplasmic accumulation. Ablation of CLIPs from MT +ends was accompanied by a seven-fold reduction in rescue frequency. Conversely, when constructs coding for the head domain only and for the Δhead-CLIP-170 were microinjected in cells (in a 10:1 molar ratio, respectively),

rescue frequencies were restored to levels comparable to control cells. It was concluded that CLIPs were able to promote rescues and that this property could be ascribed to their "head domain", composed of the two CAP-Gly domains and surrounding basic amino acidic stretches [327]. However, the properties of CLIP-115 alone have never been investigated, mainly because of its high similarity to CLIP-170 and the supposedly redundant roles that the two proteins seemed to share. A thorough examination of CLIP-115 will be made in **Chapter 4** of this thesis, in which we aim at understanding whether CLIP-115 and CLIP-170 truly have redundant functions.

CLASPs

Cytoplasmic linker associated proteins (CLASPs) were initially identified as CLIP-interacting proteins using a yeast-two-hybrid assay. The most conserved region of the coiled-coils of CLIP-170 and CLIP-115 is the 300 residue-long, N-terminal portion, which was used as "bait" in the assay [334]. Two *CLASP* genes exist in mammals: *CLASP1* (ubiquitously expressed) and *CLASP2* (enriched in the brain). "Long" protein isoforms generated by both genes, about 170 kDa in molecular weight, were named CLASP1α and CLASP2α. *CLASP2* can be alternatively transcribed by using different start sites to yield shorter isoforms, of about 140 kDa, named β- and γ- isoforms [334]. In the fission yeast *Schizosaccharomyces pombe,* the CLASP ortholog Cls1p is a thin and elongated protein. Cls1p dimerizes via its C-terminal coiled-coil domain and is able to "wrap" around a tubulin dimer [335]. Conversely, human CLASP2α was found to be predominantly present in monomeric form [336], although size-exclusion chromatography experiments also revealed the existence of CLASP dimers, indicating that both forms are possible in solution [337].

The N-terminus is the region that varies the most across the isoforms. The "α" isoforms (Figure 6) contain two TOG (tumor overexpressed gene) and one TOG-like (TOG-L) domains (TOG and TOG-L domains are explained below) [337] that are responsible for tubulin binding [335]. The β/γ isoforms, instead, lack the first TOG domain and therefore contain only two TOG domains [337]. Moreover, CLASP2β (which is brain specific) has an N-terminal palmitoylation sequence that mediates anchoring to membranes and that is not present in the other isoforms [334].

TOG domains are flat, straight paddle-like domains capable of binding tubulin along their thin edge. They consist of approximately 220-250 residues, organized in 12 α-helices consecutively paired in six HEAT repeats (Huntingtin, Elongation factor-3, A subunit of PR65, Tor-kinase repeats) [338,339]. Intra-HEAT loops on one face of the TOG domain directly contact one tubulin dimer [340]. Arrays of five TOG domains are present in the MT polymerase XMAP215/chTOG; binding in tandem of these arrays to tubulin dimers greatly enhances the MT polymerization rate [335,340,341]. In their structural studies on TOG domains of the XMAP215 family in *Drosophila* and yeast, Slep and colleagues noted the presence of discontinuous tubulin-binding determinants in two conserved central regions of the CLASP family that bore sequence similarity to TOG domain intra-HEAT loops. These conserved regions were termed "cryptic TOG-L domains" [339]. Subsequent structural studies revealed that the first TOG-L domain of human CLASP1α conforms to the "classical" TOG domain, whereas the second showed structural differences. In fact, this TOG-L (TOG-L 2) domain is curved, in contrast to the straight, flat surface as in the XMAP215 (chTOG) family [342]. Nevertheless, the authors suggested that the TOG-L2 is a *bona fide* TOG domain, given its remarkable similarity in tertiary structure to TOG domains; therefore it will be referred to as TOG2 [342].

Recently, an arched conformation was also found for the TOG domains of CLASP2α

[343]. It has been proposed that the different curvature of the TOG domains could serve as a way for CLASPs to discriminate between the tubulin states and therefore promote MT assembly and rescues [343]. In particular, the latter would be achieved through the association of the curved TOG domain to depolymerizing, curved protofilaments. Experiments with *Xenopus laevis* egg extracts showed that the TOG domains mediate MT binding, also in egg extracts immunodepleted of EB1, but failed to track +ends [337]. An interesting observation can be made at this point. The binding interface of the TOG domains with tubulin (Figure 7B and Figure 7C) strikingly overlaps with that of stathmin, a MT-depolymerizing and tubulin-sequestering protein that binds two consecutive tubulin dimers (Figure 7A) [344–346]. It is therefore tempting to speculate about a competition between CLASPs and stathmin. Tubulin dimers in the soluble cytoplasmic pool could be CLASP-bound in order to be incorporated into polymerizing MTs (according to the model by Al-Bassam *et al.* [335]) or stathmin-bound to prevent assembly.

C-terminal of the second TOG domain (for the α isoforms; after the first TOG domain for the β/γ isoforms), a serine/arginine-rich (SR-rich) region (residues 512-650 of CLASP2α) is subject to phosphorylation by the glycogen synthase kinase 3β (GSK3β), discussed later in this section. The SR-rich region is important for MT binding but especially for +end tracking [347], and contains two consecutive SxIP motifs for interactions with EBs at the hydrophobic groove in the EBH [296]. Most of the similarity between CLASP1α and CLASP2α (77% identity in primary structure) resides in this SR-rich region and in the C-terminal coiled-coil domain. This domain (residues 1171-1463 of CLASP1α) is mainly responsible for binding proteins, such as the CLIPs and LL5β, the latter mediating interactions with the cell cortex [205,348].

The MT binding ability of CLASPs relies mainly on electrostatic interactions involving the acidic C-terminal tail of tubulin. However, *in vitro* experiments showed that MTs subjected to cleavage of the tubulin tail with the protease subtilisin retained their ability to interact (to a lower extent than under non-treated conditions) with CLASPs. This indicated that additional interactions occur between CLASPs and the globular domain of tubulin subunits within the MTs [337].

The SR-rich region of CLASP2α (residues 512-650) contains nine serine residues (conserved also in CLASP1α), which constitute two consensus motifs (S/T-x-x-x-S/T) [349] for glycogen synthase kinase 3β (GSK3β) phosphorylation [350]. It has been suggested that this kinase has more predicted substrates (over 500) than any other kinase [351]. Among the experimentally-validated substrates, there are MT-associated proteins such as APC [352], the von Hippel-Lindau (VHL) protein [353], Tau [354], MAP1B [355], and CLASP2 [350,356,357]; it has been proposed that GSK3β negatively regulates MT-associated proteins via phosphorylation [358]. Indeed, phosphorylation of CLASP was found to disrupt its binding to MTs in cells [334]. In addition, when an EGFP-CLASP2 mutant construct (coding for the +end tracking domain (residues 512-650) and with the serines mentioned above mutated to alanines) was expressed in HeLa cells, the fluorescence intensity at the MT +ends was higher than the cells expressing the control construct. The fluorescence intensity decreased upon expression of a phosphomimic construct, with serines mutated to aspartate residues, similarly to what had been observed in cells expressing a constitutively active GSK3β (GSK3β(S9A)) [350]. It was found that the first SxIP motif is particularly important for the +end tracking ability, and phosphorylation of both motifs abolishes this, as well as MT binding. This indicated that CLASP2 behavior can be modulated according to the GSK3β-dependent phosphorylation status. It was later shown that phosphorylation of the same motif (in the context of a peptide including the first SxIP motif) directly controls binding to EB1, with the non-phosphorylated motif having an affinity 5-fold higher than the mono-phosphorylated peptide.

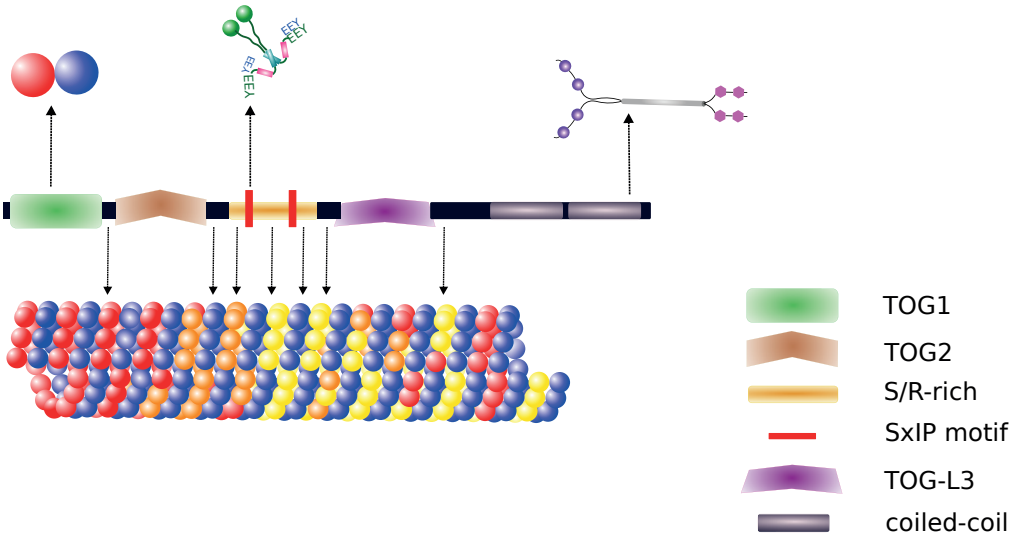

Figure 6. Domain organization of CLASPs and their interactions. Schematic representation of the α isoforms of CLASPs. Arrows represent interactions between the specific regions of CLASPs and some of the main interaction partners (tubulin dimer, EBs, MTs and CLIP-170 as represented in Figure 3). Note the multiple interactions between the MT lattice and the TOG domains, together with the positively-charged residues C-terminal of the TOG domains and within the S/R-rich region (Maki et al. 2015).

The underlying mechanism was elucidated by molecular dynamics simulations together with NMR spectroscopy; it was found that phosphoserine residues in the +end tracking domain of CLASP2α, immediately following the first SxIP motif (Ser-Lys-Ile-Pro, residues 728-731) could establish intra-molecular salt bridges with neighboring arginine residues, subtracting them from the interactions otherwise occurring with the C-terminal glutamates of EB1 [359]. On the other hand, phosphorylation of the second motif could inhibit MT binding, possibly by inducing a conformational change of CLASP. In fact, the second motif has a low affinity for MTs on its own [360] and thus it would be more likely to promote MT binding indirectly [350]. In migrating HaCaT keratinocytes, clusters of lamella MTs decorated with CLASP2 were associated to focal adhesions, possibly affecting them; this could be dependent on CLASP2 phosphorylation status, as GSK3β inhibition disrupts focal adhesion dynamics [361]. GSK3β has also been shown to be involved in the regulation of acetylcholine receptors (AChR) delivery at the post-synaptic neuromuscular junction (NMJ) by acting on CLASP2γ, the only isoform expressed in muscle [356]. In fact, expression of a construct coding for a phosphoresistant form of CLASP2 (with the nine serines mutated to alanines, as described earlier) promoted MT capture at AChR clusters and increased cluster size. Conversely, expression of the phosphomimic construct (serines to aspartates) reduced MT capture and cluster size, indicating a crucial role of this kinase at the NMJ, together with CLASP2γ expression levels [356].

CLASPs play a role in stabilizing MTs in proximity of the cell cortex by promoting rescues and inhibiting catastrophes [335,347], and at mitosis localizing at kinetochores and mediating their attachment to MTs [362]. A similar rescue-promoting role was found also for the *Schizosaccharomyces pombe* CLASP ortholog, Cls1p [363]. Studies in mitotic *Drosophila* cells showed that MAST/Orbit (the CLASP ortholog in this organism) is crucial for maintaining the length of kinetochore fibers (K-fibers, the MT bundles anchoring the kinetochores to the spindle poles) constant after their formation, contributing to proper chromosome motion.

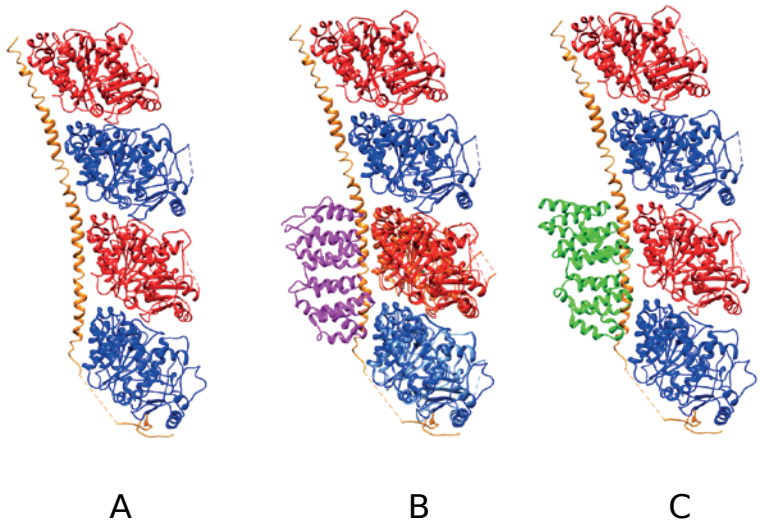

Figure 7. Comparison of TOGs-tubulin and stathmin-tubulin binding interfaces. (A) Structures of two tubulin dimers (cartoon representations) in complex with a stathmin-like domain (orange) (PDB: 1SA0 (Ravelli et al. 2004)). α- and β-tubulin are colored in blue and red, respectively. (B) Structure of the "classical" straight TOG2 domain (magenta) of the *Saccharomyces cerevisiae* Stu2p protein, ortholog of the XMAP215/chTOG MT polymerases, bound to a tubulin dimer (PDB: 4U3J (Ayaz et al. 2014)). The α-subunit (light blue cartoon) of this complex was aligned to the α-tubulin of the structure 1SA0 (dark blue cartoon) across their α-carbon traces to compare the overlapping binding interface. (C) Similarly, the α-carbon trace of the TOG2 domain (green) of human CLASP2 (PDB: 3WOY (Maki et al. 2015)) was aligned with the TOG2 domain of Stu2p, in magenta in Figure 5B. Note the arched conformation compared to the TOG2 domain of Stu2p, as well as its overlap at the tubulin-binding interface with the stathmin-like domain (orange). Figures generated with Chimera (Pettersen et al. 2004).

This is achieved due to the balance between the continuous addition of tubulin dimers at microtubule +ends (linked to the kinetochore) and their removal at the -ends within the pole. This phenomenon is termed "MT poleward flux" [364] and was completely lost in S2T *Drosophila* cells lacking MAST/Orbit, thus revealing a role of utmost importance for CLASPs [365]. Depletion of both CLASPs in HeLa cells leads to spindle defects, metaphase delay and abnormal exit from mitosis [362], but also to defects in interphase, such as decreased density of the MT network, increased MT growth rate, decreased rescue frequency, and longer (>1 μm) depolymerization events at the cell edge [347]. During neuronal development in mouse, CLASP2 expression increases steadily and it localizes preferentially at the growth cones of neurites. Knock-down experiments for CLASP2 in primary neurons showed that axons and dendrites were shorter than in wild-type; overproduction of CLASP2 led to the formation of multiple axons, enhanced dendritic branching, and Golgi condensation, highlighting its importance in neuron morphogenesis and polarization [366]. However, in another study CLASP2-depleted neurons displayed enhanced axon growth and reduced dendrite branching, whereas CLASP1 depletion had little effect [367]. Additionally, knockdown of all isoforms of *GSK3* impaired axon growth. This effect was reversed by knocking down *CLASP2*, indicating that CLASP2 is the major GSK3 target for axon growth inhibition. On the other hand, depletion of GSK3 increased branching in a CLASP2-independent fashion, thus suggesting that CLASP2 plays a major role in axon growth rather than branching, for which other proteins are

important [367]. The contrasting results between these two studies could be thus depending on the prevalent GSK3-induced phosphorylation status of CLASP2 at a given time.

The association of CLASPs to CLIP-170 was first shown in COS-1 (T-antigen of SV40 expressing AGMK cells, African Green Monkey Kidney cells) and NIH-3T3 fibroblasts and through yeast two-hybrid assays; this was corroborated by immunofluorescence experiments which revealed an overlapping distribution of CLASP2 and CLIP-170 at MT +ends. The direct interaction was confirmed with *in vitro* experiments, which indicated that the C-terminus of CLASPs is involved in such interaction with the region of the CLIP proteins located after the second CAP-Gly domain (Figure 4). CLASPs were found to accumulate at the Golgi apparatus and, in motile NIH-3T3 fibroblasts, CLASP2 accumulated at the leading edge. This localization pattern was in contrast to that of CLIPs or EB1, which localized at +ends of MTs in the cell interior, and not at the Golgi [334]. It was proposed that interactions between CLIPs and CLASPs play a fundamental role in MT dynamics in polarized cells. In particular, CLASPs could attract CLIPs to MT ends, even in conditions that would otherwise lead to CLIP dissociation (i.e., shrinking or pausing events), to promote MT rescues. These aspects are discussed in greater detail in **Chapter 4** of this thesis.

In conclusion, the +TIP networks that are established on MTs can be extremely complex and diverse. Among the roles of +TIPs we have encountered effects on MT dynamics, interactions with organelles, chromosomes and the cell cortex. We have discussed how a family of these +TIPs, CLASPs, can be regulated at a post-translational level. One of the most striking features of +TIPs, perhaps, is that a common player is usually required for proper +end binding of virtually all +TIPs: the EB proteins. Also, the observations presented in this section highlight the uniqueness of +ends themselves, which could be considered as “regulatory hubs” for MT behavior, driven by specific combinations of +TIPs.

Molecular dynamics simulations

In this section, a brief and general overview of a method used in theoretical biophysics (i.e., molecular dynamics) is provided, since the study described in **Chapter 3** has been performed using such method.

Background

Molecular dynamics (MD) simulations are a computational method to investigate the behavior of an atomic system over time; in the biological context, this system is usually represented by high-resolution atomic structures of proteins, solved by X-ray crystallography or nuclear magnetic resonance (NMR). The fields to which MD simulations can be applied are very diverse, ranging from chemistry to biology, engineering and physics. In MD simulations, atoms are treated as inelastic hard spheres - obeying the second principle of motion- and covalent bonds as springs - usually described by Hooke’s law-. Empirically-derived parameters from chemistry and physics experiments are specified by a force field (such as CHARMM [368]), which is an additive function describing the potential energy as the sum of different energy contributions in the system under study. These energy contributions are represented by “bonded” and “non-bonded” energies. The former includes the energies associated to the covalent bond interaction, the angle of the bond, and the dihedral (the angle between two intersecting planes defined by three atoms each, two of which are in common). Non-bonded energies include electrostatic and van der Waals interactions. In all-atom simulations, all atoms (therefore, including hydrogen) and bonds are subjected to classical mechanics’ laws to infer their behavior in space and time.

An essential step in performing MD simulations is represented by structure preparation and minimization. Structures determined experimentally may be incomplete or could be unrefined, displaying distorted bond lengths and angles, or may have steric clashes. Therefore, energy minimization is required before running an MD simulation, apart from refinement purposes. Energy minimization aims at finding the energy minima for each atom in the structure, to achieve a relaxed state of the system.

The first MD simulation applied to a biological macromolecule, the bovine pancreatic trypsin inhibitor (BPTI), was published in 1977 [369]. This simulation was carried out in vacuum (therefore, not in physiological conditions) and for only 9.2 ps; it corroborated the hydrogen-exchange experiments between peptides and water of Lindestrom-Lang *et al.* in 1955. It became clear that proteins were not fixed arrangements of atoms, but rather dynamic entities. In 1979, Frauenfelder *et al.* [370] proposed that thermal factors (B factors) determined from X-ray crystallography experiments could offer an estimate of such mobility and since then much effort has been invested in gaining more insight into protein dynamics, an essential prerequisite for protein function. Since the first MD simulation, the computational speed and the development of force-fields and of the simulation software increased steeply. To date, MD simulations can be performed on larger systems (hundreds of thousands of atoms), in explicit solvent (meaning that water molecules are present in the system and participating in the simulation), and for much longer times. As an example, in 2009 the supercomputer Anton, with its 512 nodes, performed MD simulations for more than one ms of biological time on the BPTI mentioned earlier, a time span 100 million times longer than the first MD simulation [371]. A general, simplified workflow for the set-up of an MD simulation is depicted in Figure 8.

Applications

MD simulations have been increasingly used in biology to understand elusive molecular mechanisms at the atomic level or to make predictions that can be cross-validated experimentally; however, estimates of systematic errors of computations have not been possible so far. Some applications consist in sampling the conformational space of an experimental structure (for example, during structure refinement): MD simulations are very often used in conjunction with NMR experiments [372]. Also, MD simulations allow analyzing the actual protein motions in time, such as for the bacterial chaperonin GroEL [373]. In this study, the structural transitions that take place between the closed and open conformations of GroEL were identified.

Another example is given by the dynamic gating of acetylcholinesterase, where a 10-ns simulation revealed details that were not deducible from experiments. In this study, MD simulations allowed the determination of conformations that govern substrate specificity of the enzyme. An “aromatic gate” represented by fluctuating side chains of aromatic residues allowed, within a short timeframe, the quick access of acetylcholine but this timeframe was insufficient for entry of bulkier substrates [374].

One of the most common fields of application of MD is drug design [375]. Design of pharmacophores and optimization of existing drugs (to enhance their selectivity, for example) rely extensively on molecular modelling and on MD simulations. They allow insight into the mode of binding of the candidate drug onto the target structure, but also about the structural consequences upon binding. Other applications of MD simulations include *in silico* protein folding studies [376], investigation of conformational and allosteric properties [377], studies on enzyme dynamics required for catalysis [378]. In conclusion, MD simulations are a powerful tool to discover or validate atomic mechanisms of dynamic processes; however, they should

always be accompanied by experimental evidence, to confirm the predictions or to improve the methodology.

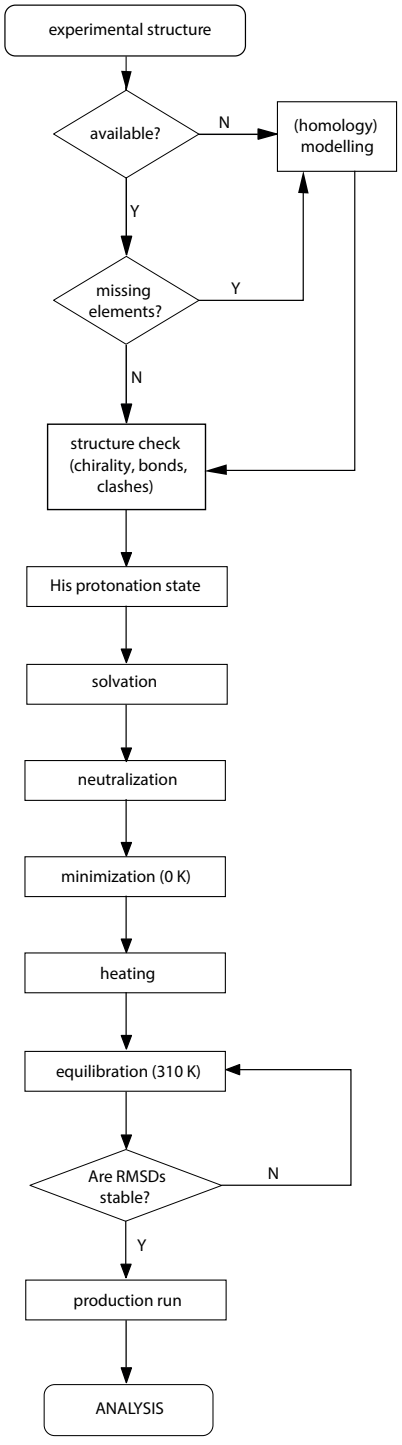

Figure 8. Simple general workflow for the preparation of a molecular dynamics simulation. The quality of the starting structure is crucial for a reliable output of an MD simulation. Structure modelling may be necessary, followed by a check of proper chirality of residues, lengths and angles of bonds and possible steric clashes between side chains; the protonation state of histidine residues must be set in function of the desired pH of the environment. The structure is solvated by adding water molecules to embed completely the protein of interest (considering also possible large structural rearrangements); the system is then made electrically neutral by adding ions accordingly. Relaxation of the protein is achieved through minimization, carried out at 0 K and followed by gradual heating up to the target temperature, usually 310 K (37°C) for biological systems. The system is considered equilibrated when RMSDs (root-mean square deviations from initial structure) do not vary steeply anymore. Once the system is equilibrated, the production run phase starts and can be carried out for the desired amount of time. At the end of the simulation, the trajectory of the molecule is analyzed with dedicated tools.

References

1. Kline-Smith, S.L., Sandall, S., and Desai, A. (2005). Kinetochore-spindle microtubule interactions during mitosis. Curr. Opin. Cell Biol. *17*, 35–46.
2. Fletcher, D.A., and Mullins, R.D. (2010). Cell mechanics and the cytoskeleton. Nature *463*, 485–92.
3. Lodish, H., Berk, A., Zipursky, S.L., Matsudaira, P., Baltimore, D., and Darnell, J. (2000). Molecular Cell Biology. 4th edition.
4. Mattila, P.K., and Lappalainen, P. (2008). Filopodia: molecular architecture and cellular functions. Nat. Rev.Mol. Cell Biol. *9*, 446–454.
5. Abercrombie, M., Joan, E., Heaysman, M., and Pegrum, S.M. (1970). The locomotion of fibroblasts in cul ture. II. "Ruffling." Exp. Cell Res. *60*, 437–444.
6. Small, J.V., Stradal, T., Vignal, E., and Rottner, K. (2002). The lamellipodium: Where motility begins. Trends Cell Biol. *12*, 112–120.
7. Cooper, G.M., and Hausman, R.E. (2007). The Cell: A Molecular Approach 2nd Edition.
8. Mehta, A.D., Rock, R.S., Rief, M., Spudich, J.A., Mooseker, M.S., and Cheney, R.E. (1999). Myosin-V is a processive actin-based motor. Nature *400*, 590–3.
9. Reymann, A.-C., Boujemaa-Paterski, R., Martiel, J.-L., Guérin, C., Cao, W., Chin, H.F., De La Cruz, E.M., Théry, M., and Blanchoin, L. (2012). Actin network architecture can determine myosin motor activity. Science *336*, 1310–4.
10. Siegrist, S.E., and Doe, C.Q. (2007). Microtubule-induced cortical cell polarity. Genes Dev. *21*, 483–96.
11. Cole, N.B., and Lippincott-Schwartz, J. (1995). Organization of organelles and membrane traffic by microtubules. Curr. Opin. Cell Biol. *7*, 55–64.
12. Sandoval, I. V., Bonifacino, J.S., Klausner, R.D., Henkart, M., and Wehland, J. (1984). Role of microtubules in the organization and localization of the Golgi apparatus. J. Cell Biol. *99*.
13. Witte, H., and Bradke, F. (2008). The role of the cytoskeleton during neuronal polarization. Curr. Opin. Neurobiol. *18*, 479–487.
14. Neukirchen, D., and Bradke, F. (2011). Neuronal polarization and the cytoskeleton. Semin. Cell Dev. Biol. *22*, 825–833.
15. De Forges, H., Bouissou, A., and Perez, F. (2012). Interplay between microtubule dynamics and intracellular organization. Int. J. Biochem. Cell Biol. *44*, 266–274.
16. Kull, F.J., and Endow, S.A. (2013). Force generation by kinesin and myosin cytoskeletal motor proteins. J. Cell Sci. *126*, 9–19.
17. Schroer, T.A., Schnapp, B.J., Reese, T.S., and Sheetz, M.P. (1988). The role of kinesin and other soluble factors in organelle movement along microtubules. J. Cell Biol. *107*, 1785–1792.
18. Rickard, J.E., and Kreis, T.E. (1996). CLIPs for organelle-microtubule interactions. Trends Cell Biol. *6*, 178–183.
19. Allan, V.J. (2011). Cytoplasmic dynein. Biochem. Soc. Trans. *39*, 1169–78.
20. Akhshi, T.K., Wernike, D., and Piekny, A. (2014). Microtubules and actin crosstalk in cell migration and division. Cytoskeleton *71*, 1–23.
21. Preciado López, M., Huber, F., Grigoriev, I., Steinmetz, M.O., Akhmanova, A., Koenderink, G.H., and Dogterom, M. (2014). Actin-microtubule coordination at growing microtubule ends. Nat. Commun. *5*, 4778.
22. Weisenberg, R.C., Borisy, G.G., and Taylor, E.W. (1968). The colchicine-binding protein of mammalian brain and its relation to microtubules. Biochemistry 7, 4466–4479.
23. Menéndez, M., Rivas, G., Díaz, J.F., and Andreu, J.M. (1998). Control of the structural stability of the tubulin dimer by one high affinity bound magnesium ion at nucleotide N-site. J. Biol. Chem. *273*, 167–176.
24. Weisenberg, R.C., Deery, W.J., and Dickinson, P.J. (1976). Tubulin-nucleotide interactions during the polymerization and depolymerization of microtubules. Biochemistry *15*, 4248–4254.
25. Löwe, J., Li, H., Downing, K.H., and Nogales, E. (2001). Refined structure of alpha beta-tubulin at 3.5 A resolution. J. Mol. Biol. *313*, 1045–57.
26. Ponstingl, H., Krauhs, E., Little, M., and Kempf, T. (1981). Complete amino acid sequence of alpha-tubulin from porcine brain. Proc. Natl. Acad. Sci. U. S. A. *78*, 4156–60.
27. Krauhs, E., Little, M., Kempf, T., Hofer-Warbinek, R., Ade, W., and Ponstingl, H. (1981). Complete amino acid

sequence of beta-tubulin from porcine brain. Proc. Natl. Acad. Sci. U. S. A. *78*, 4156–60.

28. Nogales, E., Wolf, S.G., and Downing, K.H. (1998). Structure of the alpha beta tubulin dimer by electron crystallography. Nature *391*, 199–203.
29. Downing, K.H., and Nogales, E. (1998). Tubulin and microtubule structure. Curr. Opin. Cell Biol. *10*, 16–22.
30. Alushin, G.M., Lander, G.C., Kellogg, E.H., Zhang, R., Baker, D., and Nogales, E. (2014). High-Resolution microtubule structures reveal the structural transitions in αβ-tubulin upon GTP hydrolysis. Cell *157*, 1117–1129.
31. Amos, L.A., and Löwe, J. (1999). How Taxol® stabilises microtubule structure. Chem. Biol. *6*.
32. Keskin, O., Durell, S.R., Bahar, I., Jernigan, R.L., and Covell, D.G. (2002). Relating molecular flexibility to function: a case study of tubulin. Biophys. J. *83*, 663–680.
33. Ayoub, A.T., Craddock, T.J.A., Klobukowski, M., and Tuszynski, J. (2014). Analysis of the strength of interfacial hydrogen bonds between tubulin dimers using quantum theory of atoms in molecules. Biophys. J. *107*, 740–750.
34. Roll-Mecak, A. (2015). Intrinsically disordered tubulin tails: Complex tuners of microtubule functions? Semin. Cell Dev. Biol. *37*, 11–19.
35. Campen, A., Williams, R.M., Brown, C.J., Meng, J., Uversky, V.N., and Dunker, A.K. (2008). TOP-IDP-scale: a new amino acid scale measuring propensity for intrinsic disorder. Protein Pept. Lett. *15*, 956–63.
36. Dyson, H.J., and Wright, P.E. (2002). Coupling of folding and binding for unstructured proteins. Curr. Opin. Struct. Biol. *12*, 54–60.
37. Wall, K.P., Pagratis, M., Armstrong, G., Balsbaugh, J.L., Verbeke, E., Pearson, C.G., and Hough, L.E. (2016). Molecular Determinants of Tubulin's C-Terminal Tail Conformational Ensemble. ACS Chem. Biol. *11*, 2981–2990.
38. Luchko, T., Huzil, J.T., Stepanova, M., and Tuszynski, J. (2008). Conformational analysis of the carboxy-terminal tails of human beta-tubulin isotypes. Biophys. J. *94*, 1971–1982.
39. Freedman, H., Luchko, T., Luduena, R.F., and Tuszynski, J.A. (2011). Molecular dynamics modeling of tubulin C-terminal tail interactions with the microtubule surface. Proteins Struct. Funct. Bioinforma. *79*, 2968–2982.
40. Dutcher, S.K. (2003). Long-lost relatives reappear: Identification of new members of the tubulin superfamily. Curr. Opin. Microbiol. *6*, 634–640.
41. Wade (2007). Microtubules: an overview. Methods Mol Med *137*, 1–16.
42. Ludueña, R.F., and Banerjee, A. (2008). The Isotypes of Tubulin. Role Microtubules Cell Biol. Neurobiol. Oncol., 123–175.
43. Ludueña, R.F., and Banerjee, A. (2008). The isotypes of tubulin- distribution and functional significance. In Cancer Drug Discovery and Development: The Role of Microtubules in Cell Biology, Neurobiology, and Oncology, pp. 123–175.
44. Lewis, S.A., Lee, M.G.S., and Cowan, N.J. (1985). Five mouse tubulin isotypes and their regulated expression during development. J. Cell Biol. *101*, 852–861.
45. Denoulet, P., Eddé, B., and Gros, F. (1986). Differential expression of several neurospecific beta-tubulin mRNAs in the mouse brain during development. Gene *50*, 289–297.
46. Janke, C. (2014). The tubulin code: Molecular components, readout mechanisms, functions. J. Cell Biol. *206*, 461–472.
47. Ludueña, R.F. (1993). Are tubulin isotypes functionally significant. Mol. Biol. Cell *4*, 445–457.
48. Lewis, S.A., Gu, W., and Cowan, N.J. (1987). Free intermingling of mammalian beta-tubulin isotypes among functionally distinct microtubules. Cell *49*, 539–548.
49. Panda, D., Miller, H.P., Banerjee, a, Ludueña, R.F., and Wilson, L. (1994). Microtubule dynamics in vitro are regulated by the tubulin isotype composition. Proc. Natl. Acad. Sci. U. S. A. *91*, 11358–11362.
50. Banerjee, A., Roach, M.C., Trcka, P., and Luduena, R.F. (1992). Preparation of a monoclonal antibody specific for the class IV isotype of beta-tubulin: Purification and assembly of alpha beta II, alpha beta III, and alpha beta IV tubulin dimers from bovine brain. J. Biol. Chem. *267*, 5625–5630.
51. Pamula, M.C., Ti, S.C., and Kapoor, T.M. (2016). The structured core of human β tubulin confers isotype-specific polymerization properties. J. Cell Biol. *213*, 425–433.
52. Westermann, S., and Weber, K. (2003). Post-translational modifications regulate microtubule function. Nat. Rev. Mol. Cell Biol. *4*, 938–947.
53. Verhey, K.J., and Gaertig, J. (2007). The tubulin code. Cell Cycle *6*, 2152–2160.
54. Stearns, T., and Kirschner, M. (1994). In vitro reconstitution of centrosome assembly and function: the central

role of gamma-tubulin. Cell *76*, 623–637.

55. Stearns, T., Evans, L., and Kirschner, M. (1991). Γ-Tubulin Is a Highly Conserved Component of the Centrosome. Cell *65*, 825–836.
56. Zheng, Y., Jung, M.K., and Oakley, B.R. (1991). Gamma-Tubulin is present in Drosophila melanogaster and homo sapiens and is associated with the centrosome. Cell *65*, 817–823.
57. Marziale, F., Pucciarelli, S., Ballarini, P., Melki, R., Uzun, A., Ilyin, V.A., Detrich, H.W., and Miceli, C. (2008). Different roles of two gamma-tubulin isotypes in the cytoskeleton of the Antarctic ciliate Euplotes focardii: Remodelling of interaction surfaces may enhance microtubule nucleation at low temperature. FEBS J. *275*, 5367–5382.
58. Chang, P., and Stearns, T. (2000). Tubulin and ε -tubulin : two new human centrosomal tubulins reveal new aspects of centrosome structure and function. Nat. Cell Biol. *2*, 30–5.
59. Dutcher, S.K., and Trabuco, E.C. (1998). The UNI3 Gene Is Required for Assembly of Basal Bodies of Chlamydomonas and Encodes δ-Tubulin, a New Member of the Tubulin Superfamily. Mol. Biol. Cell *9*, 1293–1308.
60. Paintrand, M., Moudjou, M., Delacroix, H., and Bornens, M. (1992). Centrosome organization and centriole architecture: Their sensitivity to divalent cations. J. Struct. Biol. *108*, 107–128.
61. Lacey, K.R., Jackson, P.K., and Stearns, T. (1999). Cyclin-dependent kinase control of centrosome duplication. Proc. Natl. Acad. Sci. U. S. A. *96*, 2817–22.
62. Bobinnec, Y., Khodjakov, A., Mir, L.M., Rieder, C.L., Eddé, B., and Bornens, M. (1998). Centriole disassembly in vivo and its effect on centrosome structure and function in vertebrate cells. J. Cell Biol. *143*, 1575–1589.
63. Turk, E., Wills, A.A., Kwon, T., Sedzinski, J., Wallingford, J.B., and Stearns, T. (2015). Zeta-tubulin is a member of a conserved tubulin module and is a component of the centriolar basal foot in multiciliated cells. Curr. Biol. *25*, 2177–2183.
64. Ruiz, F., Krzywicka, A., Klotz, C., Keller, A.M., Cohen, J., Koll, F., Balavoine, G., and Beisson, J. (2000). The SM19 gene, required for duplication of basal bodies in Paramecium, encodes a novel tubulin, η-tubulin. Curr. Biol. *10*, 1451–1454.
65. Ruiz, F., Beisson, J., Rossier, J., and Dupuis-Williams, P. (1999). Basal body duplication in Paramecium requires γ-tubulin. Curr. Biol. *9*, 43–46.
66. Ruiz, F., Dupuis-Williams, P., Klotz, C., Forquignon, F., Bergdoll, M., Beisson, J., and Koll, F. (2004). Genetic evidence for interaction between eta- and beta-tubulins. Eukaryot. Cell *3*, 212–220.
67. Arce, C.A., Rodriguez, J.A., Barra, H.S., and Caputto, R. (1975). Incorporation of L-Tyrosine, L-Phenylalanine and L-3,4-Dihydroxyphenylalanine as Single Units into Rat Brain Tubulin. Eur. J. Biochem. *59*, 145–149.
68. Barra, H.S., Arce, C.A., and Argaraña, C.E. (1988). Posttranslational tyrosination/detyrosination of tubulin. Mol. Neurobiol. *2*, 133–153.
69. Eddé, B., Rossier, J., Le Caer, J.P., Desbruyères, E., Gros, F., and Denoulet, P. (1990). Posttranslational glutamylation of alpha-tubulin. Science (80-.). *247*, 83–85.
70. Redeker, V., Melki, R., Promé, D., Le Caer, J.P., and Rossier, J. (1992). Structure of tubulin C-terminal domain obtained by subtilisin treatment The major alpha and beta tubulin isotypes from pig brain are glutamylated. FEBS Lett. *313*, 185–192.
71. L'Hernault, S.W., and Rosenbaum, J.L. (1985). Chlamydomonas alpha-tubulin is posttranslationally modified by acetylation on the epsilon-amino group of a lysine. Biochemistry *24*, 473–8.
72. Xiao, H., El Bissati, K., Verdier-Pinard, P., Burd, B., Zhang, H., Kim, K., Fiser, A., Angeletti, R.H., and Weiss, L.M. (2010). Post-translational modifications to Toxoplasma gondii alpha- and beta-tubulins include novel C-terminal methylation. J. Proteome Res. *9*, 359–372.
73. Redeker, V., Levilliers, N., Schmitter, J.M., Le Caer, J.P., Rossier, J., Adoutte, a, and Bré, M.H. (1994). Polyglycylation of tubulin: a posttranslational modification in axonemal microtubules. Science *266*, 1688–1691.
74. Magiera, M.M., and Janke, C. (2014). Post-translational modifications of tubulin. Curr. Biol. *24*, R351–R354.
75. Szyk, A., Deaconescu, A.M., Piszczek, G., and Roll-Mecak, A. (2011). Tubulin tyrosine ligase structure reveals adaptation of an ancient fold to bind and modify tubulin. Nat. Struct. Mol. Biol. *18*, 1250–1258.
76. Gundersen, G.G., Khawaja, S., and Bulinski, J.C. (1987). Postpolymerization detyrosination of alpha-tubulin: a mechanism for subcellular differentiation of microtubules. J. Cell Biol. *105*, 251–264.
77. Witte, H., Neukirchen, D., and Bradke, F. (2008). Microtubule stabilization specifies initial neuronal polarization. J. Cell Biol. *180*, 619–632.

78. Piperno, G., LeDizet, M., and Chang, X.J. (1987). Microtubules containing acetylated alpha-tubulin in mammalian cells in culture. J. Cell Biol. *104*, 289–302.

79. Hammond, J.W., Huang, C.-F., Kaech, S., Jacobson, C., Banker, G., and Verhey, K.J. (2010). Posttranslational modifications of tubulin and the polarized transport of kinesin-1 in neurons. Mol. Biol. Cell *21*, 572–583.

80. Chakraborti, S., Natarajan, K., Curiel, J., Janke, C., and Liu, J. (2016). The emerging role of the tubulin code: From the tubulin molecule to neuronal function and disease. Cytoskeleton *73*, 521–550.

81. Barra, H.S., Rodriguez, J.A., Arce, C.A., and Caputto, R. (1973). A soluble preparation from rat brain that incorporates into its own proteins [14C] arginine by a ribonuclease-sensitive system and [14C] tyrosine by a ribonuclease-insensitive system. J. Neurochem. *20*, 97–108.

82. Arce, C. a, and Barra, H.S. (1985). Release of C-terminal tyrosine from tubulin and microtubules at steady state. Biochem. J. *226*, 311–317.

83. Kreis, T.E. (1987). Microtubules containing detyrosinated tubulin are less dynamic. EMBO J. *6*, 2597–2606.

84. Peris, L., Wagenbach, M., Lafanechère, L., Brocard, J., Moore, A.T., Kozielski, F., Job, D., Wordeman, L., and Andrieux, A. (2009). Motor-dependent microtubule disassembly driven by tubulin tyrosination. J. Cell Biol. *185*, 1159–1166.

85. Prota, A.E., Magiera, M.M., Kuijpers, M., Bargsten, K., Frey, D., Wieser, M., Jaussi, R., Hoogenraad, C.C., Kammerer, R.A., Janke, C., *et al.* (2013). Structural basis of tubulin tyrosination by tubulin tyrosine ligase. J. Cell Biol. *200*, 259–270.

86. Zink, S., Grosse, L., Freikamp, a., Banfer, S., Muksch, F., and Jacob, R. (2012). Tubulin detyrosination promotes monolayer formation and apical trafficking in epithelial cells. J. Cell Sci., 5998–6008.

87. Quinones, G.B., Danowski, B.A., Devaraj, A., Singh, V., and Ligon, L.A. (2011). The posttranslational modification of tubulin undergoes a switch from detyrosination to acetylation as epithelial cells become polarized. Mol. Biol. Cell *22*, 1045–57.

88. Baas, P.W., and Black, M.M. (1990). Individual microtubules in the axon consist of domains that differ in both composition and stability. J. Cell Biol. *111*, 495–509.

89. Baas, P.W., Slaughter, T., Brown, A., and Black, M.M. (1991). Microtubule dynamics in axons and dendrites. J. Neurosci. Res. *30*, 134–153.

90. Brown, A., Li, Y., Slaughter, T., and Black, M.M. (1993). Composite microtubules of the axon: quantitative analysis of tyrosinated and acetylated tubulin along individual axonal microtubules. J. Cell Sci., 339–52.

91. Geuens, G., Gundersen, G.G., Nuydens, R., Cornelissen, F., Bulinski, J.C., and DeBrabander, M. (1986). Ultrastructural colocalization of tyrosinated and detyrosinated alpha-tubulin in interphase and mitotic cells. J. Cell Biol. *103*, 1883–1893.

92. Erck, C., Peris, L., Andrieux, A., Meissirel, C., Gruber, A.D., Vernet, M., Schweitzer, A., Saoudi, Y., Pointu, H., Bosc, C., *et al.* (2005). A vital role of tubulin-tyrosine-ligase for neuronal organization. Proc. Natl. Acad. Sci. U. S. A. *102*, 7853–7858.

93. Janke, C., and Kneussel, M. (2010). Tubulin post-translational modifications: Encoding functions on the neuronal microtubule cytoskeleton. Trends Neurosci. *33*, 362–372.

94. Berezniuk, I., Vu, H.T., Lyons, P.J., Sironi, J.J., Xiao, H., Burd, B., Setou, M., Angeletti, R.H., Ikegami, K., and Fricker, L.D. (2012). Cytosolic carboxypeptidase 1 is involved in processing alpha- and beta-tubulin. J. Biol. Chem. *287*, 6503–6517.

95. Tort, O., Tanco, S., Rocha, C., Bièche, I., Seixas, C., Bosc, C., Andrieux, A., Moutin, M.-J., Avilés, F.X., Lorenzo, J., *et al.* (2014). The cytosolic carboxypeptidases CCP2 and CCP3 catalyze posttranslational removal of acidic amino acids. Mol. Biol. Cell *25*, 3017–27.

96. Berezniuk, I., Lyons, P.J., Sironi, J.J., Xiao, H., Setou, M., Angeletti, R.H., Ikegami, K., and Fricker, L.D. (2013). Cytosolic carboxypeptidase 5 removes alpha- and gamma-linked glutamates from tubulin. J. Biol. Chem. *288*, 30445–30453.

97. Rogowski, K., van Dijk, J., Magiera, M.M., Bosc, C., Deloulme, J.C., Bosson, A., Peris, L., Gold, N.D., Lacroix, B., Grau, M.B., *et al.* (2010). A family of protein-deglutamylating enzymes associated with neurodegeneration. Cell *143*, 564–578.

98. Lafanechère, L., and Job, D. (2000). The third tubulin pool. Neurochem. Res. *25*, 11–18.

99. Paturle-Lafanechère, L., Manier, M., Trigault, N., Pirollet, F., Mazarguil, H., and Job, D. (1994). Accumulation of delta 2-tubulin, a major tubulin variant that cannot be tyrosinated, in neuronal tissues and in stable microtubule assemblies. J. Cell Sci. *107 (Pt 6*, 1529–1543.

100. Aillaud, C., Bosc, C., Saoudi, Y., Denarier, E., Peris, L., Sago, L., Taulet, N., Cieren, A., Tort, O., Magiera, M.M.,

et al. (2016). Evidence for new C-terminally truncated variants of α- and β-tubulins. Mol. Biol. Cell *27*, 640–53.

101. Miller, L.M., Menthena, A., Chatterjee, C., Verdier-Pinard, P., Novikoff, P.M., Horwitz, S.B., and Angeletti, R.H. (2008). Increased levels of a unique post-translationally modified betaIVb-tubulin isotype in liver cancer. Biochemistry *47*, 7572–82.
102. LeDizet, M., and Piperno, G. (1987). Identification of an acetylation site of Chlamydomonas alpha-tubulin. Proc. Natl. Acad. Sci. U. S. A. *84*, 5720–4.
103. Friedmann, D.R., Aguilar, A., Fan, J., Nachury, M. V, and Marmorstein, R. (2012). Structure of the α-tubulin acetyltransferase, αTAT1, and implications for tubulin-specific acetylation. Proc. Natl. Acad. Sci. U. S. A. *109*, 19655–60.
104. Coombes, C., Yamamoto, A., McClellan, M., Reid, T.A., Plooster, M., Luxton, G.W.G., Alper, J., Howard, J., and Gardner, M.K. (2016). Mechanism of microtubule lumen entry for the α-tubulin acetyltransferase enzyme αTAT1. Proc. Natl. Acad. Sci. U. S. A. *113*, E7176–E7184.
105. Shida, T., Cueva, J.G., Xu, Z., Goodman, M.B., and Nachury, M. V (2010). The major alpha-tubulin K40 acetyltransferase alphaTAT1 promotes rapid ciliogenesis and efficient mechanosensation. Proc. Natl. Acad. Sci. U. S. A. *107*, 21517–21522.
106. Schulze, E., Asai, D.J., Bulinski, J.C., and Kirschner, M. (1987). Posttranslational modification and microtubule stability. J. Cell Biol. *105*, 2167–2177.
107. Webster, D.R., and Borisy, G.G. (1989). Microtubules are acetylated in domains that turn over slowly. J. Cell Sci. *92 (Pt 1)*, 57–65.
108. Topalidou, I., Keller, C., Kalebic, N., Nguyen, K.C.Q., Somhegyi, H., Politi, K.A., Heppenstall, P., Hall, D.H., and Chalfie, M. (2012). Genetically separable functions of the MEC-17 tubulin acetyltransferase affect microtubule organization. Curr. Biol. *22*, 1057–1065.
109. Neumann, B., and Hilliard, M. (2014). Loss of MEC-17 leads to microtubule instability and axonal degeneration. Cell Rep. *6*, 93–103.
110. Kim, G.W., Li, L., Gorbani, M., You, L., and Yang, X.J. (2013). Mice lacking alpha-tubulin acetyltransferase 1 are viable but display alpha-tubulin acetylation deficiency and dentate gyrus distortion. J. Biol. Chem. *288*, 20334–20350.
111. Howes, S.C., Alushin, G.M., Shida, T., Nachury, M. V, and Nogales, E. (2014). Effects of tubulin acetylation and tubulin acetyltransferase binding on microtubule structure. Mol. Biol. Cell *25*, 257–66.
112. Janke, C., and Bulinski, J.C. (2011). Post-translational regulation of the microtubule cytoskeleton: mechanisms and functions. Nat Rev Mol Cell Biol *12*, 773–786.
113. Reed, N.A., Cai, D., Blasius, T.L., Jih, G.T., Meyhofer, E., Gaertig, J., and Verhey, K.J. (2006). Microtubule Acetylation Promotes Kinesin-1 Binding and Transport. Curr. Biol. *16*, 2166–2172.
114. Dompierre, J.P., Godin, J.D., Charrin, B.C., Cordelières, F.P., King, S.J., Humbert, S., and Saudou, F. (2007). Histone deacetylase 6 inhibition compensates for the transport deficit in Huntington's disease by increasing tubulin acetylation. J. Neurosci. *27*, 3571–3583.
115. Perdiz, D., Mackeh, R., Poüs, C., and Baillet, A. (2011). The ins and outs of tubulin acetylation: More than just a post-translational modification? Cell. Signal. *23*, 763–771.
116. Yang, P. (2013). HDAC6: Physiological function and its selective inhibitors for cancer treatment. Drug Discov. Ther. *7*, 233–242.
117. North, B.J., Marshall, B.L., Borra, M.T., Denu, J.M., and Verdin, E. (2003). The human Sir2 ortholog, SIRT2, is an NAD+-dependent tubulin deacetylase. Mol. Cell *11*, 437–444.
118. Bobrowska, A., Donmez, G., Weiss, A., Guarente, L., and Bates, G. (2012). SIRT2 ablation has no effect on tubulin acetylation in brain, cholesterol biosynthesis or the progression of Huntington's disease phenotypes in vivo. PLoS One *7*, e34805.
119. Bobrowska, A., Paganetti, P., Matthias, P., and Bates, G.P. (2011). Hdac6 knock-out increases tubulin acetylation but does not modify disease progression in the R6/2 mouse model of Huntington's disease. PLoS One *6*.
120. Fukada, M., Hanai, A., Nakayama, A., Suzuki, T., Miyata, N., Rodriguiz, R.M., Wetsel, W.C., Yao, T.P., and Kawaguchi, Y. (2012). Loss of deacetylation activity of Hdac6 affects emotional behavior in mice. PLoS One *7*.
121. Wang, B., Rao, Y.-H., Inoue, M., Hao, R., Lai, C.-H., Chen, D., McDonald, S.L., Choi, M.-C., Wang, Q., Shinohara, M.L., *et al.* (2014). Microtubule acetylation amplifies p38 kinase signalling and anti-inflammatory IL-10 production. Nat. Commun. *5*, 3479.
122. Li, L., and Yang, X.J. (2015). Tubulin acetylation: Responsible enzymes, biological functions and human diseases. Cell. Mol. Life Sci. *72*, 4237–4255.

123. Janke, C., Rogowski, K., Wloga, D., Regnard, C., Kajava, A. V, Strub, J.-M., Temurak, N., van Dijk, J., Boucher, D., van Dorsselaer, A., *et al.* (2005). Tubulin polyglutamylase enzymes are members of the TTL domain protein family. Science *308*, 1758–62.

124. van Dijk, J., Rogowski, K., Miro, J., Lacroix, B., Eddé, B., and Janke, C. (2007). A Targeted Multienzyme Mechanism for Selective Microtubule Polyglutamylation. Mol. Cell *26*, 437–448.

125. Van Dijk, J., Miro, J., Strub, J.M., Lacroix, B., Van Dorsselaer, A., Edde, B., and Janke, C. (2008). Polyglutamylation is a post-translational modification with a broad range of substrates. J. Biol. Chem. *283*, 3915–3922.

126. Redeker, V., Rossier, J., and Frankfurter, A. (1998). Posttranslational modifications of the C-terminus of α-tubulin in adult rat brain: α4 is glutamylated at two residues. Biochemistry *37*, 14838–14844.

127. Alexander, J.E., Hunt, D.F., Lee, M.K., Shabanowitz, J., Michel, H., Berlin, S.C., MacDonald, T.L., Sundberg, R.J., Rebhun, L.I., and Frankfurter, a (1991). Characterization of posttranslational modifications in neuron-specific class III beta-tubulin by mass spectrometry. Proc. Natl. Acad. Sci. U. S. A. *88*, 4685–4689.

128. Rüdiger, M., Plessman, U., Klöppel, K.D., Wehland, J., and Weber, K. (1992). Class II tubulin, the major brain ?? tubulin isotype is polyglutamylated on glutamic acid residue 435. FEBS Lett. *308*, 101–105.

129. Fouquet, J.-P., Kann, M.-L., Edde, B., Wolff, A., Desbruyeres, E., and Denoulet, P. (1994). Differential distribution of glutamylated tubulin during spermatogenesis in mammalian testis. Cell Motil. Cytoskeleton *27*, 49–58.

130. Mary, J., Redeker, V., Le Caer, J.P., Promé, J.C., and Rossier, J. (1994). Class I and IVa beta-tubulin isotypes expressed in adult mouse brain are glutamylated. FEBS Lett. *353*, 89–94.

131. Audebert, S., Desbruyères, E., Gruszczynski, C., Koulakoff, a, Gros, F., Denoulet, P., and Eddé, B. (1993). Reversible polyglutamylation of alpha- and beta-tubulin and microtubule dynamics in mouse brain neurons. Mol. Biol. Cell *4*, 615–626.

132. Audebert, S., Koulakoff, a, Berwald-Netter, Y., Gros, F., Denoulet, P., and Eddé, B. (1994). Developmental regulation of polyglutamylated alpha- and beta-tubulin in mouse brain neurons. J. Cell Sci. *107 (Pt 8*, 2313–22.

133. Wolff, A., de Néchaud, B., Chillet, D., Mazarguil, H., Desbruyères, E., Audebert, S., Eddé, B., Gros, F., and Denoulet, P. (1992). Distribution of glutamylated alpha and beta-tubulin in mouse tissues using a specific monoclonal antibody, GT335. Eur. J. Cell Biol. *59*, 425–432.

134. Kann, M.L., Soues, S., Levilliers, N., and Fouquet, J.P. (2003). Glutamylated tubulin: Diversity of expression and distribution of isoforms. Cell Motil. Cytoskeleton *55*, 14–25.

135. Kubo, T., Yanagisawa, H. aki, Yagi, T., Hirono, M., and Kamiya, R. (2010). Tubulin Polyglutamylation Regulates Axonemal Motility by Modulating Activities of Inner-Arm Dyneins. Curr. Biol. *20*, 441–445.

136. Suryavanshi, S., Eddé, B., Fox, L.A., Guerrero, S., Hard, R., Hennessey, T., Kabi, A., Malison, D., Pennock, D., Sale, W.S., *et al.* (2010). Tubulin Glutamylation Regulates Ciliary Motility by Altering Inner Dynein Arm Activity. Curr. Biol. *20*, 435–440.

137. Lacroix, B., Van Dijk, J., Gold, N.D., Guizetti, J., Aldrian-Herrada, G., Rogowski, K., Gerlich, D.W., and Janke, C. (2010). Tubulin polyglutamylation stimulates spastin-mediated microtubule severing. J. Cell Biol. *189*, 945–954.

138. Roll-Mecak, A., and Vale, R.D. (2005). The Drosophila homologue of the hereditary spastic paraplegia protein, spastin, severs and disassembles microtubules. Curr. Biol. *15*, 650–655.

139. Evans, K.J., Gomes, E.R., Reisenweber, S.M., Gundersen, G.G., and Lauring, B.P. (2005). Linking axonal degeneration to microtubule remodeling by Spastin-mediated microtubule severing. J. Cell Biol. *168*, 599–606.

140. Boucher, D., Larcher, J.C., Gros, F., and Denoulet, P. (1994). Polyglutamylation of tubulin as a progressive regulator of in vitro interactions between the microtubule-associated protein tau and tubulin. Biochemistry *33*, 12471–12477.

141. Larcher, J.C., Boucher, D., Lazereg, S., Gros, F., and Denoulet, P. (1996). Interaction of kinesin motor domains with α- and β-tubulin subunits at a tau-independent binding site: Regulation by polyglutamylation. J. Biol. Chem. *271*, 22117–22124.

142. Bonnet, C., Boucher, D., Lazereg, S., Pedrotti, B., Islam, K., Denoulet, P., and Larcher, J.C. (2001). Differential Binding Regulation of Microtubule-associated Proteins MAP1A, MAP1B, and MAP2 by Tubulin Polyglutamylation. J. Biol. Chem. *276*, 12839–12848.

143. Kimura, Y., Kurabe, N., Ikegami, K., Tsutsumi, K., Konishi, Y., Kaplan, O.I., Kunitomo, H., Iino, Y., Blacque, O.E., and Setou, M. (2010). Identification of tubulin deglutamylase among Caenorhabditis elegans and mammalian cytosolic carboxypeptidases (CCPs). J. Biol. Chem. *285*, 22936–22941.

144. Mullen, R.J., Eicher, E.M., and Sidman, R.L. (1976). Purkinje cell degeneration, a new neurological mutation in the mouse. Proc. Natl. Acad. Sci. U. S. A. *73*, 208–212.

145. Greer, C.A., and Shepherd, G.M. (1982). Mitral cell degeneration and sensory function in the neurological mutant mouse Purkinje cell degeneration (PCD). Brain Res. *235*, 156–161.

146. Wloga, D., and Gaertig, J. (2010). Post-translational modifications of microtubules. J. Cell Sci. *123*, 3447–55.

147. Wloga, D., Webster, D.M., Rogowski, K., Bré, M.H., Levilliers, N., Jerka-Dziadosz, M., Janke, C., Dougan, S.T., and Gaertig, J. (2009). TTLL3 Is a Tubulin Glycine Ligase that Regulates the Assembly of Cilia. Dev. Cell *16*, 867–876.

148. Sloboda, R.D. (2009). Posttranslational protein modifications in cilia and flagella. Methods Cell Biol. *94*, 347–363.

149. Ikegami, K., and Setou, M. (2009). TTLL10 can perform tubulin glycylation when co-expressed with TTLL8. FEBS Lett. *583*, 1957–1963.

150. Rogowski, K., Juge, F., van Dijk, J., Wloga, D., Strub, J.M., Levilliers, N., Thomas, D., Bré, M.H., Van Dorsselaer, A., Gaertig, J., *et al.* (2009). Evolutionary Divergence of Enzymatic Mechanisms for Posttranslational Polyglycylation. Cell *137*, 1076–1087.

151. Dossou, S.J.Y., Bré, M.H., and Hallworth, R. (2007). Mammalian cilia function is independent of the polymeric state of tubulin glycylation. Cell Motil. Cytoskeleton *64*, 847–855.

152. Rocha, C., Papon, L., Cacheux, W., Marques Sousa, P., Lascano, V., Tort, O., Giordano, T., Vacher, S., Lemmers, B., Mariani, P., *et al.* (2014). Tubulin glycylases are required for primary cilia, control of cell proliferation and tumor development in colon. EMBO J. *33*, 1–14.

153. Grau, M.B., Curto, G.G., Rocha, C., Magiera, M.M., Sousa, P.M., Giordano, T., Spassky, N., and Janke, C. (2013). Tubulin glycylases and glutamylases have distinct functions in stabilization and motility of ependymal cilia. J. Cell Biol. *202*, 441–451.

154. Menzl, I., Lebeau, L., Pandey, R., Hassounah, N.B., Li, F.W., Nagle, R., Weihs, K., McDermott, K.M., Goetz, S., Anderson, K., *et al.* (2014). Loss of primary cilia occurs early in breast cancer development. Cilia *3*, 7.

155. Kornberg, R.D. (1974). Chromatin structure: a repeating unit of histones and DNA. Science *184*, 868–871.

156. Kouzarides, T. (2007). Chromatin Modifications and Their Function. Cell *128*, 693–705.

157. Bannister, A.J., and Kouzarides, T. (2011). Regulation of chromatin by histone modifications. Cell Res. *21*, 381–395.

158. Park, I.Y., Powell, R.T., Tripathi, D.N., Dere, R., Ho, T.H., Blasius, T.L., Chiang, Y.C., Davis, I.J., Fahey, C.C., Hacker, K.E., *et al.* (2016). Dual Chromatin and Cytoskeletal Remodeling by SETD2. Cell *166*, 950–962.

159. Shen, Z. (2011). Genomic instability and cancer: An introduction. J. Mol. Cell Biol. *3*, 1–3.

160. Giaccia, A.J. (2016). A New Chromatin–Cytoskeleton Link in Cancer. Mol. Cancer Res. *14*, 1173 LP-1175.

161. Mandelkow, E.M., and Mandelkow, E. (1985). Unstained microtubules studied by cryo-electron microscopy. Substructure, supertwist and disassembly. J. Mol. Biol. *181*, 123–135.

162. Walker, R.A., O'Brien, E.T., Pryer, N.K., Soboeiro, M.F., Voter, W.A., Erickson, H.P., and Salmon, E.D. (1988). Dynamic instability of individual microtubules analyzed by video light microscopy: rate constants and transition frequencies. J. Cell Biol. *107*, 1437–1448.

163. Nogales, E., and Wang, H.-W. (2006). Structural mechanisms underlying nucleotide-dependent self-assembly of tubulin and its relatives. Curr. Opin. Struct. Biol. *16*, 221–229.

164. Kirschner, M.W., and Mitchison, T. (1986). Microtubule dynamics. Nature *324*, 621.

165. Etienne-Manneville, S. (2013). Microtubules in cell migration. Annu. Rev. Cell Dev. Biol. *29*, 471–99.

166. Nogales, E. (1999). A structural view of microtubule dynamics. Cell. Mol. Life Sci. C. *56*, 133–142.

167. Nogales, E., Whittaker, M., Milligan, R.A., and Downing, K.H. (1999). High-resolution model of the microtubule. Cell *96*, 79–88.

168. Yu, L., Van Hoozen, B.L., Bodnar, C.E., and Martin, D.S. (2017). A New Microtubule Gliding Assay Analysis of Microtubule Persistence Length. Biophys. J. *100*, 450a.

169. Amos, L., and Klug, a (1974). Arrangement of subunits in flagellar microtubules. J. Cell Sci. *14*, 523–549.

170. Mandelkow, E.M., Schultheiss, R., Rapp, R., and Müller, M. (1986). On the surface lattice of microtubules: Helix starts, protofilament number, seam, and handedness. J. Cell Biol. *102*, 1067–1073.

171. McEwen, B., and Edelstein, S.J. (1980). Evidence for a mixed lattice in microtubules reassembled in vitro. J. Mol. Biol. *139*, 123–143.

172. Sui, H., and Downing, K.H. (2010). Structural basis of interprotofilament interaction and lateral deformation of microtubules. Structure *18*, 1022–1031.

173. Chrétien, D., Metoz, F., Verde, F., Karsenti, E., and Wade, R.H. (1992). Lattice defects in microtubules: Protofilament numbers vary within individual microtubules. J. Cell Biol. *117*, 1031–1040.

174. Chrétien, D., and Wade, R.H. (1991). New data on the microtubule surface lattice. Biol. Cell *71*, 161–174.

175. Mitchison, T.J. (1993). Localization of an exchangeable GTP binding site at the plus end of microtubules. Science *261*, 1044–7.

176. Bornens, M. (2008). Organelle positioning and cell polarity. Nat Rev Mol Cell Biol *9*, 874–886.

177. Howard, J., and Hyman, A.A. (2003). Dynamics and mechanics of the microtubule plus end. Nature *422*, 753–758.

178. Mitchison, T., and Kirschner, M. (1984). Dynamic instability of microtubule growth. Nature *312*, 237–42.

179. Mimori-Kiyosue, Y., and Tsukita, S. (2003). "Search-and-Capture" of Microtubules through Plus-End-Binding Proteins (+TIPs). J. Biochem. *134*, 321–326.

180. Schuyler, S.C., and Pellman, D. (2001). Microtubule "plus-end-tracking proteins": The end is just the beginning. Cell *105*, 421–424.

181. David-Pfeuty, T., Erickson, H.P., and Pantaloni, D. (1977). Guanosinetriphosphatase activity of tubulin associated with microtubule assembly. Proc. Natl. Acad. Sci. *74*, 5372–5376.

182. Hyman, A.A., Salser, S., Drechsel, D.N., Unwin, N., and Mitchison, T.J. (1992). Role of GTP hydrolysis in microtubule dynamics: information from a slowly hydrolyzable analogue, GMPCPP. Mol. Biol. Cell *3*, 1155–67.

183. Arai, T., and Kaziro, Y. (1977). Role of GTP in the Assembly of Microtubules. J. Biochem. *82*, 1063.

184. Caplow, M., Ruhlen, R.L., and Shanks, J. (1994). The free energy for hydrolysis of a microtubule-bound nucleotide triphosphate is near zero: all of the free energy for hydrolysis is stored in the microtubule lattice. J. Cell Biol. *127*, 779 LP-788.

185. Carlier, M.F., and Pantaloni, D. (1981). Kinetic analysis of guanosine 5'-triphosphate hydrolysis associated with tubulin polymerization. Biochemistry *20*, 1918–1924.

186. Walker, R.A., Inoue, S., and Salmon, E.D. (1989). Asymmetric behavior of severed microtubule ends after ultraviolet-microbeam irradiation of individual microtubules in vitro. J. Cell Biol. *108*, 931–937.

187. Tran, P.T., Walker, R.A., and Salmon, E.D. (1997). A metastable intermediate state of microtubule dynamic instability that differs significantly between plus and minus ends. J. Cell Biol. *138*, 105–117.

188. Caplow, M., and Shanks, J. (1996). Evidence that a Single Monolayer Tubulin-GTP Cap Is Both Necessary and Sufficient to Stabilize Microtubules. Mol. Biol. Cell *7*, 663–675.

189. Walker, R.A., Pryer, N.K., and Salmon, E.D. (1991). Dilution of individual microtubules observed in real time in vitro: Evidence that cap size is small and independent of elongation rate. J. Cell Biol. *114*, 73–81.

190. Voter, W.A., and Erickson, H.P. (1984). The kinetics of microtubule assembly. Evidence for a two-stage nucleation mechanism. J. Biol. Chem. *259*, 10430–10438.

191. Wieczorek, M., Bechstedt, S., Chaaban, S., and Brouhard, G.J. (2015). Microtubule-associated proteins control the kinetics of microtubule nucleation. Nat Cell Biol *17*, 907–916.

192. Lin, T., Neuner, A., Flemming, D., Liu, P., Chinen, T., Jäkle, U., Arkowitz, R., and Schiebel, E. (2016). MOZART1 and γ-tubulin complex receptors are both required to turn γ-TuSC into an active microtubule nucleation template. J. Cell Biol., jcb.201606092.

193. Mozart1 orchestrates microtubule nucleation (2017). J. Cell Sci. *130*, e0204 LP-e0204.

194. Hunter, A.W., Caplow, M., Coy, D.L., Hancock, W.O., Diez, S., Wordeman, L., and Howard, J. (2003). The kinesin-related protein MCAK is a microtubule depolymerase that forms an ATP-hydrolyzing complex at microtubule ends. Mol. Cell *11*, 445–457.

195. Bieling, P., Laan, L., Schek, H., Munteanu, E.L., Sandblad, L., Dogterom, M., Brunner, D., and Surrey, T. (2007). Reconstitution of a microtubule plus-end tracking system in vitro. Nature *450*, 1100–1105.

196. Brouhard, G.J., Stear, J.H., Noetzel, T.L., Al-Bassam, J., Kinoshita, K., Harrison, S.C., Howard, J., and Hyman, A.A. (2008). XMAP215 Is a Processive Microtubule Polymerase. Cell *132*, 79–88.

197. Zanic, M., Widlund, P.O., Hyman, A. a, and Howard, J. (2013). Synergy between XMAP215 and EB1 increases microtubule growth rates to physiological levels. Nat. Cell Biol. *15*, 1–8.

198. Bornens, M. (2012). The centrosome in cells and organisms. Science (80-.). *335*, 422–426.

199. Conduit, P.T., Wainman, A., and Raff, J.W. (2015). Centrosome function and assembly in animal cells. Nat. Rev. Mol. Cell Biol. *16*, 611–624.

200. Debec, A., Sullivan, W., and Bettencourt-Dias, M. (2010). Centrioles: Active players or passengers during mitosis? Cell. Mol. Life Sci. *67*, 2173–2194.

201. Cunha-Ferreira, I., Bento, I., and Bettencourt-Dias, M. (2009). From zero to many: Control of centriole number in development and disease. Traffic *10*, 482–498.

202. Chabin-Brion, K., Marceiller, J., Perez, F., Settegrana, C., Drechou, A., Durand, G., and Poüs, C. (2001). The Golgi complex is a microtubule-organizing organelle. Mol. Biol. Cell *12*, 2047–60.

203. Rios, R.M. (2014). The centrosome-Golgi apparatus nexus. Philos. Trans. R. Soc. Lond. B. Biol. Sci. *369*, 1–10.

204. Sanders, A.A.W.M., and Kaverina, I. (2015). Nucleation and dynamics of Golgi-derived microtubules. Front. Neurosci. *9*.

205. Efimov, A., Kharitonov, A., Efimova, N., Loncarek, J., Miller, P.M., Andreyeva, N., Gleeson, P., Galjart, N., Maia, A.R.R., McLeod, I.X., *et al.* (2007). Asymmetric CLASP-Dependent Nucleation of Noncentrosomal Microtubules at the trans-Golgi Network. Dev. Cell *12*, 917–930.

206. Zhu, X., and Kaverina, I. (2013). Golgi as an MTOC: Making microtubules for its own good. Histochem. Cell Biol. *140*, 361–367.

207. Lindeboom, J.J., Nakamura, M., Hibbel, A., Shundyak, K., Gutierrez, R., Ketelaar, T., Emons, A.M.C., Mulder, B.M., Kirik, V., and Ehrhardt, D.W. (2013). A mechanism for reorientation of cortical microtubule arrays driven by microtubule severing. Science (80-.). *342*, 1245533.

208. Srayko, M., Kaya, A., Stamford, J., and Hyman, A.A. (2005). Identification and characterization of factors required for microtubule growth and nucleation in the early C. elegans embryo. Dev. Cell *9*, 223–236.

209. Bettencourt-Dias, M., and Glover, D.M. (2007). Centrosome biogenesis and function: centrosomics brings new understanding. Nat. Rev. Mol. Cell Biol. *8*, 451–63.

210. Winey, M., and O'Toole, E. (2014). Centriole structure. Philos. Trans. R. Soc. Lond. B. Biol. Sci. *369*, 20130457-.

211. Gönczy, P. (2012). Towards a molecular architecture of centriole assembly. Nat. Rev. Mol. Cell Biol. *13*, 425–435.

212. Brito, D.A., Gouveia, S.M., and Bettencourt-Dias, M. (2012). Deconstructing the centriole: Structure and number control. Curr. Opin. Cell Biol. *24*, 4–13.

213. Sir, J.H., Pütz, M., Daly, O., Morrison, C.G., Dunning, M., Kilmartin, J. V., and Gergely, F. (2013). Loss of centrioles causes chromosomal instability in vertebrate somatic cells. J. Cell Biol. *203*, 747–756.

214. Sorokin, S.P. (1968). Reconstructions of centriole formation and ciliogenesis in mammalian lungs. J. Cell Sci. *3*, 207–30.

215. Satir, P., Pedersen, L.B., and Christensen, S.T. (2010). The primary cilium at a glance. J Cell Sci *123*, 499–503.

216. Oh, E.C., and Katsanis, N. (2012). Cilia in vertebrate development and disease. Development *139*, 443–448.

217. Nauli, S.M., Alenghat, F.J., Luo, Y., Williams, E., Vassilev, P., Li, X., Elia, A.E.H., Lu, W., Brown, E.M., Quinn, S.J., *et al.* (2003). Polycystins 1 and 2 mediate mechanosensation in the primary cilium of kidney cells. Nat. Genet. *33*, 129–37.

218. Praetorius, H.A., and Spring, K.R. (2003). Removal of the MDCK cell primary cilium abolishes flow sensing. J. Membr. Biol. *191*, 69–76.

219. Summers, K.E., and Gibbons, I.R. (1971). Adenosine Triphosphate-Induced Sliding of Tubules in Trypsin-Treated Flagella of Sea-Urchin Sperm. Proc. Natl. Acad. Sci. *68*, 3092–3096.

220. Basten, S.G., and Giles, R.H. (2013). Functional aspects of primary cilia in signaling, cell cycle and tumorigenesis. Cilia *2*, 6.

221. Azimzadeh, J., Wong, M.L., Downhour, D.M., Alvarado, A.S., and Marshall, W.F. (2012). Centrosome Loss in the Evolution of Planarians. Science (80-.). *335*, 461–463.

222. Courtois, A., Schuh, M., Ellenberg, J., and Hiiragi, T. (2012). The transition from meiotic to mitotic spindle assembly is gradual during early mammalian development. J. Cell Biol. *198*, 357–370.

223. Kalab, P., and Heald, R. (2008). The RanGTP gradient - a GPS for the mitotic spindle. J. Cell Sci. *121*, 1577–86.

224. Gruss, O.J., Wittmann, M., Yokoyama, H., Pepperkok, R., Kufer, T., Silljé, H., Karsenti, E., Mattaj, I.W., and Vernos, I. (2002). Chromosome-induced microtubule assembly mediated by TPX2 is required for spindle formation in HeLa cells. Nat. Cell Biol. *4*, 871–9.

225. Wittmann, T., Wilm, M., Karsenti, E., and Vernos, I. (2000). TPX2, a novel Xenopus MAP involved in spindle pole organization. J. Cell Biol. *149*, 1405–1418.

226. Roostalu, J., Cade, N.I., and Surrey, T. (2015). Complementary activities of TPX2 and chTOG constitute an efficient importin-regulated microtubule nucleation module. Nat. Cell Biol. *17*, 1422–1434.

227. Dogterom, M., Kerssemakers, J.W.J., Romet-Lemonne, G., and Janson, M.E. (2005). Force generation by

dynamic microtubules. Curr. Opin. Cell Biol. *17*, 67–74.

228. Murphy, D.B., and Borisy, G.G. (1975). Association of high-molecular-weight proteins with microtubules and their role in microtubule assemble in vitro. Proc. Natl. Acad. Sci. U. S. A. *72*, 2696–2700.
229. Weisenberg, R.C. (1972). Microtubule Formation in vitro in Solutions Containing Low Calcium Concentrations. Science (80-.). *177*, 1104–1105.
230. Shelanski, M.L., Gaskin, F., and Cantor, C.R. (1973). Microtubule assembly in the absence of added nucleotides. Proc. Natl. Acad. Sci. U. S. A. *70*, 765–8.
231. Amos, L.A., and Schlieper, D. (2005). Microtubules and maps. Adv. Protein Chem. *71*, 257–298.
232. Fourest-Lieuvin, A., Peris, L., Gache, V., Garcia-Saez, I., Juillan-Binard, C., Lantez, V., and Job, D. (2006). Microtubule regulation in mitosis: tubulin phosphorylation by the cyclin-dependent kinase Cdk1. Mol Biol Cell *17*, 1041–1050.
233. Masson, D., and Kreis, T.E. (1995). Binding of E-MAP-115 to microtubules is regulated by cell cycle-dependent phosphorylation. J. Cell Biol. *131*, 1015–1024.
234. Drewes, G., Ebneth, A., Preuss, U., Mandelkow, E.M., and Mandelkow, E. (1997). MARK, a novel family of protein kinases that phosphorylate microtubule-associated proteins and trigger microtubule disruption. Cell *89*, 297–308.
235. Ookata, K., Hisanaga, S.I., Bulinski, J.C., Murofushi, H., Aizawa, H., Itoh, T.J., Hotani, H., Okumura, E., Tachibana, K., and Kishimoto, T. (1995). Cyclin B interaction with microtubule-associated protein 4 (MAP4) targets p34(cdc2) kinase to microtubules and is a potential regulator of M-phase microtubule dynamics. J. Cell Biol. *128*, 849–862.
236. Hoffman, A., Taleski, G., and Sontag, E. (2017). The protein serine/threonine phosphatases PP2A, PP1 and calcineurin: A triple threat in the regulation of the neuronal cytoskeleton. Mol. Cell. Neurosci.
237. Fernandez, J., Portilho, D.M., Danckaert, A., Munier, S., Becker, A., Roux, P., Zambo, A., Shorte, S., Jacob, Y., Vidalain, P.O., *et al.* (2015). Microtubule-associated proteins 1 (MAP1) promote human immunodeficiency virus type I (HIV-1) intracytoplasmic routing to the nucleus. J. Biol. Chem. *290*, 4631–4646.
238. Andrieux, A., Salin, P.A., Vernet, M., Kujala, P., Baratier, J., Gory-Fauré, S., Bosc, C., Pointu, H., Proietto, D., Schweitzer, A., *et al.* (2002). The suppression of brain cold-stable microtubules in mice induces synaptic defects associated with neuroleptic-sensitive behavioral disorders. Genes Dev. *16*, 2350–2364.
239. Bosc, C., Andrieux, A., and Job, D. (2003). STOP Proteins. Biochemistry *42*, 12125–12132.
240. Zhou, Y., Yang, S., Mao, T., and Zhang, Z. (2015). MAPanalyzer: a novel online tool for analyzing microtubule-associated proteins. Database J. Biol. Databases Curation *2015*, bav108.
241. Madden, T. (2013). The BLAST sequence analysis tool. BLAST Seq. Anal. Tool, 1–17.
242. Hirokawa, N., and Tanaka, Y. (2015). Kinesin superfamily proteins (KIFs): Various functions and their relevance for important phenomena in life and diseases. Exp. Cell Res. *334*, 16–25.
243. Goulet, A., Behnke-Parks, W.M., Sindelar, C. V., Major, J., Rosenfeld, S.S., and Moores, C.A. (2012). The structural basis of force generation by the mitotic motor kinesin-5. J. Biol. Chem. *287*, 44654–44666.
244. Rice, S., Lin, A.W., Safer, D., Hart, C.L., Naber, N., Carragher, B.O., Cain, S.M., Pechatnikova, E., Wilson-Kubalek, E.M., Whittaker, M., *et al.* (1999). A structural change in the kinesin motor protein that drives motility. Nature *402*, 778–84.
245. Vinogradova, M. V., Reddy, V.S., Reddy, A.S.N., Sablin, E.P., and Fletterick, R.J. (2004). Crystal structure kinesin regulated by Ca2+-calmodulin. J. Biol. Chem. *279*, 23504–23509.
246. Vale, R.D., Funatsu, T., Pierce, D.W., and Romberg, L. (1996). Direct observation of single kinesin molecules moving along microtubules. Nature *380*, 451–453.
247. Valentine, M.T., Fordyce, P.M., Krzysiak, T.C., Gilbert, S.P., and Block, S.M. (2006). Individual dimers of the mitotic kinesin motor Eg5 step processively and support substantial loads in vitro. Nat. Cell Biol. *8*, 470–6.
248. Manning, A.L., Ganem, N.J., Bakhoum, S.F., Wagenbach, M., Wordeman, L., and Compton, D.A. (2007). The Kinesin-13 Proteins Kif2a, Kif2b, and Kif2c/MCAK Have Distinct Roles during Mitosis in Human Cells. Mol. Biol. Cell *18*, 2970–2979.
249. Desai, A., Verma, S., Mitchison, T.J., and Walczak, C.E. (1999). Kin I kinesins are microtubule-destabilizing enzymes. Cell *96*, 69–78.
250. Seog, D.H., Lee, D.H., and Lee, S.K. (2004). Molecular Motor Proteins of the Kinesin Superfamily Proteins (KIFs): Structure, Cargo and Disease. J. Korean Med. Sci. *19*, 1–7.
251. Jana, B., Hyeon, C., and Onuchic, J.N. (2012). The Origin of Minus-end Directionality and Mechanochemistry

of Ncd Motors. PLoS Comput. Biol. *8*.

252. Svoboda, K., Schmidt, C.F., Schnapp, B.J., and Block, S.M. (1993). Direct Observation of Kinesin Stepping by Optical Trapping Interferometry. NatureNature *365*, 721–727.
253. Schnitzer, M.J., and Block, S.M. (1997). Kinesin hydrolyses one ATP per 8-nm step. Nature *388*, 386–90.
254. Coy, D.L., Wagenbach, M., and Howard, J. (1999). Kinesin takes one 8-nm step for each ATP that it hydrolyzes. J. Biol. Chem. *274*, 3667–3671.
255. Hua, W., Young, E.C., Fleming, M.L., and Gelles, J. (1997). Coupling of kinesin steps to ATP hydrolysis. Nature *388*, 390–393.
256. Asbury, C.L. (2005). Kinesin: World's tiniest biped. Curr. Opin. Cell Biol. *17*, 89–97.
257. Howard, J., Hudspeth, A.J., and Vale, R.D. (1989). Movement of microtubules by single kinesin molecules. Nature *342*, 154–158.
258. Block, S.M., Goldstein, L.S., and Schnapp, B.J. (1990). Bead movement by single kinesin molecules studied with optical tweezers. Nature *348*, 348–52.
259. Visscher, K., Schnitzer, M.J., and Block, S.M. (1999). Single kinesin molecules studied with a molecular force clamp. Nature *400*, 184–9.
260. Thiede, C., Fridman, V., Gerson-Gurwitz, A., Gheber, L., and Schmidt, C.F. (2012). Regulation of bi-directional movement of single kinesin-5 Cin8 molecules. Bioarchitecture *2*, 70–74.
261. Roostalu, J., Hentrich, C., Bieling, P., Telley, I.A., Schiebel, E., and Surrey, T. (2011). Directional Switching of the Kinesin Cin8 Through Motor Coupling. Science (80-.). *332*, 94–99.
262. Shapira, O., and Gheber, L. (2016). Motile properties of the bi-directional kinesin-5 Cin8 are affected by phosphorylation in its motor domain. Sci. Rep. *6*, 25597.
263. Wozniak, M.J., Milner, R., and Allan, V. (2004). N-terminal kinesins: Many and various. Traffic *5*, 400–410.
264. Roberts, A.J., Kon, T., Knight, P.J., Sutoh, K., and Burgess, S. a (2013). Functions and mechanics of dynein motor proteins. Nat. Rev. Mol. Cell Biol. *14*, 713–26.
265. Gibbons, I.R. (1963). Studies on the protein components of cilia from Tetrahymena Pyriformis. Proc. Natl. Acad. Sci. U. S. A. *50*, 1002–1010.
266. Hirokawa, N., and Takemura, R. (2004). Molecular motors in neuronal development, intracellular transport and diseases. Curr. Opin. Neurobiol. *14*, 564–573.
267. Vallee, R.B., Williams, J.C., Varma, D., and Barnhart, L.E. (2004). Dynein: An Ancient Motor Protein Involved in Multiple Modes of Transport. J. Neurobiol. *58*, 189–200.
268. Ishikawa, T. (2012). Structural biology of cytoplasmic and axonemal dyneins. J. Struct. Biol. *179*, 229–234.
269. Burgess, S. a, Walker, M.L., Sakakibara, H., Knight, P.J., and Oiwa, K. (2003). Dynein structure and power stroke. Nature *421*, 715–718.
270. Samsó, M., and Koonce, M.P. (2004). 25 Å resolution structure of a cytoplasmic dynein motor reveals a seven-member planar ring. J. Mol. Biol. *340*, 1059–1072.
271. Serohijos, A.W., Chen, Y., Ding, F., Elston, T.C., and Dokholyan, N. V (2006). A structural model reveals energy transduction in dynein. Proc Natl Acad Sci U S A *103*, 18540–18545.
272. Vaughan, K.T., and Vallee, R.B. (1995). Cytoplasmic dynein binds dynactin through a direct interaction between the intermediate chains and p150Glued. J. Cell Biol. *131*, 1507–1516.
273. Vaughan, P.S., Leszyk, J.D., and Vaughan, K.T. (2001). Cytoplasmic Dynein Intermediate Chain Phosphorylation Regulates Binding to Dynactin. J. Biol. Chem. *276*, 26171–26179.
274. Kardon, J.R., and Vale, R.D. (2009). Regulators of the cytoplasmic dynein motor. Nat. Rev. Mol. Cell Biol. *10*, 854–865.
275. Chowdhury, S., Ketcham, S. a, Schroer, T. a, and Lander, G.C. (2015). Structural organization of the dynein–dynactin complex bound to microtubules. Nat. Struct. Mol. Biol. *advance on*, 1–6.
276. Karki, S., and Holzbaur, E.L. (1999). Cytoplasmic dynein and dynactin in cell division and intracellular transport. Curr. Opin. Cell Biol. *11*, 45–53.
277. Chen, X.-J., Xu, H., Cooper, H.M., and Liu, Y. (2014). Cytoplasmic dynein: a key player in neurodegenerative and neurodevelopmental diseases. Sci. China Life Sci. *57*, 372–377.
278. Krysten J. Palmer, Helen Hughes, and D.J.S. (2009). Specificity of Cytoplasmic Dynein Subunits in Discrete Membrane-trafficking Steps. Mol. Biol. Cell *82*, 327–331.
279. Vaisberg, E.A., Grissom, P.M., and McIntosh, J.R. (1996). Mammalian cells express three distinct dynein heavy

chains that are localized to different cytoplasmic organelles. J. Cell Biol. *133*, 831–842.

280. Gibbons, B.H., Asai, D.J., Tang, W.-J.Y., Hays, T.S., and Gibbons, I.R. (1994). Phylogeny and expression of axonemal and cytoplasmic dynein genes in sea urchins. Mol. Biol. Cell *5*, 57–70.
281. Criswell, P.S., Ostrowski, L.E., and Asai, D.J. (1996). A novel cytoplasmic dynein heavy chain: expression of DHC1b in mammalian ciliated epithelial cells. J. Cell Sci. *109 (Pt 7*, 1891–8.
282. Porter, M.E., Bower, R., Knott, J.A., Byrd, P., and Dentler, W. (1999). Cytoplasmic dynein heavy chain 1b is required for flagellar assembly in Chlamydomonas. Mol. Biol. Cell *10*, 693–712.
283. DeWitt, M.A., Chang, A.Y., Combs, P.A., and Yildiz, A. (2012). Cytoplasmic dynein moves through uncoordinated stepping of the AAA+ ring domains. Science *335*, 221–5.
284. Qiu, W., Derr, N.D., Goodman, B.S., Villa, E., Wu, D., Shih, W., and Reck-Peterson, S.L. (2012). Dynein achieves processive motion using both stochastic and coordinated stepping. Nat. Struct. Mol. Biol. *19*, 193–200.
285. Kollman, J.M., Merdes, A., Mourey, L., and Agard, D.A. (2011). Microtubule nucleation by γ-tubulin complexes. Nat. Rev. Mol. Cell Biol. *12*, 709–21.
286. Meng, W., Mushika, Y., Ichii, T., and Takeichi, M. (2008). Anchorage of Microtubule Minus Ends to Adherens Junctions Regulates Epithelial Cell-Cell Contacts. Cell *135*, 948–959.
287. Baines, A.J., Bignone, P.A., King, M.D.A., Maggs, A.M., Bennett, P.M., Pinder, J.C., and Phillips, G.W. (2009). The CKK domain (DUF1781) binds microtubules and defines the CAMSAP/ssp4 family of animal proteins. Mol. Biol. Evol. *26*, 2005–2014.
288. Goodwin, S.S., and Vale, R.D. (2010). Patronin Regulates the Microtubule Network by Protecting Microtubule Minus Ends. Cell *143*, 263–274.
289. Gimona, M., Djinovic-Carugo, K., Kranewitter, W.J., and Winder, S.J. (2002). Functional plasticity of CH domains. FEBS Lett. *513*, 98–106.
290. Akhmanova, A., and Hoogenraad, C.C. (2015). Microtubule minus-end-targeting proteins. Curr. Biol. *25*, R162–R171.
291. Perez, F., Diamantopoulos, G.S., Stalder, R., and Kreis, T.E. (1999). CLIP-170 highlights growing microtubule ends in vivo. Cell *96*, 517–527.
292. Akhmanova, A., and Steinmetz, M.O. (2010). Microtubule+ TIPs at a glance. J. Cell Sci. *123*, 3415–3419.
293. Maurer, S.P., Fourniol, F.J., Bohner, G., Moores, C.A., and Surrey, T. (2012). EBs recognize a nucleotide-dependent structural cap at growing microtubule ends. Cell *149*, 371–382.
294. Zanic, M., Stear, J.H., Hyman, A.A., and Howard, J. (2009). EB1 recognizes the nucleotide state of tubulin in the microtubule lattice. PLoS One *4*.
295. Maurer, S.P., Bieling, P., Cope, J., Hoenger, A., and Surrey, T. (2011). GTPgammaS microtubules mimic the growing microtubule end structure recognized by end-binding proteins (EBs). Proc. Natl. Acad. Sci. U. S. A. *108*, 3988–3993.
296. Kumar, P., and Wittmann, T. (2012). +TIPs: SxIPping along microtubule ends. Trends Cell Biol. *22*, 418–428.
297. Galjart, N. (2010). Plus-end-tracking proteins and their interactions at microtubule ends. Curr. Biol. *20*.
298. Su, L.K., and Qi, Y. (2001). Characterization of human MAPRE genes and their proteins. Genomics *71*, 142–9.
299. Tirnauer, J.S., and Bierer, B.E. (2000). EB1 proteins regulate microtubule dynamics, cell polarity, and chromosome stability. J. Cell Biol. *149*, 761–766.
300. Alberico, E.O., Zhu, Z.C., Wu, Y.F.O., Gardner, M.K., Kovar, D.R., and Goodson, H. V. (2016). Interactions between the Microtubule Binding Protein EB1 and F-Actin. J. Mol. Biol. *428*, 1304–1314.
301. Dugina, V., Alieva, I., Khromova, N., Kireev, I., Gunning, P.W., and Kopnin, P. (2015). Interaction of microtubules with the actin cytoskeleton via cross-talk of EB1-containing +TIPs and γ-actin in epithelial cells. Oncotarget *7*, 18–20.
302. Stroud, M.J., Nazgiewicz, A., McKenzie, E.A., Wang, Y., Kammerer, R.A., Ballestrem, C., Alves-Silva, J., Sanchez-Soriano, N., Beaven, R., Klein, M., *et al.* (2014). GAS2-like proteins mediate communication between microtubules and actin through interactions with end-binding proteins. J. Cell Sci. *127*, 2672–82.
303. Jimenez-Mateos, E.M., Paglini, G., Gonzalez-Billault, C., Caceres, A., and Avila, J. (2005). End binding protein-1 (EB1) complements microtubule-associated protein-1B during axonogenesis. J. Neurosci. Res. *80*, 350–359.
304. De Groot, C.O., Jelesarov, I., Damberger, F.F., Bjelić, S., Schärer, M.A., Bhavesh, N.S., Grigoriev, I., Buey, R.M., Wüthrich, K., Capitani, G., *et al.* (2010). Molecular insights into mammalian end-binding protein

heterodimerization. J. Biol. Chem. *285*, 5802–5814.

305. Nakagawa, H., Koyama, K., Murata, Y., Morito, M., Akiyama, T., and Nakamura, Y. (2000). EB3, a novel member of the EB1 family preferentially expressed in the central nervous system, binds to a CNS-specific APC homologue. Oncogene *19*, 210–216.
306. Zhang, R., Alushin, G.M., Brown, A., and Nogales, E. (2015). Mechanistic origin of microtubule dynamic instability and its modulation by EB proteins. Cell *162*, 849–859.
307. Maurer, S.P., Cade, N.I., Bohner, G., Gustafsson, N., Boutant, E., and Surrey, T. (2014). EB1 accelerates two conformational transitions important for microtubule maturation and dynamics. Curr. Biol. *24*, 372–384.
308. Vitre, B., Coquelle, F.M., Heichette, C., Garnier, C., Chrétien, D., and Arnal, I. (2008). EB1 regulates microtubule dynamics and tubulin sheet closure in vitro. Nat. Cell Biol. *10*, 415–421.
309. Duellberg, C., Cade, N.I., Holmes, D., and Surrey, T. (2016). The size of the EB cap determines instantaneous microtubule stability. Elife *5*.
310. Carlier, M.F., Hill, T.L., and Chen, Y. (1984). Interference of GTP hydrolysis in the mechanism of microtubule assembly: an experimental study. Proc. Natl. Acad. Sci. U. S. A. *81*, 771–775.
311. Gard, D.L., and Kirschner, M.W. (1987). Microtubule assembly in cytoplasmic extracts of Xenopus oocytes and eggs. J. Cell Biol. *105*, 2091–2201.
312. Rickard, J.E., and Kreis, T.E. (1990). Identification of a novel nucleotide-sensitive microtubule-binding protein in HeLa cells. J. Cell Biol. *110*, 1623–1633.
313. Pierre, P., Scheel, J., Rickard, J.E., and Kreis, T.E. (1992). CLIP-170 links endocytic vesicles to microtubules. Cell *70*, 887–900.
314. Weisbrich, A., Honnappa, S., Jaussi, R., Okhrimenko, O., Frey, D., Jelesarov, I., Akhmanova, A., and Steinmetz, M.O. (2007). Structure-function relationship of CAP-Gly domains. Nat. Struct. Mol. Biol. *14*, 959–967.
315. Mishima, M., Maesaki, R., Kasa, M., Watanabe, T., Fukata, M., Kaibuchi, K., and Hakoshima, T. (2007). Structural basis for tubulin recognition by cytoplasmic linker protein 170 and its autoinhibition. Proc. Natl. Acad. Sci. U. S. A. *104*, 10346–10351.
316. Lansbergen, G., Komarova, Y., Modesti, M., Wyman, C., Hoogenraad, C.C., Goodson, H. V., Lemaitre, R.P., Drechsel, D.N., Van Munster, E., Gadella, T.W.J., *et al.* (2004). Conformational changes in CLIP-170 regulate its binding to microtubules and dynactin localization. J. Cell Biol. *166*, 1003–1014.
317. Gupta, K.K., Paulson, B.A., Folker, E.S., Charlebois, B., Hunt, A.J., and Goodson, H. V. (2009). Minimal plus-end tracking unit of the cytoplasmic linker protein CLIP-170. J. Biol. Chem. *284*, 6735–6742.
318. Hayashi, I., Plevin, M.J., and Ikura, M. (2007). CLIP170 autoinhibition mimics intermolecular interactions with p150Glued or EB1. Nat. Struct. Mol. Biol. *14*, 980–981.
319. Bieling, P., Kandels-Lewis, S., Telley, I.A., Van Dijk, J., Janke, C., and Surrey, T. (2008). CLIP-170 tracks growing microtubule ends by dynamically recognizing composite EB1/tubulinbinding sites. J. Cell Biol. *183*, 1223–1233.
320. Ligon, L.A., Shelly, S.S., Tokito, M.K., and Holzbaur, E.L.F. (2006). Microtubule binding proteins CLIP-170, EB1, and p150Glued form distinct plus-end complexes. FEBS Lett. *580*, 1327–1332.
321. Akhmanova, A., Mausset-Bonnefont, A.L., Van Cappellen, W., Keijzer, N., Hoogenraad, C.C., Stepanova, T., Drabek, K., Van Der Wees, J., Mommaas, M., Onderwater, J., *et al.* (2005). The microtubule plus-end-tracking protein CLIP-170 associates with the spermatid manchette and is essential for spermatogenesis. Genes Dev. *19*, 2501–2515.
322. Coquelle, F.M., Caspi, M., Cordelières, F.P., Dompierre, J.P., Dujardin, D.L., Koifman, C., Martin, P., Hoogenraad, C.C., Akhmanova, A., Galjart, N., *et al.* (2002). LIS1 , CLIP-170 ' s Key to the Dynein / Dynactin Pathway. Mol. Cell. Biol. *22*, 3089–3102.
323. Lewkowicz, E., Herit, F., Clainche, C. Le, Bourdoncle, P., Perez, F., and Niedergang, F. (2008). The microtubule-binding protein CLIP-170 coordinates mDia1 and actin reorganization during CR3-mediated phagocytosis. J. Cell Biol. *183*, 1287–1298.
324. Henty-Ridilla, J.L., Rankova, A., Eskin, J.A., Kenny, K., and Goode, B.L. (2016). Accelerated actin filament polymerization from microtubule plus ends. Science (80-.). *352*, 1004–1009.
325. Stepanova, T., Smal, I., Van Haren, J., Akinci, U., Liu, Z., Miedema, M., Limpens, R., Van Ham, M., Van Der Reijden, M., Poot, R., *et al.* (2010). History-dependent catastrophes regulate axonal microtubule behavior. Curr. Biol. *20*, 1023–1028.
326. Fukata, M., Watanabe, T., Noritake, J., Nakagawa, M., Yamaga, M., Kuroda, S., Matsuura, Y., Iwamatsu, A., Perez, F., and Kaibuchi, K. (2002). Rac1 and Cdc42 capture microtubules through IQGAP1 and CLIP-170. Cell

109, 873–885.

327. Komarova, Y.A., Akhmanova, A.S., Kojima, S.I., Galjart, N., and Borisy, G.G. (2002). Cytoplasmic linker proteins promote microtubule rescue in vivo. J. Cell Biol. *159*, 589–599.

328. Hoogenraad, C.C., Akhmanova, a, Grosveld, F., De Zeeuw, C.I., and Galjart, N. (2000). Functional analysis of CLIP-115 and its binding to microtubules. J. Cell Sci. *113 (Pt 1*, 2285–97.

329. De Zeeuw, C.I., Hoogenraad, C.C., Goedknegt, E., Hertzberg, E., Neubauer, A., Grosveld, F., and Galjartt, N. (1997). CLIP-115, a novel brain-specific cytoplasmic linker protein, mediates the localization of dendritic lamellar bodies. Neuron *19*, 1187–1199.

330. Francke, U. (1999). Williams-Beuren syndrome: Genes and mechanisms. Hum. Mol. Genet. *8*, 1947–1954.

331. Hoogenraad, C.C., Akhmanova, A., Galjart, N., and De Zeeuw, C.I. (2004). LIMK1 and CLIP-115: Linking cytoskeletal defects to Williams Syndrome. BioEssays *26*, 141–150.

332. Hamosh, A., Scott, A.F., Amberger, J.S., Bocchini, C.A., and McKusick, V.A. (2005). Online Mendelian Inheritance in Man (OMIM), a knowledgebase of human genes and genetic disorders. Nucleic Acids Res. *33*.

333. Hoogenraad, C.C., Koekkoek, B., Akhmanova, A., Krugers, H., Dortland, B., Miedema, M., van Alphen, A., Kistler, W.M., Jaegle, M., Koutsourakis, M., *et al.* (2002). Targeted mutation of Cyln2 in the Williams syndrome critical region links CLIP-115 haploinsufficiency to neurodevelopmental abnormalities in mice. Nat. Genet. *32*, 116–27.

334. Akhmanova, A., Hoogenraad, C.C., Drabek, K., Stepanova, T., Dortland, B., Verkerk, T., Vermeulen, W., Burgering, B.M., De Zeeuw, C.I., Grosveld, F., *et al.* (2001). CLASPs are CLIP-115 and -170 associating proteins involved in the regional regulation of microtubule dynamics in motile fibroblasts. Cell *104*, 923–935.

335. Al-Bassam, J., Kim, H., Brouhard, G., van Oijen, A., Harrison, S.C., and Chang, F. (2010). CLASP promotes microtubule rescue by recruiting tubulin dimers to the microtubule. Dev. Cell *19*, 245–258.

336. Drabek, K., van Ham, M., Stepanova, T., Draegestein, K., van Horssen, R., Sayas, C.L., Akhmanova, A., ten Hagen, T., Smits, R., Fodde, R., *et al.* (2006). Role of CLASP2 in Microtubule Stabilization and the Regulation of Persistent Motility. Curr. Biol. *16*, 2259–2264.

337. Patel, K., Nogales, E., and Heald, R. (2012). Multiple domains of human CLASP contribute to microtubule dynamics and organization in vitro and in Xenopus egg extracts. Cytoskeleton *69*, 155–165.

338. Al-Bassam, J., Larsen, N.A., Hyman, A.A., and Harrison, S.C. (2007). Crystal Structure of a TOG Domain: Conserved Features of XMAP215/Dis1-Family TOG Domains and Implications for Tubulin Binding. Structure *15*, 355–362.

339. Slep, K.C., and Vale, R.D. (2007). Structural Basis of Microtubule Plus End Tracking by XMAP215, CLIP-170, and EB1. Mol. Cell *27*, 976–991.

340. Ayaz, P., Ye, X., Huddleston, P., Brautigam, C.A., and Rice, L.M. (2012). A TOG: -tubulin Complex Structure Reveals Conformation-Based Mechanisms for a Microtubule Polymerase. Science (80-.). *337*, 857–860.

341. Widlund, P.O., Stear, J.H., Pozniakovsky, A., Zanic, M., Reber, S., Brouhard, G.J., Hyman, A.A., and Howard, J. (2011). XMAP215 polymerase activity is built by combining multiple tubulin-binding TOG domains and a basic lattice-binding region. Proc. Natl. Acad. Sci. U. S. A. *108*, 2741–6.

342. Leano, J.B., Rogers, S.L., and Slep, K.C. (2013). A cryptic TOG domain with a distinct architecture underlies CLASP-dependent bipolar spindle formation. Structure *21*, 939–950.

343. Maki, T., Grimaldi, A.D., Fuchigami, S., Kaverina, I., and Hayashi, I. (2015). CLASP2 has two distinct TOG domains that contribute differently to microtubule dynamics. J. Mol. Biol. *427*, 2379–2395.

344. Duncan, J.E., Lytle, N.K., Zuniga, A., and Goldstein, L.S.B. (2013). The Microtubule Regulatory Protein Stathmin Is Required to Maintain the Integrity of Axonal Microtubules in Drosophila. PLoS One *8*.

345. Barbier, P., Dorl??ans, A., Devred, F., Sanz, L., Allegro, D., Alfonso, C., Knossow, M., Peyrot, V., and Andreu, J.M. (2010). Stathmin and interfacial microtubule inhibitors recognize a naturally curved conformation of tubulin dimers. J. Biol. Chem. *285*, 31672–31681.

346. Ravelli, R.B.G., Gigant, B., Curmi, P.A., Jourdain, I., Lachkar, S., Sobel, A., and Knossow, M. (2004). Insight into tubulin regulation from a complex with colchicine and a stathmin-like domain. Nature *428*, 198–202.

347. Mimori-Kiyosue, Y., Grigoriev, I., Lansbergen, G., Sasaki, H., Matsui, C., Severin, F., Galjart, N., Grosveld, F., Vorobjev, I., Tsukita, S., *et al.* (2005). CLASP1 and CLASP2 bind to EB1 and regulate microtubule plus-end dynamics at the cell cortex. J. Cell Biol. *168*, 141–153.

348. Lansbergen, G., Grigoriev, I., Mimori-Kiyosue, Y., Ohtsuka, T., Higa, S., Kitajima, I., Demmers, J., Galjart, N., Houtsmuller, A.B., Grosveld, F., *et al.* (2006). CLASPs Attach Microtubule Plus Ends to the Cell Cortex through a Complex with LL5β. Dev. Cell *11*, 21–32.

349. Beurel, E., Grieco, S.F., and Jope, R.S. (2015). Glycogen synthase kinase-3 (GSK3): Regulation, actions, and diseases. Pharmacol. Ther. *148*, 114–131.

350. Kumar, P., Lyle, K.S., Gierke, S., Matov, A., Danuser, G., and Wittmann, T. (2009). GSK33 phosphorylation modulates CLASP-microtubule association and lamella microtubule attachment. J. Cell Biol. *184*, 895–908.

351. Linding, R., Jensen, L.J., Ostheimer, G.J., van Vugt, M.A.T.M., Jørgensen, C., Miron, I.M., Diella, F., Colwill, K., Taylor, L., Elder, K., *et al.* (2007). Systematic Discovery of In Vivo Phosphorylation Networks. Cell *129*, 1415–1426.

352. Zumbrunn, J., Kinoshita, K., Hyman, A.A., and Näthke, I.S. (2001). Binding of the adenomatous polyposis coli protein to microtubules increases microtubule stability and is regulated by GSK3β phosphorylation. Curr. Biol. *11*, 44–49.

353. Hergovich, A., Lisztwan, J., Thoma, C.R., Wirbelauer, C., Barry, R.E., and Krek, W. (2006). Priming-dependent phosphorylation and regulation of the tumor suppressor pVHL by glycogen synthase kinase 3. Mol. Cell. Biol. *26*, 5784–96.

354. Cho, J.H., and Johnson, G.V.W. (2003). Glycogen synthase kinase 3β phosphorylates tau at both primed and unprimed sites: Differential impact on microtubule binding. J. Biol. Chem. *278*, 187–193.

355. Trivedi, N., Marsh, P., Goold, R.G., Wood-Kaczmar, A., and Gordon-Weeks, P.R. (2005). Glycogen synthase kinase-3beta phosphorylation of MAP1B at Ser1260 and Thr1265 is spatially restricted to growing axons. J. Cell Sci. *118*, 993–1005.

356. Basu, S., Sladecek, S., Pemble, H., Wittmann, T., Slotman, J.A., Van Cappellen, W., Brenner, H.R., and Galjart, N. (2014). Acetylcholine receptor (AChR) clustering is regulated both by glycogen synthase kinase 3β (GSK3β)-dependent Phosphorylation and the level of CLIP-associated protein 2 (CLASP2) mediating the capture of microtubule plus-ends. J. Biol. Chem. *289*, 30857–30867.

357. Watanabe, T., Noritake, J., Kakeno, M., Matsui, T., Harada, T., Wang, S., Itoh, N., Sato, K., Matsuzawa, K., Iwamatsu, A., *et al.* (2009). Phosphorylation of CLASP2 by GSK-3beta regulates its interaction with IQGAP1, EB1 and microtubules. J. Cell Sci. *122*, 2969–2979.

358. Cassimeris, L., and Spittle, C. (2001). Regulation of microtubule-associated proteins. Int. Rev. Cytol. *210*, 163–226.

359. Kumar, P., Chimenti, M.S., Pemble, H., Schönichen, A., Thompson, O., Jacobson, M.P., and Wittmann, T. (2012). Multisite phosphorylation disrupts arginine-glutamate salt bridge networks required for binding of cytoplasmic linker-associated protein 2 (CLASP2) to end-binding protein 1 (EB1). J. Biol. Chem. *287*, 17050–17064.

360. Wittmann, T., and Waterman-Storer, C.M. (2005). Spatial regulation of CLASP affinity for microtubules by Rac1 and GSK3β in migrating epithelial cells. J. Cell Biol. *169*, 929–939.

361. Kobayashi, T., Hino, S., Oue, N., Asahara, T., Zollo, M., Yasui, W., and Kikuchi, A. (2006). Glycogen synthase kinase 3 and h-prune regulate cell migration by modulating focal adhesions. Mol. Cell. Biol. *26*, 898–911.

362. Mimori-Kiyosue, Y., Grigoriev, I., Sasaki, H., Matsui, C., Akhmanova, A., Tsukita, S., and Vorobjev, I. (2006). Mammalian CLASPs are required for mitotic spindle organization and kinetochore alignment. Genes to Cells *11*, 845–857.

363. Bratman, S. V., and Chang, F. (2007). Stabilization of Overlapping Microtubules by Fission Yeast CLASP. Dev. Cell *13*, 812–827.

364. Mitchison, T.J. (1989). Polewards microtubule flux in the mitotic spindle: Evidence from photoactivation of fluorescence. J. Cell Biol. *109*, 637–652.

365. Maiato, H., Khodjakov, A., and Rieder, C.L. (2005). Drosophila CLASP is required for the incorporation of microtubule subunits into fluxing kinetochore fibres. Nat. Cell Biol. *7*, 42–47.

366. Beffert, U., Dillon, G.M., Sullivan, J.M., Stuart, C.E., Gilbert, J.P., Kambouris, J. a., and Ho, a. (2012). Microtubule Plus-End Tracking Protein CLASP2 Regulates Neuronal Polarity and Synaptic Function. J. Neurosci. *32*, 13906–13916.

367. Hur, E.M., Saijilafu, Lee, B.D., Kim, S.J., Xu, W.L., and Zhou, F.Q. (2011). GSK3 controls axon growth via CLASP-mediated regulation of growth cone microtubules. Genes Dev. *25*, 1968–1981.

368. Brooks, B.R., Bruccoleri, R.E., Olafson, B.D., States, D.J., Swaminathan, S., and Karplus, M. (1983). CHARMM: A program for macromolecular energy, minimization, and dynamics calculations. J. Comput. Chem. *4*, 187–217.

369. McCammon, J.A., Gelin, B.R., and Karplus, M. (1977). Dynamics of folded proteins. Nature *267*, 585–590.

370. Frauenfelder, H., Petsko, G.A., and Tsernoglou, D. (1979). Temperature-dependent X-ray diffraction as a probe of protein structural dynamics. Nature *280*, 558–563.

371. Shaw, D.E., Bowers, K.J., Chow, E., Eastwood, M.P., Ierardi, D.J., Klepeis, J.L., Kuskin, J.S., Larson, R.H., Lindorff-Larsen, K., Maragakis, P., *et al.* (2009). Millisecond-scale molecular dynamics simulations on Anton. Proc. Conf. High Perform. Comput. Netw. Storage Anal. SC 09, 1.

372. Linge, J.P., Williams, M.A., Spronk, C.A.E.M., Bonvin, A.M.J.J., and Nilges, M. (2003). Refinement of protein structures in explicit solvent. Proteins Struct. Funct. Genet. *50*, 496–506.

373. Ma, J., Sigler, P.B., Xu, Z., and Karplus, M. (2000). A dynamic model for the allosteric mechanism of GroEL1. J. Mol. Biol. *302*, 303–313.

374. Tai, K., Shen, T., Börjesson, U., Philippopoulos, M., McCammon, J.A., Borjesson, U., Philippopoulos, M., and McCammon, J.A. (2001). Analysis of a 10-ns Molecular Dynamics Simulation of Mouse Acetylcholinesterase. Biophys J *81*, 715–724.

375. Wong, C.F., and McCammon, J.A. (2003). Protein simulation and drug design. Adv. Protein Chem. *66*, 87–121.

376. Day, R., and Daggett, V. (2003). All-atom simulations of protein folding and unfolding. Adv. Protein Chem. *66*, 373–403.

377. Kim, H.W., Shen, T.J., Sun, D.P., Ho, N.T., Madrid, M., Tam, M.F., Zou, M., Cottam, P.F., and Ho, C. (1994). Restoring allosterism with compensatory mutations in hemoglobin. Proc. Natl. Acad. Sci. U. S. A. *91*, 11547–51.

378. Warshel, A. (2003). Computer Simulations of Enzyme Catalysis: Methods, Progress, and Insights. Annu. Rev. Biophys. Biomol. Struct. *32*, 425–443.

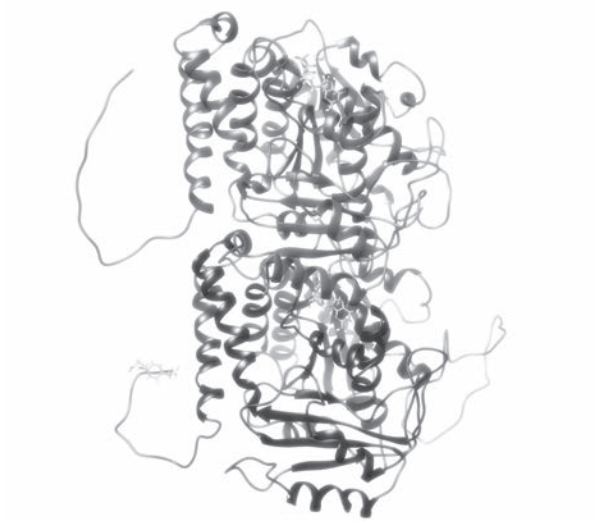

Chapter 2

Isolation of functional tubulin dimers and of tubulin-associated proteins from mammalian cells

Nuo Yu[1]*, **Luca Signorile**[1]*, Sreya Basu[1], Sophie Ottema[1], Joyce H. G. Lebbink[1,4], Kris Leslie[1], Ihor Smal[2], Dick Dekkers[3], Jeroen Demmers[3], and Niels Galjart[1#].

1) Department of Cell Biology and Genetics, Erasmus MC, P.O. Box 2040, 3000 CA Rotterdam, The Netherlands;
2) Biomedical Imaging Group Rotterdam, Erasmus Medical Center, 3015 GE, Rotterdam, The Netherlands;
3) Proteomics Centre, Erasmus MC, P.O. Box 2040, 3000 CA Rotterdam, The Netherlands;
4) Department of Radiation Oncology, ErasmusMC, Rotterdam, The Netherlands.

***: these authors contributed equally to the results described in this paper**
#: Author for correspondence: n.galjart@erasmusmc.nl

Current Biology 26(13):1728-36 (2016)

CellPress

Current Biology
Report

Isolation of Functional Tubulin Dimers and of Tubulin-Associated Proteins from Mammalian Cells

Nuo Yu,[1,5] Luca Signorile,[1,5] Sreya Basu,[1] Sophie Ottema,[1] Joyce H.G. Lebbink,[1,4] Kris Leslie,[1] Ihor Smal,[2] Dick Dekkers,[3] Jeroen Demmers,[3] and Niels Galjart[1,*]
[1]Department of Cell Biology and Genetics, Erasmus Medical Center, P.O. Box 2040, 3000 CA Rotterdam, the Netherlands
[2]Biomedical Imaging Group Rotterdam, Erasmus Medical Center, 3015 GE, Rotterdam, the Netherlands
[3]Proteomics Centre, Erasmus Medical Center, P.O. Box 2040, 3000 CA Rotterdam, the Netherlands
[4]Department of Radiation Oncology, Erasmus Medical Center, Rotterdam, the Netherlands
[5]Co-first author
*Correspondence: n.galjart@erasmusmc.nl
http://dx.doi.org/10.1016/j.cub.2016.04.069

SUMMARY

The microtubule (MT) cytoskeleton forms a dynamic filamentous network that is essential for many processes, including mitosis, cell polarity and shape, neurite outgrowth and migration, and ciliogenesis [1, 2]. MTs are built up of α/β-tubulin heterodimers, and their dynamic behavior is in part regulated by tubulin-associated proteins (TAPs). Here we describe a novel system to study mammalian tubulins and TAPs. We co-expressed equimolar amounts of triple-tagged α-tubulin and β-tubulin using a 2A "self-cleaving" peptide and isolated functional fluorescent tubulin dimers from transfected HEK293T cells with a rapid two-step approach. We also produced two mutant tubulins that cause brain malformations in tubulinopathy patients [3]. We then applied a paired mass-spectrometry-based method to identify tubulin-binding proteins in HEK293T cells and describe both novel and known TAPs. We find that CKAP5 and the CLASPs, which are MT plus-end-tracking proteins with TOG(L)-domains [4], bind tubulin efficiently, as does the Golgi-associated protein GCC185, which interacts with the CLASPs [5]. The N-terminal TOGL domain of CLASP1 contributes to tubulin binding and allows CLASP1 to function as an autonomous MT-growth-promoting factor. Interestingly, mutant tubulins bind less well to a number of TAPs, including CLASPs and GCC185, and incorporate less efficiently into cellular MTs. Moreover, expression of these mutants in cells impairs several MT-growth-related processes involving TAPs. Thus, stable tubulin-TAP interactions regulate MT nucleation and growth in cells. Combined, our results provide a resource for investigating tubulin interactions and functions and widen the spectrum of tubulin-related disease mechanisms.

RESULTS AND DISCUSSION

Production of Functional Tubulin in Mammalian Cells

Microtubules (MTs) are filaments composed α/β-tubulin heterodimers that interact in a head-to-tail manner to form protofilaments, 13 of which fold up through lateral interactions to make a hollow MT tube. Assembly, or disassembly, of a MT occurs by the addition, or removal, of tubulin dimers at the ends. One end of a MT, called the minus end, is often embedded in a protective structure such as the centrosome, whereas the plus end undergoes cycles of polymerization, pausing, and depolymerization, a behavior termed dynamic instability [6].

Functional (i.e., assembly-competent) tubulin can be purified from pig or cow brain tissue through repeated cycles of polymerization, high-speed sedimentation of MTs, and depolymerization [7]. Brain tubulin is widely used in in vitro studies, but since multiple α- and β-tubulin isotypes exist that are encoded by different genes [8], brain-derived MTs are of a mixed isotype composition. Efforts toward isolating recombinant tubulin isotypes are hampered by the fact that tubulin biosynthesis is quite complex, involving chaperones that bind to nascent tubulin polypeptides, cytosolic chaperonins (CCTs) that facilitate folding of intermediate tubulin monomers, and tubulin-specific folding cofactors that allow formation of native heterodimers [9]. Nevertheless, purified assembly-competent recombinant human tubulin was recently obtained from baculovirus-infected insect cells, allowing studies of isotype function [10]. However, non-cleavable affinity tags were placed at the C terminus of both the α- and β-tubulin subunits, and these may influence MT behavior. Furthermore, expression in insect cells precludes analysis of mammalian-specific tubulin-associated proteins (TAPs).

We designed a so-called "dual" tubulin expression construct (Figure 1A) for the production and isolation of recombinant tubulins in mammalian cells. This construct consists of a fusion cDNA encoding β-tubulin (TUBB3) followed by a short sequence encoding a P2A "self-cleaving" peptide [11] and triple-tagged α-tubulin (TUBA1A). The triple tag, which was placed at the N terminus, contains a biotin-recognition sequence (biotinylated by the bacterial BirA enzyme), a Sumo* substrate peptide (recognized by Sumo* protease), and GFP (Figure 1A, top). Upon translation of the "dual" construct mRNA, the short P2A peptide

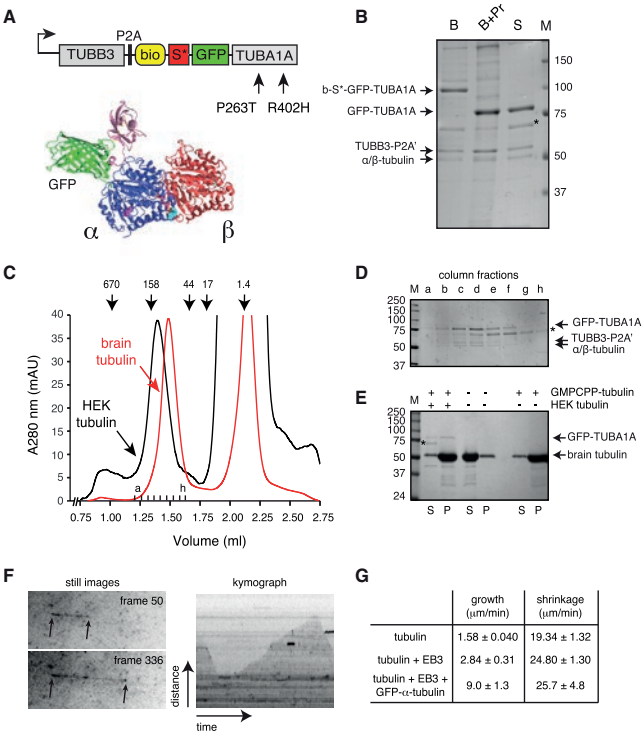

	growth (μm/min)	shrinkage (μm/min)
tubulin	1.58 ± 0.040	19.34 ± 1.32
tubulin + EB3	2.84 ± 0.31	24.80 ± 1.30
tubulin + EB3 + GFP-α-tubulin	9.0 ± 1.3	25.7 ± 4.8

Figure 1. Isolation of Functional Tubulin

(A) Schematic representation of the "dual" tubulin expression construct (top) and ribbon visualization of triple-tagged α/β-tubulin (bottom). The position of the single point mutations is indicated. In the model, α-tubulin is in blue, β-tubulin is in red, GFP is in green, Sumo* is in pink, and the bio tag is in orange. Amino acids P263 (cyan) and R402 (magenta) are indicated.

(B) Coomassie-stained gel showing purification and cleavage of tubulins, derived from "dual" tubulin expression in HEK293T cells. B, beads; B+Pr, Sumo* protease-treated beads; S, soluble proteins released from beads after Sumo* protease treatment; M, marker lane (molecular weights are indicated to the right). The asterisk indicates proteins of 70 kDa co-purifying with GFP-tubulin.

(C) Size-exclusion chromatography of GFP-tagged tubulin purified from HEK293T cells (HEK tubulin) and brain tubulin. Proteins were run separately on a Superdex 200 column, and elution profiles were monitored using absorbance at 280 nm. Size markers (M_r, indicated in kDa above the graph) were independently applied to the same column.

(D) Coomassie-stained gel of column fractions a–h from size-exclusion chromatography in (C). Dimeric GFP-tubulin peaks in fractions c and d, whereas complexes of GFP-tubulin with ~70 kDa HSPA proteins (*) peak in fractions e and f. M, marker lane (molecular weights are indicated to the left).

(E) Coomassie-stained gel showing result of MT sedimentation assay. After sedimentation, the supernatant (S) and pellet (P) fraction of each experiment was loaded on gel. M, marker lane (molecular weights are indicated to the left).

(F) In vitro MT polymerization assay showing that purified GFP-tubulin incorporates into MTs. The left panels show still images (see Movie S1 for the corresponding time-lapse experiment). Arrows indicate the MT ends of the GFP-TUBA1A-reconstituted fluorescent MT. The right panel is a kymograph (distance versus time plot) showing the dynamic behavior of a single MT.

(G) Parameters of dynamic MTs incubated with the indicated proteins. Data are shown ±SD. The average growth speed of MTs incubated with fluorescent α-tubulin is higher than that of MTs with EB3 only, whereas shrinkage speeds are similar. For comparison, see Figure 2E.

See also Figure S1 and Movie S1.

cleaves in an autocatalytic fashion, resulting in the production of equimolar amounts of TUBB3 with part of the P2A peptide at its C terminus (TUBB3-P2A) and tagged TUBA1A. Analysis of the modeled structure of the tagged α/β-tubulin dimer indicated that bio-Sumo*-GFP at the N terminus of α-tubulin is not in the vicinity of the α/β-tubulin dimer interface (Figure 1A, bottom). As controls for the "dual" construct, we made "single" bio-Sumo*-GFP-TUBA1A constructs, as well as another "dual" version in which we placed a bio-Sumo*-tag at the N terminus of β-tubulin instead of α-tubulin (Figure S1A).

We expressed "single" or "dual" constructs in HEK293T cells together with a plasmid encoding the BirA biotin ligase. Transfected cells were lysed, and biotinylated tubulin was purified using streptavidin-coated magnetic beads. After washing, proteins were cleaved off of the beads with Sumo* protease. SDS-PAGE followed by Coomassie staining (Figures 1B and S1B) or western blotting (Figures S1C and S1D) was used to examine protein expression, purification, and cleavage. We detected biotinylated and Sumo*-GFP-tagged α-tubulin (~110 kDa) on beads after purification. Cleavage with Sumo* protease resulted in the disappearance of the ~110 kDa protein and the appearance of GFP-α-tubulin (~85 kDa). In addition, we co-purified proteins of ~55kDa (Figures 1B and S1B), which were identified as tubulins by western blot (Figures S1C and S1D), and proteins of ~70 kDa (asterisks in Figures 1B and S1B), which are discussed below. When wild-type GFP-TUBA1A was expressed using the "dual" construct, the amount of β-tubulin that co-purified with GFP-TUBA1A was higher compared to the "single" construct due to increased TUBB3-P2A (compare Figure 1B with Figure S1B). This indicates that simultaneous synthesis of α- and β-tubulin polypeptides promotes dimer formation. Furthermore, tubulin dimer pull-down was less efficient when the biotin tag was placed at the N terminus of β-tubulin (data not shown). Taken together, these data suggest that our production and isolation method yields soluble recombinant tubulin and that dimer pull-down is most effective when α-tubulin is tagged.

The conformation of HEK293T-purified wild-type tubulin was examined by gel filtration. Compared to brain tubulin, which

eluted as a single dimeric species, HEK-purified GFP-tagged tubulin eluted slightly earlier (Figure 1C), consistent with the presence of a GFP moiety on tubulin. SDS-PAGE and Coomassie staining of eluted fractions suggested that this peak consisted of GFP-α-tubulin/β-tubulin heterodimers and complexes of GFP-tubulin with ~70 kDa proteins. A mass-spectrometry-based analysis of purified fractions revealed that the latter are HSPA heat shock proteins (data not shown). We next mixed HEK-purified tubulin with brain tubulin and GMPCPP (a slowly hydrolyzable GTP analog), allowed MTs to form, and performed a MT sedimentation assay. Approximately 70% of the total HEK-purified GFP-α-tubulin incorporated into MTs (Figure 1E). Furthermore, an in vitro total internal reflection fluorescence (TIRF)-microscopy-based assay [12], in which a mixture of purified GFP-TUBA1A, brain tubulin, and other components was added to a functionalized chamber with GMPCPP-stabilized MT seeds, revealed incorporation of fluorescent tubulin into dynamic MTs (Figure 1F; Movie S1). Thus, GFP-tagged tubulin produced using the "dual" strategy is assembly competent.

The importance of the different tubulin isotypes for neuronal function is underscored by the finding of mutations in the tubulin genes that give rise to a spectrum of human neuro-developmental disorders. These are collectively called tubulinopathies, and they arise because of problems in neuronal migration or differentiation [3]. To study mutant tubulins, we introduced two mutations (P263T and R402H) into TUBA1A (Figure 1A) that lead to problems in vivo [13] but that do not impair the capacity of mutant tubulins to form heterodimers in vitro [14]. Expression of the P263T and R402H mutants in differentiating N1E-115 cells indeed affected neurite outgrowth (Figures S1E and S1F). The tagged mutant tubulins were purified in soluble form from HEK293T cells and were cleaved with Sumo* protease, like wild-type tubulin (Figure S1D).

Collectively, our data demonstrate that the isolation of recombinant tubulin from transiently transfected HEK293T cells using a "dual" expression method followed by biotin-streptavidin pull-down and Sumo* protease cleavage yields assembly-competent fluorescent α/β-tubulin dimers. This approach can be further developed to study tubulin isotypes, also from different species, and the effect of tubulin mutations on MT behavior in vitro. It should be noted that tubulins undergo a number of posttranslational modifications (PTMs), some of which occur on the C-terminal residues of α- and β-tubulin [15]. In our "dual" expression approach, the C terminus of β-tubulin contains part of the P2A "self-cleaving" peptide; this is highly likely to impair C-terminal PTMs on this subunit.

Identification of Tubulin Associated Proteins

The dynamic behavior of MTs is regulated both by TAPs and MT-associated proteins (MAPs). The latter are often divided into subgroups according to their mode of association with MTs. For example, "classic" MAPs, like MAP2, MAP1B, and MAP4, bind along the MT lattice, motor proteins move along MTs, and MT plus-end-tracking proteins (+TIPs) associate specifically with the ends of growing MTs. Although many MAPs and +TIPs have been identified over the years, we are aware of only two unbiased approaches to detect TAPs. In the first, a tubulin affinity matrix was used; this strategy yielded 122 potential plant TAPs, of which one was a tubulin chaperone and six others, including plant CLASP, were similar to known MAPs [16]. In the second approach, a tubulin-antibody matrix was used to isolate TAPs from extracts of HeLa cells [17]; however, this indirect approach did not yield a high number of proteins.

To identify mammalian TAPs, we expressed tagged tubulins in HEK293T cells, purified them on streptavidin beads, and used a paired mass-spectrometry-based approach to screen for interaction partners. In this strategy, one sample contained proteins that were boiled off streptavidin beads and identified by mass spectrometry, whereas in a second sample the streptavidin-linked material was treated with Sumo* protease and the released proteins were analyzed by mass spectrometry. The rationale behind this approach is that proteins that show a strong preference for tubulin-bound streptavidin beads and that are efficiently released by Sumo* protease are likely to be TAPs. By contrast, contaminants such as endogenously biotinylated mitochondrial proteins should be present in the bead fractions of the different samples, including the negative control (Bio-Sumo*-GFP), but not in Sumo*-protease-released fractions.

We obtained 3,091 entries for proteins co-purifying with "dual" tubulin (Table S1). Although most TAPs were novel, some were previously shown to bind tubulin, validating our approach. In addition, we did not detect MAP1B, MAP2, or MAP4, the +TIPs EB1 or EB3, or conventional kinesin, indicating that the pull-downs were specific for TAPs. We verified mass spectrometry results using western blot analysis and showed that four prominent TAPs (i.e., CKAP5, CLASP1, CLASP2, and GCC185 [or GCC2]) did bind tubulin, whereas EB1, the "core" +TIP that recruits many other +TIPs to MT ends [18], did not (Figure S2A). We also showed that the "dual" construct depicted in Figure 1A brings down TAPs more efficiently than other constructs (Figures S1A and S2B). Together, these results indicate that the proteins listed in Table S1 represent a considerable fraction of the HEK293T cell "tubulome."

By applying stringent criteria (see the Supplemental Experimental Procedures for explanation) we selected the 45 most prominent TAPs and classified these according to known function or localization (Table 1). Of these TAPs, the majority (80%) are novel. To estimate their abundance, we examined the HEK293T transcriptome using next-generation sequencing. This revealed that most TAPs are expressed at considerably lower levels than the chaperonins, which have FPKM (fragments per kilobase of transcript per million mapped reads) values of well over a 100 (data not shown). Thus, the presence of the TAPs in Table 1 appears to reflect an affinity for α-tubulin, rather than cellular abundance.

We observed several general features in Table 1. First, many of the TAPs interact with other TAPs, often of the same category. For example, CEP97 and CCP110 are interacting centrosomal proteins with a role in preventing excessive centriole growth [19]. Also, CLIP-115 binds the CLASPs [20], and SLAINs have been shown to interact with CLASPs, CKAP5, and CLIP-115 [21]. These results suggest the existence of higher-order tubulin-TAP complexes with important functions in MT and/or centrosome and/or cilia behavior. For example, the tubulin-binding +TIPs might form a core network that promotes MT growth at plus ends and other intracellular sites. A second observation, which was verified by western blot (Figure S2C), was that for a number of TAPs, including the CLASPs, GCC185, and

Table 1. Characterization of Mammalian Tubulin-Associated Proteins

Description[a]	Symbol	RNA[b]	WT-a[c] b	WT-a a	P263T b	P263T a	R402H b	R402H a	WT-b b	WT-b a	T[d]	Interactions[e]
+TIPs												
Cytoskeleton-associated protein 5	CKAP5	53	98	102	96	94	100	99	42	3	Y	TACCs, SLAINs
CLIP-associating protein 1	CLASP1	4.9	49	41	31	27	46	26			I	CLIP2, GCC2, SLAINs
CLIP-associating protein 2	CLASP2	6.1	30	25	10	7	18	7			I	CLIP2, GCC2, SLAINs
Transforming acidic coiled-coil-containing protein 1	TACC1	4.7	15	20	16	25	15	19			N	CKAP5
SLAIN-motif-containing protein 1	SLAIN1	9.4	12	9	12	8	14	8			N	CLASPs, CLIPs, CKAP5, TACC2, KIF2A
SLAIN-motif-containing protein 2	SLAIN2	2.9	11	8	10	7	11	7			N	CLASPs, CLIPs, CKAP5, TACC2, KIF2A
CAP-Gly domain-containing linker protein 2	CLIP2	2.4	6	8			2				I	CLASPs, CKAP5, SLAINs
Adenomatous polyposis coli protein	APC	2.1	6		5		5				N	
Centrosomal												
Centrosomal protein of 290 kDa	CEP290	9.8	67	12	64	10	45	4			N	CCP110, CEP97, IQCB1
Transforming acidic coiled-coil-containing protein 2	TACC2	2.1	35	41	41	44	41	42			N	CKAP5, SLAINs
Centrosomal protein of 170 kDa protein B	CEP170B (KIAA0284)	7.8	29	16	10	5					N	KIF2b, but not KIF2a or KIF2c
Centromere protein J	CENPJ	4.8	29	4	24	5	26	4			Y	
Centriolar coiled-coil protein of 110 kDa	CCP110 (CEP110)	3.7	27	18	21	20	20	16			N	CEP97, Neurl4, CEP290
Centrosomal protein of 97 kDa	CEP97	4.5	16	14	13	17	10	9			N	CCP110, Neurl4 (indirectly), CEP290, CEP97
Abnormal spindle-like microcephaly-associated protein	ASPM	1.6	20	2	9		28				N	
WD-repeat-containing protein 62	WDR62	11	18		13		2		1		N	CEP170
Ninein	NIN	14	9		13		12				N	CEP170
Pericentriolar material 1 protein	PCM1	7.4	9		7		3				N	
Centrosomal protein of 85 kDa like	CEP85L (C6orf204)	4.2	5	4	11	6	15	5			N	
Motor												
Kinesin-like protein KIF14	KIF14	6.8	32	9	29	4	22	5	2		Y	KIF4A(*)
Chromosome-associated kinesin KIF4A	KIF4A	17	27	27	9	7	10				N	KIF14
Kinesin-like protein KIF2A	KIF2A	17	26	30	25	27	17	18	1	2	N	
MT Associated												
MAP7 domain-containing protein 1	MAP7D1	25	26	26	13	11	27	23	9	6	N	NEURL4
Janus kinase and microtubule-interacting protein 1	JAKMIP1	3.2	16	2	4		5				N	
Ensconsin	MAP7	7.4	10	9	3	3	5	7	4	3	N	
Not Categorized												
GRIP and coiled-coil-domain-containing protein 2	GCC2	5.2	26	38	2	9	6	11			N	CLASPs
Lamin-B1	LMNB1	89	15		21	1	22		6		N	LMNA
Alpha-internexin	INA	1.4	13		9		9		5		N	PP1CA
Lamin-B2	LMNB2	61	13		11		12		2		N	LMNA
Prelamin-A/C	LMNA	31	10		13		6				N	LMNB1/2
Serine/arginine-rich splicing factor 1	SRSF1	96	9		10	5	8	2	5		N	
KIAA1671 [hgnc:29345]	KIAA1671	3.2	9		4		5		4		N	
HCLS1-associated protein X-1	HAX1	150	8	6	9	8	9	9	1	3	Y	HSPs
rRNA 2′-O-methyltransferase fibrillarin	FBL	591	8		9		7		3		Y	

(*Continued on next page*)

Table 1. *Continued*

Description[a]	Symbol	RNA[b]	WT-a[c] b	WT-a[c] a	P263T b	P263T a	R402H b	R402H a	WT-b b	WT-b a	T[d]	Interactions[e]
Casein kinase I isoform alpha	CSNK1A1	40	8	6					1		N	HMMR1, FAM83D, APC
Zinc-finger C2HC domain-containing protein 1A	ZC2HC1A	2.6	7	8	5	8	11	5			N	
Tubulin-folding cofactor B	TBCB	55	7	6			8	7	3	2	Y	tubulins
Hyaluronan-mediated motility receptor	HMMR	21	7	15							N	CSNK1A1
IQ calmodulin-binding motif-containing protein 1	IQCB1	35	6		7						N	CEP290
Zinc-finger and BTB domain-containing protein 21	ZBTB21 (ZNF295)	4.6	6	3			3				N	
Protein FAM83D	FAM83D	12	6	7	2						N	CSNK1A1
Mitochondrial inner membrane protein	IMMT	63	5		10		3				N	HSPs
Protein phosphatase 1 regulatory subunit 12A	PPP1R12A	10.8	5	4			4	2			N	
T-complex protein 11-like protein 2	TCP11L2	1.7	5	5	8	6	18	16	2		N	
Catenin beta-1	CTNNB1	71.9	5	2	2		6	4	2		N	

See also Figure S2 and Table S1.

[a]TAPs were categorized into groups based on localization or function. In each group, proteins were sorted in descending preference for the "b" fraction of tagged wild-type α-tubulin. For the underlined TAPs, the corresponding gene was found mutated in a brain malformation and/or ciliopathy patient.

[b]mRNA levels in HEK293T cells as determined by RNA sequencing (FPKM values).

[c]Unique peptides from the paired mass spectrometry analysis. WT-a, pull-down with tagged wild-type α-tubulin; P263T and R402H: pull-down with the respective tagged mutant α-tubulins; WT-b, pull-down with tagged wild-type β-tubulin. b, proteins boiled off the streptavidin beads (i.e., before cleavage); a, proteins released by Sumo* protease (i.e., after cleavage).

[d]Column lists whether a TAP is known (Y) or novel (N) or whether tubulin binding can be inferred (I) based on data with similar proteins from lower eukaryotes.

[e]Interactions with other TAPs in the table, based on Uniprot database and literature searches.

various centrosomal components, fewer unique peptides were found in the mass-spectrometry-based pull-downs of the mutant tubulins (Tables 1 and S1). Finally, several TAPs (underlined in Table 1) have been found mutated in patients with brain malformations or ciliopathies. This underscores the importance of TAPs for brain development and ciliogenesis. It would be interesting to investigate whether other TAPs in Table 1 are mutated in patients with neurological symptoms.

Tubulin Binding Stimulates the MT-Growth-Promoting Capacity of CLASP1

Among the highest-ranking TAPs in the "tubulome" of HEK cells are CKAP5 (also called XMAP215 or Ch-TOG) and the CLASPs, which are +TIPs with similar domains, termed TOG in the case of CKAP5 and TOGL in the case of CLASPs [4]. CKAP5 acts as a MT polymerase by binding tubulin subunits with its TOG domains and mediating the incorporation of tubulin at MT ends [22]. Tubulin binding has also been described for yeast CLASP, which was suggested to promote MT rescue by recruiting tubulin dimers to the MT [23], but not for mammalian CLASP1 and CLASP2. These proteins are encoded by different genes and exist as multiple isoforms [20], the longest of which (α) contains three TOGL domains, whereas shorter isoforms (β, γ) only have two (Figure 2A). Recent studies suggest that the TOGL domains in CLASP2γ do not have an optimal tubulin-binding interface as they assume a curved conformation; these domains were instead proposed to have a preference for MTs [27]. To examine tubulin binding by CLASP isoforms, we co-expressed biotinylated and GFP-tagged "dual" tubulin together with YFP, YFP-CLASP1α, or YFP-CLASP2γ, pulled down biotinylated tubulin, and found that YFP-CLASP1α co-precipitated much more efficiently than YFP-CLASP2γ (Figure 2A, bottom). These results suggest that the TOGL1 domain contributes significantly to tubulin binding of CLASP1α.

The majority of +TIPs, including the CLASPs, have been shown to harbor a small domain (called the SxIP motif) with which they interact with EB proteins and that allows them to accumulate at growing MT ends [18]. In fact, the EB proteins are seen as the "core" +TIPs because they attract most other +TIPs yet bind MT ends in an autonomous fashion [12]. We purified GFP-tagged CLASP1α and CLASP2γ from HEK293T cells (Figures 2B, S3A, and S3B), as well as GFP-tagged and non-tagged ("dark") EB3 (Figures S3C and S3D and data not shown), and examined binding of CLASP isoforms to in vitro-grown MTs, as well as their effect on MT dynamics, using the aforementioned TIRF-microscopy-based assay. CLASP2γ displayed typical +TIP behavior as it accumulated on MT ends in the presence of EB3 (Figures 2C and 2D) and did not bind MTs in the absence of EB3 (data not shown). Strikingly, CLASP1α bound to MT ends and the MT lattice in the absence of EB3; addition of the "core" +TIP shifted CLASP1α binding toward the MT end (Figures 2C and 2D). Thus, the presence of the tubulin-binding TOGL1 domain allows CLASP1α to bind MTs and MT ends autonomously.

We then measured dynamic parameters of in vitro-polymerizing MTs grown in the presence or absence of EB3 and the

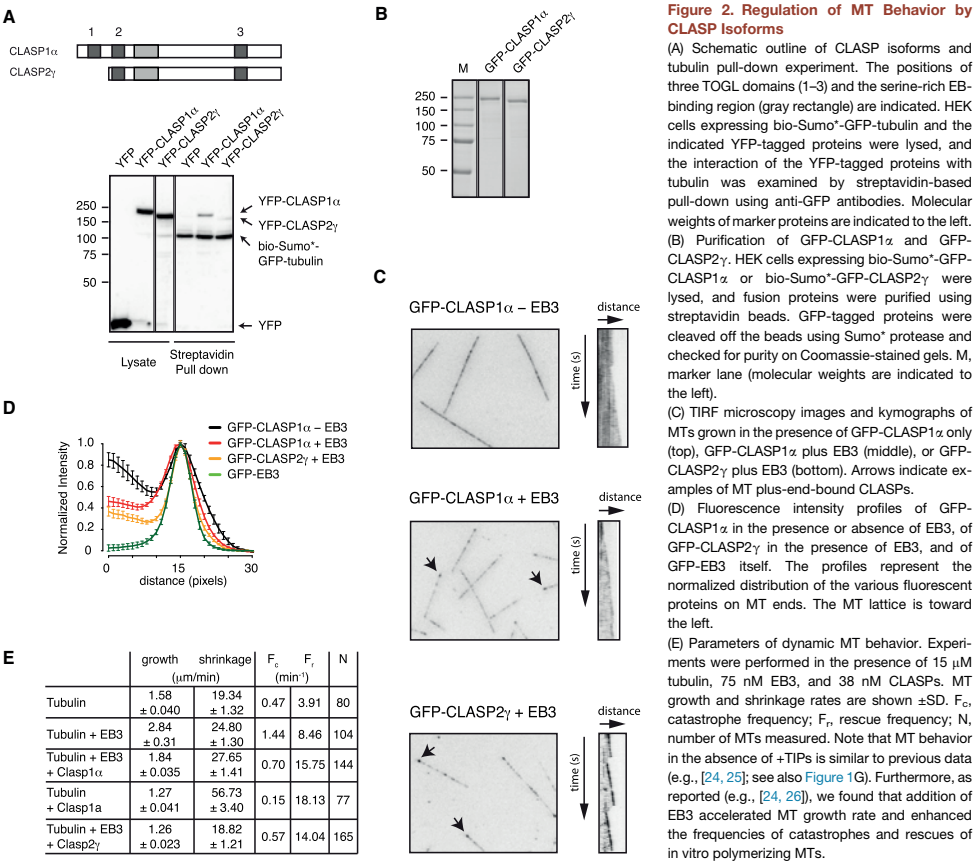

E

	growth (μm/min)	shrinkage (μm/min)	F_c (min^{-1})	F_r (min^{-1})	N
Tubulin	1.58 ± 0.040	19.34 ± 1.32	0.47	3.91	80
Tubulin + EB3	2.84 ± 0.31	24.80 ± 1.30	1.44	8.46	104
Tubulin + EB3 + Clasp1α	1.84 ± 0.035	27.65 ± 1.41	0.70	15.75	144
Tubulin + Clasp1a	1.27 ± 0.041	56.73 ± 3.40	0.15	18.13	77
Tubulin + EB3 + Clasp2γ	1.26 ± 0.023	18.82 ± 1.21	0.57	14.04	165

Figure 2. Regulation of MT Behavior by CLASP Isoforms

(A) Schematic outline of CLASP isoforms and tubulin pull-down experiment. The positions of three TOGL domains (1–3) and the serine-rich EB-binding region (gray rectangle) are indicated. HEK cells expressing bio-Sumo*-GFP-tubulin and the indicated YFP-tagged proteins were lysed, and the interaction of the YFP-tagged proteins with tubulin was examined by streptavidin-based pull-down using anti-GFP antibodies. Molecular weights of marker proteins are indicated to the left.

(B) Purification of GFP-CLASP1α and GFP-CLASP2γ. HEK cells expressing bio-Sumo*-GFP-CLASP1α or bio-Sumo*-GFP-CLASP2γ were lysed, and fusion proteins were purified using streptavidin beads. GFP-tagged proteins were cleaved off the beads using Sumo* protease and checked for purity on Coomassie-stained gels. M, marker lane (molecular weights are indicated to the left).

(C) TIRF microscopy images and kymographs of MTs grown in the presence of GFP-CLASP1α only (top), GFP-CLASP1α plus EB3 (middle), or GFP-CLASP2γ plus EB3 (bottom). Arrows indicate examples of MT plus-end-bound CLASPs.

(D) Fluorescence intensity profiles of GFP-CLASP1α in the presence or absence of EB3, of GFP-CLASP2γ in the presence of EB3, and of GFP-EB3 itself. The profiles represent the normalized distribution of the various fluorescent proteins on MT ends. The MT lattice is toward the left.

(E) Parameters of dynamic MT behavior. Experiments were performed in the presence of 15 μM tubulin, 75 nM EB3, and 38 nM CLASPs. MT growth and shrinkage rates are shown ±SD. F_c, catastrophe frequency; F_r, rescue frequency; N, number of MTs measured. Note that MT behavior in the absence of +TIPs is similar to previous data (e.g., [24, 25]; see also Figure 1G). Furthermore, as reported (e.g., [24, 26]), we found that addition of EB3 accelerated MT growth rate and enhanced the frequencies of catastrophes and rescues of in vitro polymerizing MTs.

See also Figure S3.

CLASPs. The addition of EB3 and GFP-CLASP1α or of EB3 and GFP-CLASP2γ caused a general dampening of MT dynamic behavior compared to MTs grown in the presence of EB3 only (Figure 2E). Interestingly, when added on its own GFP-CLASP1α also reduced MT growth rates, and it virtually eliminated MT catastrophes while increasing rescue frequency (Figure 2E). Thus, consistent with cellular data [28], CLASPs stabilize MT growth by acting both as anti-catastrophe and rescue factors. However, while CLASP2γ only exerts its function in the presence of EB proteins, the tubulin-binding TOGL1-domain allows CLASP1α to promote continuous MT growth in an autonomous fashion. These data suggest that CLASP isoforms use different mechanisms to stimulate MT growth.

Stable Tubulin-TAP Interactions Are Required for Efficient MT Nucleation and Growth

Mutations that give rise to tubulinopathies are thought to perturb neuronal migration and differentiation because of defective tubulin dimer formation, hampered MT dynamics, and/or reduced binding of MAPs to MTs [29–31]. However, our finding that mutant tubulins interact less well with a selected number of TAPs suggested that MT-based processes that depend on these TAPs might also be perturbed in tubulinopathy patients. We therefore examined the intracellular behavior of the P263T and R402H mutants in more detail.

We first confirmed that wild-type and mutant GFP-tubulins are expressed at similar levels in RPE1 cells (Figure S4A). We then examined live RPE1 cells, and we observed fluorescent MT networks less frequently in cells expressing mutant tubulins (Figure S4B). These mutants appeared to be assembly competent, as we detected MTs in virtually all cells after the addition of paclitaxel, a MT-stabilizing agent (Figure S4B). However, the fluorescence intensity of mutant MTs was less than that of MTs containing GFP-tagged wild-type tubulin (Figure S4C), suggesting that mutant tubulins incorporate less efficiently into MTs. To examine GFP-tubulin properties in more detail, we turned to fixed cells.

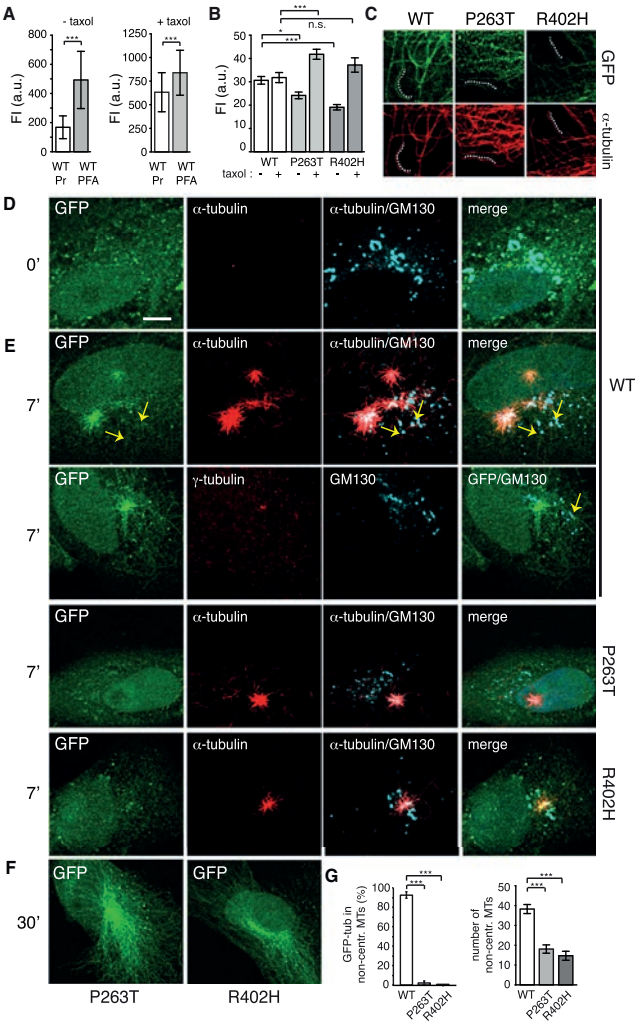

Figure 3. Defects in MT-Based Processes in Cells Expressing Mutant Tubulins

(A) MT incorporation of wild-type GFP-tubulin. Transfected HEK293T cells were either treated with paclitaxel for 2 hr (+ taxol) or not treated (– taxol) and were then either pre-extracted for 1 min and fixed with paraformaldehyde (WT Pr) or only fixed with paraformaldehyde (WT PFA). The fluorescence intensity (FI) of the whole cell was measured in a.u. In the WT Pr sample, in which soluble tubullin is washed away, the FI reflects the amount of GFP-tubulin incorporated into MTs; in the WT PFA sample, the FI reflects both soluble and MT-bound GFP-tubulin.

(B and C) Efficiency of MT incorporation of wild-type and mutant GFP-tubulins. HEK293T cells were transfected with wild-type (WT) or mutant (P263T and R402H) GFP-tubulin and were then pre-extracted and fixed. After fixation, cells were stained with anti-tubulin antibodies. Images in (C) show insets of cells shown in Figure S4E. Using α-tubulin staining, MT segments were outlined (stippled lines show examples, placed adjacent to the corresponding MTs), and the FI of the GFP signal on the MT was measured in a.u. Quantifications are shown in (B).

(A and B) Data are shown ±SD, and t tests were done to examine significance of differences (*$p < 0.05$, ***$p < 0.0001$).

(D–F) MT re-growth in cells after nocodazole washout. RPE1 cells were transfected with wild-type (WT) or mutant (P263T and R402H) GFP-tubulin. After 1 day, cells were treated for 2 hr with 2.5 μg/ml nocodazole and fixed at the indicated times after washout (D, 0 min; E, 7 min; F, 30 min). Cells were stained with either anti-α-tubulin or anti-γ-tubulin antibodies (red) to mark MTs or centrosomes, respectively, and with anti-GM130 antibodies (cyan) to mark the Golgi. Yellow arrows indicate examples of non-centrosomal Golgi-derived MTs. Scale bar, 5 μm.

(G) Quantification of the number of cells with GFP-tubulin incorporated into non-centrosomal MTs (left), or with number of non-centrosomal MTs per cell (right). Data are shown ±SEM, and t tests were done to examine significance of differences (***$p < 0.0001$).

See also Figure S4.

Control experiments indicated that a quick pre-extraction of cells prior to fixation removes soluble GFP signal without affecting the MT network (Figure S4D). To measure the level of MT-bound GFP-tubulin, we therefore analyzed fluorescence in cells that were first pre-extracted and then fixed with paraformaldehyde. To measure the total amount of GFP-tubulin (i.e., soluble and MT bound), we examined cells that were fixed in paraformaldehyde without pre-extraction. We found that 34% of GFP-tubulin was in MTs in cells cultured under normal conditions (Figure 3A, left). By contrast, in cells treated with paclitaxel, 75% of GFP-tubulin was MT bound (Figure 3A, right), suggesting that 75% of wild-type GFP-tubulin is assembly competent. This result is consistent with our MT pelleting result in Figure 1E.

We next compared the capacity of wild-type and mutant tubulins to incorporate into MTs by measuring fluorescence intensities of MT segments in pre-extracted, fixed cells (Figure 3B; note that MTs were outlined with the help of anti-tubulin antibodies, see Figure 3C). In cells cultured under normal conditions, the mutant tubulins incorporated less efficiently into MTs as compared to the wild-type (Figures 3B, 3C, and S4E), in line with results in live RPE1 cells (Figure S4C). Strikingly, in paclitaxel-treated cells, the mutants incorporated better than wild-type tubulin (Figures 3B, 3C, and S4E). These data strongly suggest that mutant tubulins are fully assembly

competent, raising the question of why they do not incorporate efficiently into MTs under normal conditions. We propose that the reduced binding of mutant tubulins to CLASPs and CKAP5 (Figure S2C) contributes to their reduced incorporation into MT ends. We furthermore note that the improved incorporation of mutant tubulins after paclitaxel treatment opens perspectives for treatment of tubulinopathy patients, not with paclitaxel, as this compound does not pass the blood-brain barrier, but perhaps with epothilone B, a MT-stabilizing agent that does [32].

Tubulin dimers have an intrinsic capacity to self-organize into MTs in a process known as MT nucleation. However, the kinetic barrier is high, meaning that the efficiency with which MTs spontaneously nucleate is very low. In cells MT nucleation therefore occurs in MT -organizing centers (MTOCs), of which the centrosome is the major one. However, non-centrosomal MT nucleation, for example at the Golgi apparatus, is also common in cells. As Golgi-mediated MT nucleation depends on GCC185 and the CLASPs [5] and mutant tubulins bind these proteins less efficiently, we investigated whether expression of the mutants affects this process. We treated RPE1 cells with nocodazole, a MT-depolymerizing agent, and first examined incorporation of GFP-tubulin at the centrosome and Golgi after nocodazole washout. Nocodazole treatment almost completely abolished the MT network and caused dispersal of the Golgi (Figure 3D). Seven minutes after washout, GFP-labeled centrosomal and non-centrosomal MTs were detected in cells transfected with wild-type tubulin, but in cells expressing TUBA1A-P263T or TUBA1A-R402H we did not observe any incorporation of mutant tubulin into regrowing MTs (Figure 3E; see also quantification in Figure 3G). By contrast, 30 min after washout, we did observe MTs with fluorescent TUBA1A-P263T or TUBA1A-R402H (Figure 3F).

To examine re-growth of the complete MT network, we stained cells with anti-α-tubulin. This revealed that MTs do form early on after washout (Figure 3E). Interestingly, although the mutant tubulins themselves did not incorporate into Golgi-derived MTs at early time points, their presence did hamper formation of these MTs (Figure 3G). MT nucleation at the Golgi has been suggested to proceed in a step-wise fashion, with GCC185 providing a Golgi-based docking platform for the CLASPs and the CLASPs in turn stimulating MT growth by binding nascent MTs [5]. Our in vitro results support the idea that CLASPs promote MT growth. However, GCC185 also binds tubulin; in fact, like the CLASPs, GCC185 is one of the prominent TAPs identified in this study (Tables 1 and S1). As mutant tubulins bind less efficiently to CLASPs and GCC185 and expression of these mutants hampers Golgi-mediated MT nucleation in cells, we propose that tubulin-CLASP, tubulin-GCC185, and CLASP-GCC185 interactions are all important for setting up a platform at the Golgi for efficient MT nucleation.

Finally, since mutant tubulins also interacted less efficiently with TAPs that are important for cilia formation, we tested whether ciliogenesis is affected in RPE1 cells expressing the mutants. We found that the percentage of RPE1 cells with cilia was reduced upon expression of both mutants; in addition, TUBA1A-R402H expression affected ciliary length (Figures S4F and S4G). We conclude that mutant tubulins hamper both ciliogenesis and non-centrosomal MT nucleation. The P263T and R402H mutants may affect these processes by competing with normal tubulin for TAPs. It is noteworthy that Golgi-mediated MT nucleation contributes to directed cell motility [33] and that cilia are important for directed neuronal migration [34]. Thus, reduced tubulin-TAP interactions may cause neuronal migration problems in tubulinopathy patients due to defective cilia and Golgi-based MT nucleation. Together, our data widen the spectrum of MT-mediated processes that are deregulated in the tubulinopathies.

Conclusions

We have developed an approach to express and purify functional mammalian tubulin dimers from transiently transfected cells. We used this method to identify TAPs in cultured HEK293T cells. This ''tubulome,'' which contains many novel factors, includes CKAP5 and the CLASPs, which are MT plus-end-tracking proteins with multiple TOG(L)-domains, and GCC185, a Golgi-associated protein that binds CLASPs. We show that the N-terminal TOGL1 domain is required for efficient tubulin binding by CLASP1 and allows CLASP1 to promote MT growth in an autonomous manner. Furthermore, two mutant tubulins, known to cause brain malformation and neuronal differentiation defects in tubulinopathy patients, bind less efficiently to certain TAPs, incorporate less well into MTs, and impair intracellular processes involving TAPs. Thus, stable tubulin-TAP interactions, which are perturbed by tubulin mutations, are required for efficient MT nucleation and growth. Our results provide a resource for investigating tubulin interactions and functions and widen the spectrum of tubulin-related disease mechanisms.

ACCESSION NUMBERS

The protein interactions from this publication have been submitted to the IMEx (http://www.imexconsortium.org) consortium through IntAct [35] and assigned the identifier IM-25115.

SUPPLEMENTAL INFORMATION

Supplemental Information includes Supplemental Experimental Procedures, four figures, one table, and one movie and can be found with this article online at http://dx.doi.org/10.1016/j.cub.2016.04.069.

AUTHOR CONTRIBUTIONS

All authors designed and performed subsets of experiments, analyzed data belonging to those experiments, and helped to write the paper. N.G. conceived and supervised the project.

ACKNOWLEDGMENTS

We thank Dave Lammers for preparing the Bio-Sumo*-GFP-CLASP constructs. This work was supported by Netherlands Organization for Scientific Research (NWO) Chemical Sciences (700.59.011) and Graduate Program (022.004.002) grants. This work is also part of the project Proteins At Work, a program of The Netherlands Proteomics Centre financed by the NWO as part of the National Roadmap Large-Scale Research Facilities of the Netherlands (project number 184.032.201).

Received: January 21, 2015
Revised: March 15, 2016
Accepted: April 26, 2016
Published: June 9, 2016

CellPress

REFERENCES

1. de Forges, H., Bouissou, A., and Perez, F. (2012). Interplay between microtubule dynamics and intracellular organization. Int. J. Biochem. Cell Biol. *44*, 266–274.
2. Kapitein, L.C., and Hoogenraad, C.C. (2015). Building the neuronal microtubule cytoskeleton. Neuron *87*, 492–506.
3. Breuss, M., and Keays, D.A. (2014). Microtubules and neurodevelopmental disease: the movers and the makers. Adv. Exp. Med. Biol. *800*, 75–96.
4. Al-Bassam, J., and Chang, F. (2011). Regulation of microtubule dynamics by TOG-domain proteins XMAP215/Dis1 and CLASP. Trends Cell Biol. *21*, 604–614.
5. Efimov, A., Kharitonov, A., Efimova, N., Loncarek, J., Miller, P.M., Andreyeva, N., Gleeson, P., Galjart, N., Maia, A.R., McLeod, I.X., et al. (2007). Asymmetric CLASP-dependent nucleation of noncentrosomal microtubules at the trans-Golgi network. Dev. Cell *12*, 917–930.
6. Desai, A., and Mitchison, T.J. (1997). Microtubule polymerization dynamics. Annu. Rev. Cell Dev. Biol. *13*, 83–117.
7. Miller, H.P., and Wilson, L. (2010). Preparation of microtubule protein and purified tubulin from bovine brain by cycles of assembly and disassembly and phosphocellulose chromatography. Methods Cell Biol. *95*, 3–15.
8. Ludueña, R.F. (1998). Multiple forms of tubulin: different gene products and covalent modifications. Int. Rev. Cytol. *178*, 207–275.
9. Tian, G., Huang, Y., Rommelaere, H., Vandekerckhove, J., Ampe, C., and Cowan, N.J. (1996). Pathway leading to correctly folded beta-tubulin. Cell *86*, 287–296.
10. Minoura, I., Hachikubo, Y., Yamakita, Y., Takazaki, H., Ayukawa, R., Uchimura, S., and Muto, E. (2013). Overexpression, purification, and functional analysis of recombinant human tubulin dimer. FEBS Lett. *587*, 3450–3455.
11. Kim, J.H., Lee, S.-R., Li, L.-H., Park, H.-J., Park, J.-H., Lee, K.Y., Kim, M.-K., Shin, B.A., and Choi, S.-Y. (2011). High cleavage efficiency of a 2A peptide derived from porcine teschovirus-1 in human cell lines, zebrafish and mice. PLoS ONE *6*, e18556.
12. Bieling, P., Laan, L., Schek, H., Munteanu, E.L., Sandblad, L., Dogterom, M., Brunner, D., and Surrey, T. (2007). Reconstitution of a microtubule plus-end tracking system in vitro. Nature *450*, 1100–1105.
13. Bahi-Buisson, N., Poirier, K., Fourniol, F., Saillour, Y., Valence, S., Lebrun, N., Hully, M., Bianco, C.F., Boddaert, N., Elie, C., et al.; LIS-Tubulinopathies Consortium (2014). The wide spectrum of tubulinopathies: what are the key features for the diagnosis? Brain *137*, 1676–1700.
14. Tian, G., Jaglin, X.H., Keays, D.A., Francis, F., Chelly, J., and Cowan, N.J. (2010). Disease-associated mutations in TUBA1A result in a spectrum of defects in the tubulin folding and heterodimer assembly pathway. Hum. Mol. Genet. *19*, 3599–3613.
15. Janke, C. (2014). The tubulin code: molecular components, readout mechanisms, and functions. J. Cell Biol. *206*, 461–472.
16. Chuong, S.D., Good, A.G., Taylor, G.J., Freeman, M.C., Moorhead, G.B., and Muench, D.G. (2004). Large-scale identification of tubulin-binding proteins provides insight on subcellular trafficking, metabolic channeling, and signaling in plant cells. Mol. Cell. Proteomics *3*, 970–983.
17. Gache, V., Louwagie, M., Garin, J., Caudron, N., Lafanechere, L., and Valiron, O. (2005). Identification of proteins binding the native tubulin dimer. Biochem. Biophys. Res. Commun. *327*, 35–42.
18. Honnappa, S., Gouveia, S.M., Weisbrich, A., Damberger, F.F., Bhavesh, N.S., Jawhari, H., Grigoriev, I., van Rijssel, F.J., Buey, R.M., Lawera, A., et al. (2009). An EB1-binding motif acts as a microtubule tip localization signal. Cell *138*, 366–376.
19. Spektor, A., Tsang, W.Y., Khoo, D., and Dynlacht, B.D. (2007). Cep97 and CP110 suppress a cilia assembly program. Cell *130*, 678–690.
20. Akhmanova, A., Hoogenraad, C.C., Drabek, K., Stepanova, T., Dortland, B., Verkerk, T., Vermeulen, W., Burgering, B.M., De Zeeuw, C.I., Grosveld, F., and Galjart, N. (2001). Clasps are CLIP-115 and -170 associating proteins involved in the regional regulation of microtubule dynamics in motile fibroblasts. Cell *104*, 923–935.
21. van der Vaart, B., Manatschal, C., Grigoriev, I., Olieric, V., Gouveia, S.M., Bjelic, S., Demmers, J., Vorobjev, I., Hoogenraad, C.C., Steinmetz, M.O., and Akhmanova, A. (2011). SLAIN2 links microtubule plus end-tracking proteins and controls microtubule growth in interphase. J. Cell Biol. *193*, 1083–1099.
22. Brouhard, G.J., Stear, J.H., Noetzel, T.L., Al-Bassam, J., Kinoshita, K., Harrison, S.C., Howard, J., and Hyman, A.A. (2008). XMAP215 is a processive microtubule polymerase. Cell *132*, 79–88.
23. Al-Bassam, J., Kim, H., Brouhard, G., van Oijen, A., Harrison, S.C., and Chang, F. (2010). CLASP promotes microtubule rescue by recruiting tubulin dimers to the microtubule. Dev. Cell *19*, 245–258.
24. Montenegro Gouveia, S., Leslie, K., Kapitein, L.C., Buey, R.M., Grigoriev, I., Wagenbach, M., Smal, I., Meijering, E., Hoogenraad, C.C., Wordeman, L., et al. (2010). In vitro reconstitution of the functional interplay between MCAK and EB3 at microtubule plus ends. Curr. Biol. *20*, 1717–1722.
25. Odde, D.J., Cassimeris, L., and Buettner, H.M. (1995). Kinetics of microtubule catastrophe assessed by probabilistic analysis. Biophys. J. *69*, 796–802.
26. Maurer, S.P., Cade, N.I., Bohner, G., Gustafsson, N., Boutant, E., and Surrey, T. (2014). EB1 accelerates two conformational transitions important for microtubule maturation and dynamics. Curr. Biol. *24*, 372–384.
27. Maki, T., Grimaldi, A.D., Fuchigami, S., Kaverina, I., and Hayashi, I. (2015). CLASP2 has two distinct TOG domains that contribute differently to microtubule dynamics. J. Mol. Biol. *427*, 2379–2395.
28. Mimori-Kiyosue, Y., Grigoriev, I., Lansbergen, G., Sasaki, H., Matsui, C., Severin, F., Galjart, N., Grosveld, F., Vorobjev, I., Tsukita, S., and Akhmanova, A. (2005). CLASP1 and CLASP2 bind to EB1 and regulate microtubule plus-end dynamics at the cell cortex. J. Cell Biol. *168*, 141–153.
29. Tian, G., Kong, X.P., Jaglin, X.H., Chelly, J., Keays, D., and Cowan, N.J. (2008). A pachygyria-causing alpha-tubulin mutation results in inefficient cycling with CCT and a deficient interaction with TBCB. Mol. Biol. Cell *19*, 1152–1161.
30. Niwa, S., Takahashi, H., and Hirokawa, N. (2013). β-Tubulin mutations that cause severe neuropathies disrupt axonal transport. EMBO J. *32*, 1352–1364.
31. Tischfield, M.A., Baris, H.N., Wu, C., Rudolph, G., Van Maldergem, L., He, W., Chan, W.-M., Andrews, C., Demer, J.L., Robertson, R.L., et al. (2010). Human TUBB3 mutations perturb microtubule dynamics, kinesin interactions, and axon guidance. Cell *140*, 74–87.
32. Ruschel, J., Hellal, F., Flynn, K.C., Dupraz, S., Elliott, D.A., Tedeschi, A., Bates, M., Sliwinski, C., Brook, G., Dobrindt, K., et al. (2015). Axonal regeneration. Systemic administration of epothilone B promotes axon regeneration after spinal cord injury. Science *348*, 347–352.
33. Miller, P.M., Folkmann, A.W., Maia, A.R., Efimova, N., Efimov, A., and Kaverina, I. (2009). Golgi-derived CLASP-dependent microtubules control Golgi organization and polarized trafficking in motile cells. Nat. Cell Biol. *11*, 1069–1080.
34. Métin, C., and Pedraza, M. (2014). Cilia: traffic directors along the road of cortical development. Neuroscientist *20*, 468–482.
35. Orchard, S., Ammari, M., Aranda, B., Breuza, L., Briganti, L., Broackes-Carter, F., Campbell, N.H., Chavali, G., Chen, C., del-Toro, N., et al. (2014). The MIntAct project–IntAct as a common curation platform for 11 molecular interaction databases. Nucleic Acids Res. *42*, D358–D363.

For copyright reasons chapters 3,4 and 5 are still under embargo

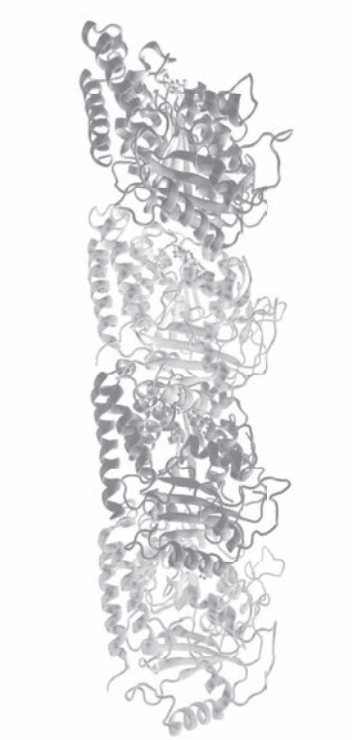

Chapter 3

α-Tubulin mutations causing brain malformations investigated by all-atom molecular dynamics simulations

Luca Signorile[†], Kris Leslie[‡], Niels Galjart[†1]

[†] Department of Cell Biology, Erasmus Medical Center Faculty Building, PO Box 2040, 3000CA Rotterdam, the Netherlands.

[1] Corresponding author. E-mail: n.galjart@erasmusmc.nl

[‡] Present address: School of Human and Life Sciences, Canterbury Christ Church University, North Holmes Road, Canterbury, Kent CT1 1QU, United Kingdom.

Manuscript in preparation

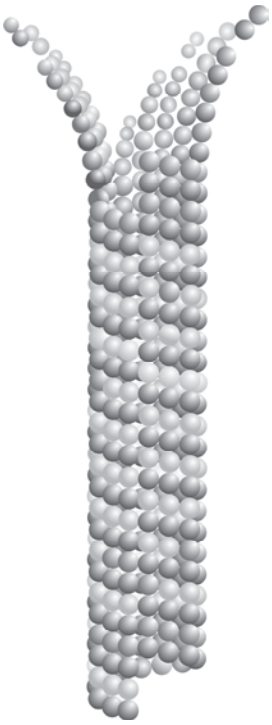

Chapter 4

CLIPs regulate microtubule, centrosome and ciliary behavior by linking protein complexes to specific conformations of tyrosinated tubulin

Luca Signorile[1], Marja Miedema[1], Sreya Basu[1], Malgorzata Grosbart[2], Nuo Yu[1], Sophie Ottema[1], Yulia Komarova[1], Jeffrey van Haren[1], Michael Olvedy[1], Ihor Smal[3], Nanda Keijzer[1], Dick Dekkers[4], Isabelle Arnal[5], Claire Wyman[2], Jeroen Demmers[4], Frank Grosveld[1], Niels Galjart[#1].

1) Department of Cell Biology, Erasmus Medical Center Faculty Building, PO Box 2040, 3000CA Rotterdam, The Netherlands.

2) Department of Molecular Genetics, Erasmus Medical Center Faculty Building, PO Box 2040, 3000CA Rotterdam, The Netherlands.

3) Biomedical Imaging Group Rotterdam, Erasmus Medical Center, 3015 GE, Rotterdam, The Netherlands.

4) Proteomics Centre, Erasmus MC, P.O. Box 2040, 3000 CA Rotterdam, The Netherlands.

5) Grenoble Institute des Neurosciences, Grenoble, France

[#] Corresponding author. E-mail: n.galjart@erasmusmc.nl

Manuscript in preparation

Chapter 5

General Discussion

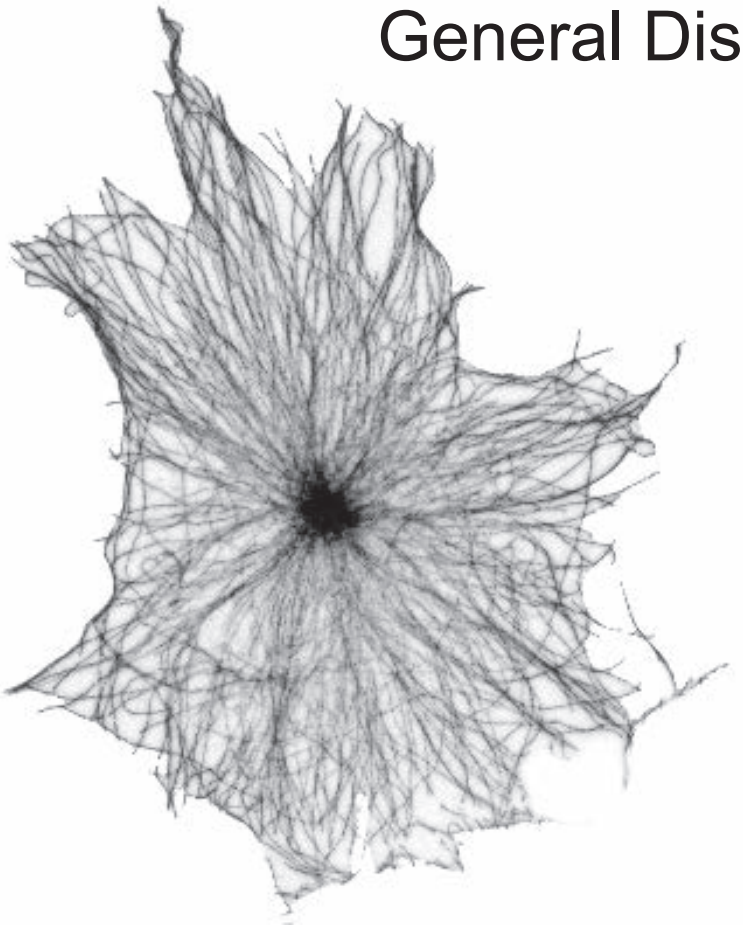

Addendum

Curriculum vitae

PERSONAL DETAILS

Name	Luca Signorile
Date of birth	11 February 1986
Place of birth	Bari, Italy

EDUCATION

2013-2017	PhD program at Erasmus Medical Center Department of Cell Biology, Erasmus Medical Center, Rotterdam, The Netherlands
2010-2012	Master of Science in Molecular Medicine Erasmus Medical Center, Rotterdam, The Netherlands
2006-2010	Bachelor of Science in Pharmaceutical and Health Biotechnologies, University of Bari, Italy
2000-2005	Scientific High School “A. Scacchi”, Bari, Italy

RESEARCH

2013-2017	PhD research Department of Cell Biology, Erasmus MC, Rotterdam, The Netherlands (Prof.dr. D. Huylebroeck, Prof.dr. F.G. Grosveld and Dr.ir. N.J. Galjart)
2011-2012	MSc research project Department of Cell Biology, Erasmus MC, Rotterdam, The Netherlands (Dr. R.A. Poot)
2011	MSc research project Department of Orthopaedics and Otorhinolaringology, Erasmus MC, Rotterdam, The Netherlands (Dr. R. Narcisi and Prof.dr. G.J.V.M. van Osch)

Publications

“Isolation of Functional Tubulin Dimers and of Tubulin-Associated Proteins from Mammalian Cells.” Yu N*, **Signorile L*,** Basu S, Ottema S, Lebbink JH, Leslie K, Smal I, Dekkers D, Demmers J, Galjart N. Curr Biol. 2016 Jul 11;26(13):1728-36. [* shared first author]

”ACTG2 variants impair actin polymerization in sporadic Megacystis Microcolon Intestinal Hypoperistalsis Syndrome.” Halim D, Hofstra RM, **Signorile L**, Verdijk RM, van der Werf CS, Sribudiani Y, Brouwer RW, van IJcken WF, Dahl N, Verheij JB, Baumann C, Kerner J, van Bever Y, Galjart N, Wijnen RM, Tibboel D, Burns AJ, Muller F, Brooks AS, Alves MM. Hum Mol Genet. 2016 Feb 1;25(3):571-83.

“Proteins that bind regulatory regions identified by histone modification chromatin immunoprecipitations and mass spectrometry.” Engelen E, Brandsma JH, Moen MJ, **Signorile L**, Dekkers DH, Demmers J, Kockx CE, Ozgür Z, van IJcken WF, van den Berg DL, Poot RA. Nat Commun. 2015 May 20;6:7155.

“TGFβ inhibition during expansion phase increases the chondrogenic re-differentiation capacity of human articular chondrocytes.” Narcisi R, **Signorile L**, Verhaar JA, Giannoni P, van Osch GJ. Osteoarthritis Cartilage. 2012 Oct;20(10):1152-60.

PhD Portfolio

Name student	Luca Signorile
Erasmus MC Department	Cell Biology
Research school	Graduate School MGC
PhD period	March 2013-September 2017
Promoters	Danny Huylebroeck, Frank G. Grosveld
co-promoter	Niels J. Galjart

PhD training

Courses

2013	Basic Course on R (Rotterdam)
2013	Genetics (Rotterdam)
2013	Safely working in the laboratory (Leiden)
2013	Biochemistry and Biophysics (Rotterdam)
2014	Microscopic Image Analysis (Rotterdam)
2014	Cell and Developmental Biology (Rotterdam)
2014	Biostatistical Methods (Rotterdam)
2015	Scientific Integrity (Rotterdam)
2015	Linux and Basic Scripting Course (Leiden)
2016	English Biomedical Writing (Rotterdam)

Workshops, Symposia and Conferences

2017	27th MGC symposium, Rotterdam, The Netherlands (oral presentation)
2017	1st Meeting ACE Systems Biomedicine, Rotterdam, The Netherlands
2013-2017	Department Meetings
2013	20th MGC PhD workshop, Luxembourg, Luxembourg
2013	23rd MGC Symposium, Rotterdam, The Netherlands
2014	EMBO conference: Microtubules: Structure, regulation and functions, Hei delberg, Germany (poster presentation)
2014	21st MGC PhD workshop, Münster, Germany (poster presentation)
2014	24th MGC Symposium, Rotterdam, The Netherlands
2015	22nd MGC PhD workshop, Maastricht, The Netherlands (oral presentation)
2015	25th MGC Symposium, Leiden, The Netherlands
2016	23rd MGC PhD workshop, Dortmund, Germany (oral presentation)
2016	2nd European Meeting of Neuroscience for PhD students, Grenoble Institute of Neuroscience, France (oral presentation)

Teaching activities

2014	BSc Nanobiology Program, supervision of 2 students
2015-2016	BSc student supervision
2015	Teaching assistant for Protein Structure Course for BSc Nanobiology Program (Rotterdam)
2017	Teaching assistant for Protein Structure Course for PhD Program (Rotterdam)

Additional Activities

2013-2017	Department Server Administrator

Acknowledgements

First of all, I would like to express my gratitude to my promoters, **Danny** and **Frank**. **Danny**, thanks for your critical insight and helpful comments not only for this thesis, but also throughout my PhD. You had always time for me even in the most hectic moments, thank you. **Frank**, thank you for all the advice you gave me during these years, and thank you for the nice discussions about cell biology, biochemistry, chemistry and physics! **Niels**, it seems like yesterday we first had our first chat about microtubules: I still cannot believe 4 years have passed since then. Thank you for your guidance, your openness to new ideas, your positive and encouraging attitude (also when I was frustrated because of failed experiments!) and for your support and understanding. I have learned a lot from you, thank you. **Gert**, **Marileen**, **Isabelle**, **Joyce** and **Kris**: I could have not asked for better committee members; thank you for being part of it! **Isabelle**, I still have great memories from the time I visited your lab two years ago, thank you so much for your time and help! **Joyce**, I was very happy when you asked me if I could help you out with the Protein Structure course. I enjoyed it and I learned a lot from your teaching, as well as when we were talking about structural studies and biochemistry, and when you taught me how to perform gel filtration and surface plasmon experiments. Thank you very much for all your help! **Kris**, although you left the group shortly after I had started my PhD, you have been of great help, supportive and a great teacher. It is to you that I mainly owe my passion for structural biology, molecular modeling and molecular dynamics studies (let's discuss another time about quantum mechanics, better with a couple of pints of ale!). **Ihor**: thank you very much for the custom-made plugin you made for MT dynamics parameters! And of course for all your help on image processing, analysis, R, statistics, Linux tips, etc.! I think I am forgetting more things, but I thank you also for them! Best of luck for your career!! **Maarten**, thanks for your prompt help with R. A big thank you to the whole **Optical Imaging Center!** Special thanks to **Martijn** for all the help and training on the TIRF, and for being always so patient and kind whenever I bothered him!

Marike, thank you so much for all the help, especially towards the defence! You are great! To my friends and paranymphs **Andrea, Martì** and **Enrico**: I cannot say how much I am grateful for your (practical and psychological) support and how much I enjoyed the great times we had, not only during these last crazy months of my PhD, but during all these years. I was really lucky having you beside me, thank you! (**Andrea**, grazie ancora per il "supporto logistico" al mio trentesimo compleanno: e chi se lo scorda? **Enrico**, daje, manca poco anche a te!! **Martì**, you are very close to finishing as well: best of luck to you and **Marta**!!) **Claire**, thank you for your collaboration, your availability, for the input you provided and for the stimulating conversations. SFM is cool! And of course **Gosia**, lots of good luck for your future! Thanks for all the work you have done for the SFM included in Chapter 4. **Lena**, "the TIRFer", first of all a huge thank you for designing the magnificent cover of this thesis!! I am so happy I asked you (who knows what could have been of it, otherwise!!). Best of luck for your future, please let's keep in touch! I will miss our weekend drinks and conversations about Tool! To the present and past members of Lab1030: **Sreya**, thank you for the nice chats and support during our late hours at work, and thanks also for your patience and the help in the lab; good luck with your career! **Nuo**, it has been great working with you, especially for the paper we co-authored. And keep on smiling as you always do! Best of luck to you and Oliver. **Sophie**, I will never forget the good times in the lab and in Heidelberg! **Katja**, **Yannicka**, **Arie**, **Enzo** and **Mingkun**: good luck! **Kerstin**, thanks for your help and advice not only for work-related matters, but also for my future: thank you! **Raymond** and **Erik**, it is in your lab that I learned a lot of biochemistry and molecular biology techniques: thank you.

A big thank you to the band **The Microtubules**! **Marti, Enrico, Lennart**: you see? I have said it! Guys, thanks a lot for the great fun during our rehearsals and during the post-rehearsals beers and hamburgers! **Aristea**, thank you so much for your help, best of luck in Sweden!! **Sarra**, good luck for your future, but try to work a bit less... **Irene, Judith, Lize, Ilias, Pablo, Rodrigo, Jente**: thank you for the fun times and good luck with your PhDs, you will do great! **Eskeww**, it is great to see you again in the EMC! I am passing on to you the responsibility of Kolossus: treat it well!

To the whole Cell Biology Department and in particular to **Mieke, Ser, Sylvia, Martjin** (thanks for the help with the layout of the last days and, of course, for the ultracentrifuge tubes!)**, Evelien**: keep up with the fun borrels and parties (and good science!). **Rick**, the first and only Dutch man to prefer wine and gin over beer: it has been nice sharing some enological thoughts with you (besides scientific ones, of course)! **Mateusz**, good luck in finishing your PhD! The "IT team": **Toon, Nils,** and especially **Sjozef**: thank you so much for helping me out with server matters and Linux issues (sorry for having hassled you so much Sjozef! I learned a lot from you). **Johannes, Cristina, Yasemin** and **Mariangela**: such crazy days at the PhD workshops! Hang in there for a bit more, you are very close to finishing!

And now, the "Italian gang": **Isa** (per favore, sii meno gentile e disponibile col prossimo! Scherzo...non cambiare, sei una persona squisita!! Ricordo ancora che sei stata la prima persona che ho conosciuto a Rotterdam...In bocca al lupo per tutto e grazie ancora per gli splendidi giorni a Chiavenna), **Jessica** (grazie per tutte le risate, le cene, i consigli lavorativi e di shopping, l'aiuto con il forno sotto il diluvio, etc... ed ovviamente per essermi sempre stata accanto anche nei momenti più difficili. In bocca al lupo per tutto!!!), **Thomas** (lots of good luck for your future man! Hope to visit you soon!), **Chris** (sooner or later I will make it to Edinburgh! And yes, you are Italian!), **Jovana ed Enrico** (un ultimo sforzo, ci siete quasi! Mi prenoto giá per venire a Meolo e per fare una ferrata sulle Dolomiti!), **Flavia e Simone** (grazie per tutte le risate e i manicaretti! E chi se le scorda le magnate insieme?), **Marta** (ci vediamo a Stoccolma! Sono sicuro ti troverai bene), e poi **Federica, Ale, Agnese**, **Friedemann, Fabrizia** e **Hegias** (in bocca al lupo a tutti voi!). **Chiara** e **Domenico** (sono stato davvero contento di avervi incontrato! In bocca al lupo!), **Alessia** (come non ricordare i mercoledí sera al Bird in compagnia di **Enrico** e degli infiniti giri di Maredsous! Per non parlare del pranzo di Pasqua... Ci vediamo a Bologna!) e **Sabrina** (in bocca al lupo per il tuo futuro, nella vita lavorativa e non solo!). **Adela**, moltes gràcies per tindre tanta paciencia amb mi durant aquests últims i estresants mesos, i moltes gràcies per tots els bons moments i riures que hem tingut junts en totes les circumstàncies! Et desitge el millor, tinc moltes ganes de veure't de nou prompte!

Marco, Giovanni e **Alessandro**, amici storici, anzi fratelli. Ho così tanti ricordi che non saprei da dove iniziare. Siete grandi e sappiate che ci sono sempre per voi. Davvero non posso esprimere la mia riconoscenza per essermi stati vicini da subito così come i vostri genitori (**Daniela, Emanuele, Gianna, Domenico, Antonietta** e **Gino**: un grazie stragrande per avermi sempre accolto come un figlio), senza se e senza ma, e sempre pronti ad aiutarmi. **Patrizia**, quando andiamo in bosco? Grazie per essermi stata accanto. Un grazie a tutti i miei parenti. **Clara**, sei la donna piú forte e testarda che conosca: continua cosí! Ai miei zii teutonici **Valentina** e **Hermann** (vielen Dank für ihre Hilfe in diesen Jahren!) e a quelli meno teutonici **Mirella** e **Mimmo**: grazie mille per tutto quello che avete fatto per me, soprattutto da quando avevo 15 anni. Non lo scorderò mai ed è in gran parte merito vostro se ho raggiunto questo traguardo. Siete un esempio per me. Grazie, grazie, grazie.